A STUDY OF SECONDARY BONDING EFFECTS IN WERNER CLATHRATES

A thesis submitted to the
UNIVERSITY OF CAPE TOWN
in fulfilment of the requirements for the degree of
MASTER OF SCIENCE

by

ADRIAN PHILIP SUCKLING
B.Sc(Hons) (CAPE TOWN)

Department of Physical Chemistry
University of Cape Town
Rondebosch
7700
Republic of South Africa

July 1988

ACKNOWLEDGEMENTS

I wish to extend sincere thanks to:

Professor L.R Nassimbeni and Dr M.L. Niven for their enthusiastic supervision.

All colleagues for their help and interest, especially to Michael Taylor.

The University of Cape Town and C.S.I.R for the financial assistance.

This work is dedicated to my parents

PUBLICATIONS

Studies in Werner Clathrates. Part 8. Secondary bonding to halogenated guest molecules. L.R Nassimbeni, M.L Niven and A.P Suckling, Inorganica Chimica Acta, in publication.

ABSTRACT

The crystal structures of $Ni(NCS)_2(4\text{-}ViPy)_2.nG$ where nG = $2CH_2Cl_2$ **(I)**, $2CCl_4$ **(II)**, $1.8CH_2I_2$ **(III)** and CHI_3 **(IV)**, as well as the crystal structure of $[Ni(NCS)_2(4\text{-}ViPy)_4]$. $[Ni(NCS)_2(4\text{-}ViPy)_3(thf)].2CHI_3$ **(V)** have been elucidated. The diiodomethane guest molecules in STRUCTURE III were severely disordered at room temperature and so this structure was solved at -40°C.

The dichloromethane clathrate is isomorphous with the chloroform clathrate of the same host, and both these clathrates have a similar packing to the carbon tetrachloride clathrate.

There is significant secondary bonding between the sulphur (donor) of the isothiocyanate ligand of the host and the iodines (acceptor) of the halogenated guest molecules in compounds III, IV and V. The iodoform clathrates, compounds IV and V, also show strong similarities in their packings.

Particular attention has been paid to the shape and size of the cavities in which the guest molecules find themselves, in order to gain a better understanding of the nature of these clathrates. This has also shed some light on the probable cause of the disordered diiodomethane molecules in STRUCTURE III. Packing densities and volume comparisons of the $[Ni(NCS)_2(4\text{-}ViPy)_2]$ clathrates have been carried out.

Solid - state U.V/visible spectroscopy was used to obtain information on the host conformation, and thermal analysis (thermogravimatry and differential thermal analysis) was used to obtain insight into the host - guest interactions of these clathrates.

CONTENTS PAGE

CHAPTER 1

Introduction

1.1 INCLUSION COMPOUNDS

1.1.1 THE NATURE OF INCLUSION COMPOUNDS

The term inclusion compounds is a general one which covers a broad range of compounds, referred to as the host, which have the ability, owing to their suitable steric properties, to enclose another molecule, referred to as the guest. Although the host molecule may crystallise in a close packed-array in the absence of guest, when guest molecules are present it must have the ability to form cavities of molecular dimensions. The shape of this cavity is dramatically influenced by the nature of the host. The mixed hexacyanoferrate(II), $K_2Zn_3[Fe(CN)_6]_2.xH_2O$ is zeolitic in nature, with the crystal lattice being criss - crossed by channels interconnected by cavities[1·1]. This allows the reversible absorption and desorption of water as well as the replacement of water by other guest molecules such as CO, N_2, C_2H_4 and C_2H_6. These crystals remain thermally stable up to about 270 °C and thus permits their use for chromatographic purposes at higher temperatures.
The cavities in clathrates of Dianin's compound, 4-p-hydroxyphenyl-2,2,4-trimethylchroman, are formed by a network of hydrogen bonding between the hydroxyl groups which results in a cage structure for the ethanol[1·2], chloroform[1·2] and n - heptanol[1·3] complexes (fig 1.1).

The nature of the host-guest interaction is not so much influenced by the chemical affinity or the presence of certain groups, but rather by the spatial arrangements and interactions, where primarily van der Waals forces and

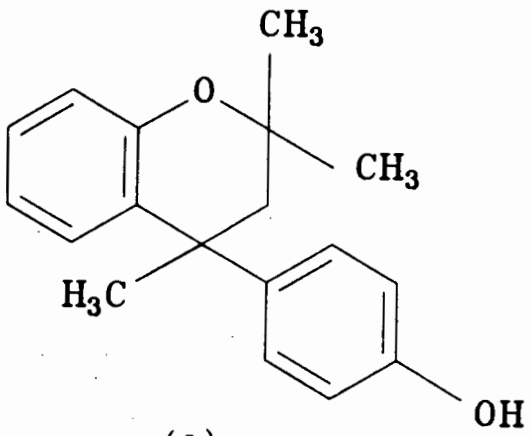

(a)

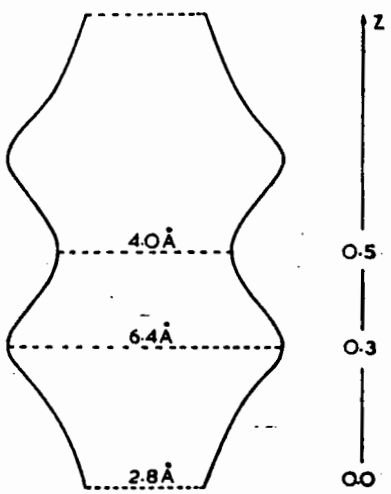

(b)

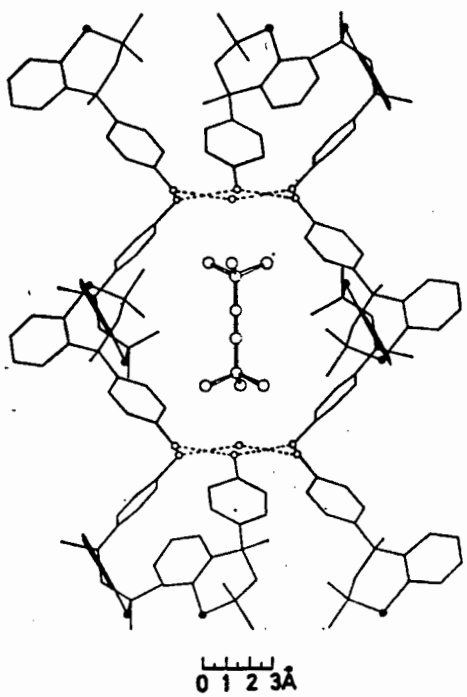

(c)

Cryptato - clathrate

fig 1.1 (a) Dianin´s compound, 4 - p - hydroxyphenyl - 2,2,4 - trimethylchroman. (b) Section through the van der Waals´ surface of the cavity of the thio analogue of (a), showing the space available for guest accomodation. (c) A view normal to the c - axis of the thio derivative, showing a guest molecule in the cavity. Two host molecules have been excluded apart from their hydroxy - oxygen atoms to show the cavity more clearly.
Taken from D.D MacNicol and F.B Wilson[1.4].

oriented dipoles play a major role in the formation of inclusion compounds.

The chemistry of inclusion compounds was born with the publication of a paper by H.M Powell in 1947[1·5] describing the clathrating ability of quinol. Prior to this, however, quite a few inclusion compounds had been prepared, but their nature had not been not elucidated. It was Powell who realised that compounds could unite to form a stereospecific complex, and that bond formation need not take place. Some of the earlier examples of inclusion compounds are: 1823 Faraday[1·6] reported the preparation of the chlorine clathrate hydrate, the preparation of graphite intercalates[1·7] in 1841, the preparation of cyclodextrin inclusion compounds[1·8] in 1891. Since these early days the extent of compounds exhibiting inclusion phenomena has grown considerably. Many of these possess similar properties and structures, and so certain classes of inclusion compounds have emerged, as well as a need to classify them. The classification adopted here is that proposed by Weber and Josel[1·9]. This classification is illustrated in TABLE 1.1.

The main division is that into complexes and clathrates. When the guest is coordinatively bound to the host then this belongs to the class of <u>complexes</u>. C.J Pedersen synthesised the first crown ethers[1·10], which are macrocyclic polyethers and J.M Lehn synthesised the cryptands[1·11]. These compounds have the ability to form 1:1 inclusion complexes with the alkaline and alkaline earth cations, in which the cation is held in the central cavity of the host molecule. The overall geometrical shape of the ligand, the ligand topology, determines the way in which ligand and cation interact and so ligands may be designed which exhibit selectivity for certain cations. On complexation the ligand should be able to replace as completely as possible the solvation shell of the cation. Since the alkaline and alkaline earth cations

TABLE 1.1 Classification of host - guest compounds.

HOST - GUEST COMPOUNDS

I	II
Coordination - type aggregate	Lattice - type aggregate
I (II) Lattice - assisted complex clathratocomplex	CLATHRATE
II(I) Coordination - assisted clathrate coordinatoclathrate	
COMPLEX	

Host - Guest type	and	Host - Guest interaction
1.Ionic(charged)		1.Ion - Ion
2.Polar		2.Ion - Dipole
3.Neutral		3.Dipole - Dipole
		4.Donor - Acceptor
		5.van der Waals
		6.Hydrophobic effect
		7.Steric barrier

A.	B.
INCLUSION compound	ADDITION compound
Intramolecular host - guest aggregate(host cavity)	Extramolecular host - guest aggregate(no host cavity)
cavitate	adduct

Topology		
	a. Layer,sandwich	: Intercalate
	b. Ring	: Coronate,Podate
	c. Channel	: Tubulate
	d. Pocket,Niche	: Aediculate
	e. Cage	: Cryptate

are spherical, the optimum ligand should contain an intramolecular, closed, spherical cavity. The size of the cavity should also be equal to the size of the cation to be recognized. The development of ligands which have a high selectivity for alkaline and alkaline earth cations can have many consequences, a few being:

(1) Control over the stability and selectivity of the complexes both within the two groups (M_1^+/M_3^+ selectivity) and between these groups (M_1^+/M_3^{2+} selectivity).

(2) Possibility of producing anion activation if complexation of the cation leads to dissolution of salts in organic solvents accompanied by ion-pair separation.

(3) The crown ethers have also been applied to the problem of bioorganic modelling, with the design of crown ethers as model systems for enzyme catalysis (fig 1.2) [1.12]. The transport of cations through membranes is an important biological process(the role of Na^+ and K^+ in the propagation of nerve impulses), and so these ligands can serve as models for these processes.

Clathrates are inclusion compounds where the guest is retained by steric barriers formed by the host lattice. These different forces involved in host - guest interaction result in complexes retaining their identity in solution, whereas clathrates normally decompose on dissolution. Examples of clathrates are the host - guest compounds formed by Dianin's compound, already mentioned, by urea[1.13,1.14]and by graphite[1.15]. Urea crystallises in a tetragonal lattice, whereas, in the presence of a suitable guest, it crystallises in an hexagonal arrangement with a one dimensional open channel with a diameter of 5 Å, which

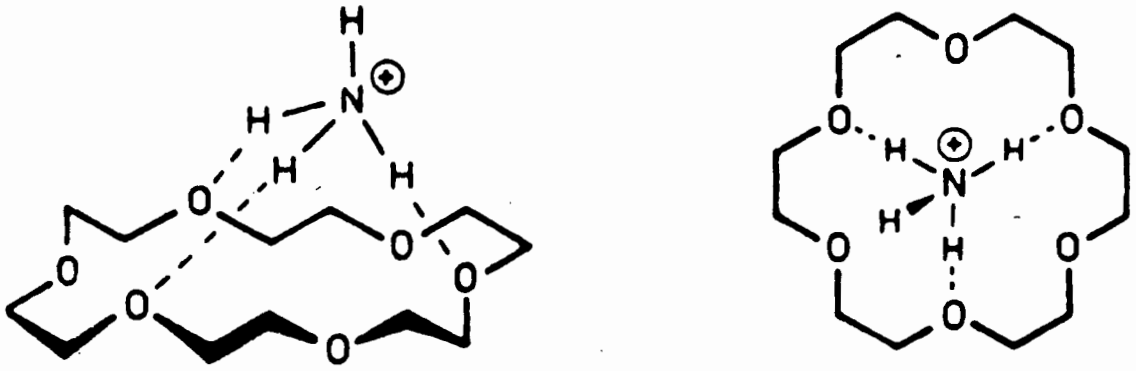

(a) *Coronato - complex* (b)

fig 1.2 (a) [18] crown - 6 , showing the three point bonding of an ammonium cation. The crown ethers can be used to mimic enzymic chemistry by using as guest an ammonium ion with group R on which a reaction is to be carried out and then modify as desired the periphery of the crown ether[1.12].

(b) [18] crown - 6 viewed from above.

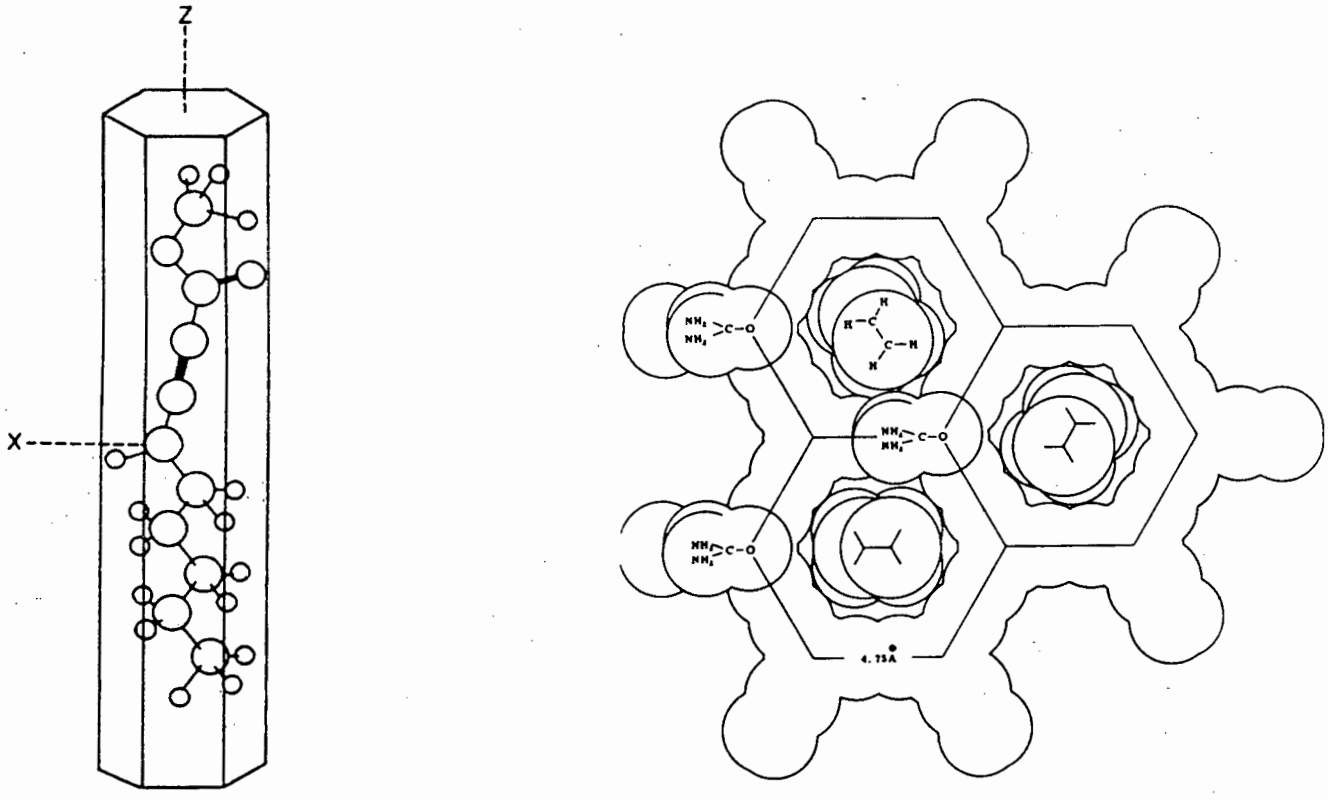

tubulato - clathrate

(a) (b)

fig 1.3 (a) A schematic diagram showing methyl - 2 - nonynoate inside the hexagonal crystalline matrix of urea[1.14].

(b) Cross - sectional view of a urea - n - paraffin inclusion compound[1.15].

allows the incorporation of straight chain aliphatics, but not hydrocarbons with branched chains or larger substituents(fig 1.3). Intercalates are systems where the guest is accommodated in interlayer spaces. The simplest compound to have a layered structure is one of the allotropes of carbon,viz, graphite (fig 1.4). The large interlayer separation of 335 pm and the consequent weak vàn der waals forces allows atoms and molecules to penetrate between the layers. A variety of species such as K, CrO_3, SbF_5, and $AlCl_3$ form graphite intercalates. These intercalates have found some use in synthetic organic chemistry[1-16]. Comparison of the reactivity of intercalated species with that of the bulk reagent reveals differences in reaction rates because of the necessity for the reacting molecule to diffuse into the graphite structure. The intercalates also display a selectivity depending on the size of the molecule because of the limitation imposed by the interlayer spacing.

It has been shown that some intercalated species have considerable translational mobility within the graphite lattice[1-18]. If blocking groups were present between the layers then this mobility would be reduced and the intercalated species would be contained in a void formed in the host lattice. Such blocking groups cannot be incorporated into the graphite structure but they are present in the Hofmann - type inclusion compounds, Fig 1.5. The structure is similar to that of graphite in that it consists of planar layers containing the metal atoms and the cyanide groups with the NH_3 groups protruding above and below these layers. The NH_3 groups then define the void wherein the guest molecule resides. Since the c dimension is essentially fixed the $Ni(NH_3)_2Ni(CN)_4$ host lattice displays a selectivity towards the length of the molecule, being able to accommodate benzene but not the longer toluene molecule. The basic Hofmann - type host lattice can be modified in two

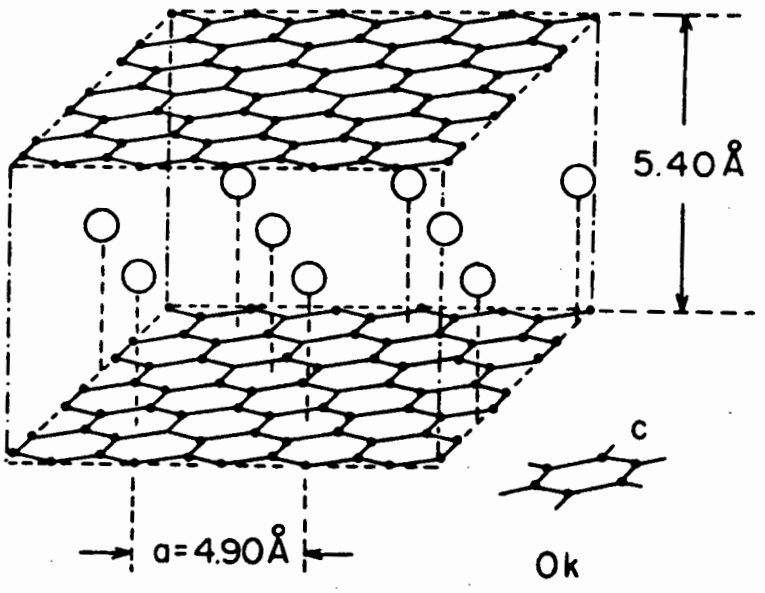

Intercalato - clathrate

fig 1.4 Potassium in graphite - C_8K. The planar distance of of graphite has increased from 3.35Å to 5.40Å to accomodate the K atoms (the covalent radius of K is 2.03Å)[1.17].

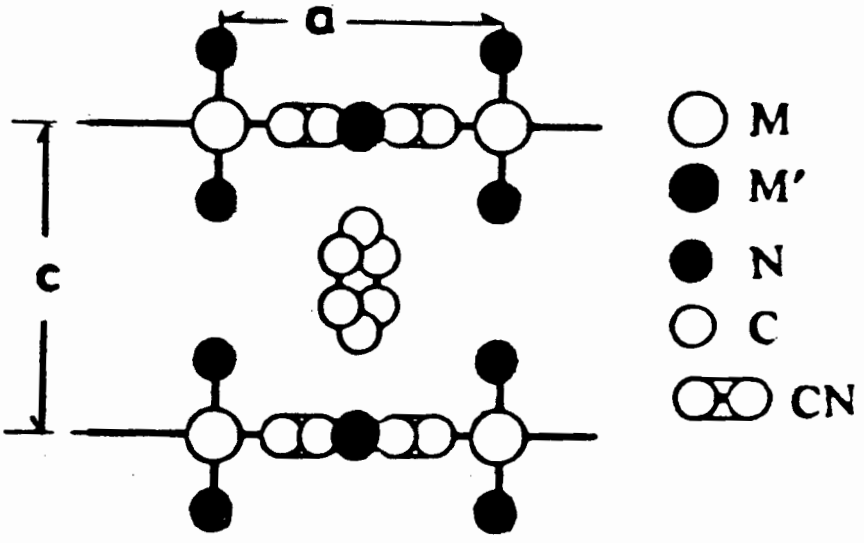

Fig 1.5 The structure of the Hofmann - type inclusion compound $Ni(NH_3)_2Ni(CN)_4.2C_6H_6$

ways[1·18]. The NH_3 groups can be replaced by molecules such as 1,2 - diaminoethane which bridge the interlayer spacing, and the square planar $Ni(CN)_4^{2-}$ group can be replaced by tetrahedral groups such as $Cd(CN)_4^{2-}$ and $Hg(CN)_4^{2-}$.

The cyclodextrins are cycloamyloses consisting of six(α), seven(β) or eight(γ) glucose units. The diameter of this cyclic oligosaccharide thus depends on the number of glucose units, and like the crown ethers and cryptands they show a selectivity for the guest whose dimensions best match the cavity dimensions[1·19]. They have a height of about 800 pm and the internal diameter ranges from about 500 pm in α - cyclodextrin to 800 pm in γ - cyclodextrin. Unlike the other clathrates discussed, the cyclodextrin inclusion compounds are stable in solution as well as in the solid state.

Some inclusion compounds are borderline cases which can be treated as complex/clathrate hybrids. One case is the coordinatoclathrates which have definite clathrate character, yet there is a certain degree of coordination between the host and guest.e.g 1,1-binaphthyl-2,2-dicarboxylic acid which forms coordinato clathrates with different -OH,-NH and -CH acidic guest compounds[1·20]. The iodoform clathrates studied in this project may also be regarded as coordinatoclathrates with secondary bonding between the iodine containing guest and the sulphur of the -NCS moiety of the host, $Ni(NCS)_2(4\text{-ViPy})_4$.

The great majority of the crown ether complexes with neutral guest molecules[1·21] are examples of clathratocomplexes.

The inclusion compounds can also be classified with regard to their topology. So we can distinguish between inclusion compounds (intramolecular host - guest aggregates) which operate via any sort of host cavity (cavitate), and addition compounds (adducts) which do not contain a host cavity

(extramolecular host - guest aggregates), such examples being the charge - transfer adduct between benzene - bromine[1·22] and trimethylamine - iodine[1·23].

Thus as the cavitates display increasing encapsulation their topology ranges from:

(1) The two-dimensional open-layer displayed by graphite, layered silicates[1·24] and transition metal disulphides[1·25];

(2) to the sandwich structures(the intercalate type);

(3) to the coronate type exhibited by the crown ether [18] crown - 6 (fig 1.2) and the podate ring structures[1·26];

(4) the one-dimensional open channel structures(the tubulates) such as the urea/n-paraffin inclusion compounds, and also those of α -cyclodextrin[1·19] and the choleic acids[1·27].

(5) and finally , the totally enclosed cage structures (the cryptates).

A class of compounds which exhibits a wide range of inclusion phenomena are the Werner clathrates, which are discussed below.

1.2 Werner clathrates.

Werner clathrates can be represented by the general formula MX_2A_4 where M stands for a divalent cation [Fe(II),Co(II),Ni(II),Cu(II),Zn(II),Cd(II),Mn(II),Hg(II), Cr(II)] and X denotes anionic ligands [NCS^-,NCO^-,CN^-,NO_3^- ,NO_2^-,Cl^-,Br^-,I^-] and A stands for electrically neutral

ligand substituted pyridines, α - arylalkylamines or isoquinoline. From a combination of these substituents many thousand complexes may be constructed. Great interest has been shown in Werner clathrates, not only for their ability to entrap a wide range of compounds, ranging e.g from the noble gases[1·28] to condensed aromatic hydrocarbons[1·29], but also for their selectivity for molecules as possible guests which differ in shape but not necessarily in physico-chemical properties. The clathrating properties of Werner clathrates were initially investigated with the intention of using them to separate petroleum fractions, and this has led to these complexes being employed in "clathrate chromatography", where for instance, the quantitative analysis of complex mixtures, especially isomers, can be determined accurately[1·30].

One of the possible reasons to explain the formation of clathrates by these kinds of inorganic complexes is the rotational freedom about the Ni-N coordination bonds. This supposedly allows adjustment of the substituted pyridines to accomodate the various guest molecules.

$Ni(NCS)_2(4\text{-}ViPy)_4$ has been the most thoroughly studied complex thus far, and represents typical properties for the MX_2A_4 group. The host can trap different guests in cavities of the channel, layer or cage type. The conformational freedom of the pyridine rings as they rotate around the corresponding Ni - N bonds is restricted to a certain extent. The dihedral angles between a pyridine ring and the N11-N21-N31-N41 molecular plane cannot assume any value e.g. coplanar arrangement of the four picolines is impossible because of steric hindrances at hydrogen atoms in α - position with respect to nitrogens. This leads to a number of preferred conformations which can be described in terms of four torsion angles,viz; N1 - Ni - N(x1) - C(x2)

where x=1-4 and the four carbon atoms of the rings lie on the same side of the Ni-N_{py} molecular plane (see fig 1.6). The host molecules can be located in general positions, in which case all four torsion angles are independent of one another, or else on a diad or centre of inversion, so that there are two pairs of symmetry related angles. When the host molecule is located on a diad , the axis is normally found to lie between the pyridine bases, although it is sometimes found to pass through a pair of trans pyridine bases, lying on a N_{py} - Ni - N_{py} line. The trans isothiocyanate groups have occasionally been found to lie along the diad[1,31].

The most common conformation of the host molecules is the propeller conformation where the four torsion angles have positive values (+ + + + conformation). The (+ + - -) conformation is found when a host molecule sits on a centre of symmetry. This situation is of higher potential energy than the previous one , and is subsequently less commonly observed. The (+ - + -) conformation has not been found in any studies.

1.2.1 Molecular packing

The non - clathrating phase of Werner clathrates has been termed the α - phase where the molecular packing of the host molecules is unable to form any suitable voids in the crystal lattice due to reasons such as steric or electronic interactions. Many of the 4 - methyl , 4 - ethyl and 4 - vinyl pyridine clathrates have been found to crystallise in the tetragonal $I4_1/a$ space - group, and this packing arrangement has become known as the β - phase. X - ray analysis of these structures reveals that the host molecules have two fold axial symmetry and that the void space between the host molecules is zeolitic in nature, i.e there is a three-dimensional set of cavities interconnected by means of

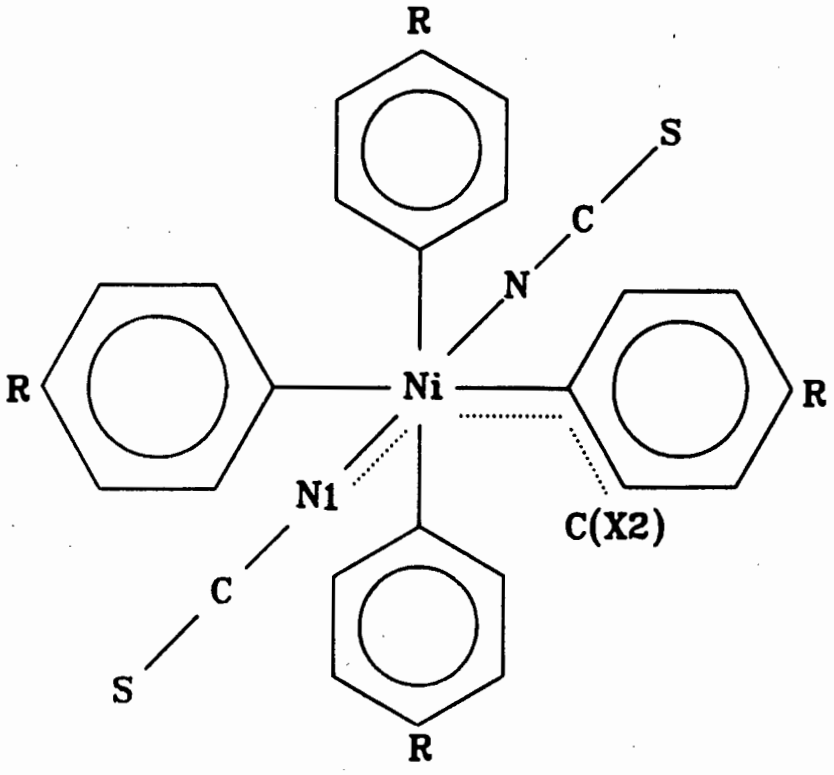

Fig 1.6 Host molecule of $Ni(NCS)_2(4\text{-subst.pyridine})_4$; altering the R group can have dramatic effects on the mode of clathration. The dotted line indicates the torsion angles used in describing the host molecule conformation.

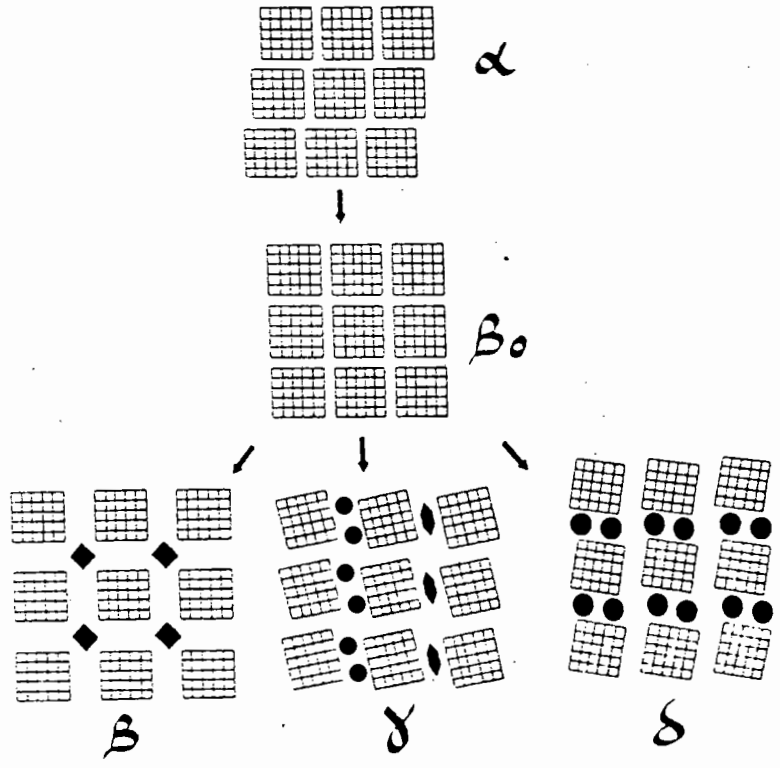

Fig 1.7 Illustration of a proposed route for the enclathration process of Werner clathrates. Taken from M.H Moore et al[1.34], adapted from a similar scheme first proposed by J. Lipkowski[1.35].

channels. The dimensions of the cavities and channels are defined not only by the packing mode of the host but strongly depend on the molecular shape of the guest[1·32] and its content in the clathrate. Lipkowski and Majchzak[1·33] report a significant β - lattice dilation when a guest is absorbed. The dilation reaches as much as 10% of total volume of the crystals. Other modifications are possible such as the δ - phase where pairs of guest molecules are located in channels[1·34]. In the γ- phase the clathrates have $P\bar{1}$ symmetry with two independent host molecules per unit cell[1·34]. The unit cell parameters are similar in length to those of the β - phase clathrates (ca. 17Å x 17Å x 27Å) and it was found that these structures could be transformed to the tetragonal I centred cell. This pseudo β - phase modification, although similar to the traditional $I4_1/a$ clathrates, exhibits a different mode of packing and thus represents another phase.

The enclathration process is believed to require the α - phase structure to change to a β_o - phase, in which the host molecules have realigned to form interstices. The guest molecules then act as a template so that as they enter these cavities the β_o - structure rearranges to form the various β,γ,δ phases etc. The latter phases arise from the different host:guest ratios and from the varied molecular shapes of the guest molecules. This is illustrated in fig 1.7. The β_o - phase is only an intermediate step in the enclathration process , the various phases only being stable in the presence of guest molecules so that the closest one can approximate a β_o - phase is a clathrate containing very small guest molecules. Lipkowski et al [1·32] have determined the structure of $Ni(NCS)_2$(4-methylpyridine)$_4$.2MeOH which must be very close to that of the β_o - phase for $Ni(NCS)_2$(4-methylpyridine)$_4$.

Many complexes have been synthesised which do not form clathrates e.g $Co(NCS)_2Py_4$, in the centrosymmetric conformation[1·36]. The pyridine rings of the adjacent molecules are parallel and molecular packing in the crystal leaves no space available for guest molecules. The replacement of the pyridines by the bulkier 4-methylpyridine ligands, still within the centrosymmetric conformation, affords similar but much less efficient packing[1·37]. The bulkier ligand allows for the inclusion of guest molecules.

TABLE 1.2 lists a number of clathrates in which $Ni(NCS)_2(4\text{-}MePy)_4$ acts as the host. These structures can be classified in terms of packing, so that structures having relatively high host/guest molar ratios e.g methylnaphthalene clathrates, are of layer like type. Such packing may be obtained with either an asymmetric or a centrosymmetric host. This transformation from a centrosymmetric to an asymmetric conformation of the host results in a dilation of the crystalline structure. In terms of molar volume ,when going from the 2-methylnaphthalene to the 1-methylnaphthalene clathrate of the same host/guest ratio and analogous type of packing, but having propeller shaped host molecules, the dilation is equal to 25 cm^3 per mole of the host.

The conformation of the isothiocyanate ligands also plays an important role in that they sub-divide the voids between the close-packed layers into cavities which are occupied by guest molecules.

1.2.2 Host - guest interaction in Werner clathrates

Studies on host - guest interactions in clathrates is important since this can supply information about reasons for clathration selectivity.

TABLE 1.2 Types of packing in clathrates of $Ni(NCS)_2(4\text{-MePy})_4$

Type of packing	guest	Host:Guest molar ratio	Crystal data (lengths in Å)
Channel			Tetragonal space- group
	benzene	1:1.50	$I4_1/a$ a=b=17.02 c=23.18
	p-xylene	1:0.88	$I4_1/a$ a=b=16.98 c=23.62
	4-MePy	1:1	$I4_1/a$ a=b=17.09 c=23.44
	p-dichlorobenzene	1:1	$I4_1/a$ a=b=17.30 c=22.68
	methanol	1:1.83	$I4_1/a$ a=b=16.99 c=22.29
Layer			Monoclinic and triclinic
	naphthalene	1:2	C_c a=16.27 b=16.46 c=31.93 β=89.3°
	1-Me-naphthalene	1:1.51	$P2_1/c$ a=11.53 b=11.89 c=32.85 β=94.3°
	2-Me-naphthalene	1:1.73	$P\bar{1}$ a=11.31 b=9.58 c=11.66 α=115.5° β=82.0 γ=108.7°
	o-xylene	1:2	$P2_1/c$ a=11.48 b=11.49 c=32.72 β=96.6°
	p-terphenyl	1:1	$P\bar{1}$ a=11.25 b=9.56 c=10.73 α=83.3° β=80.7 γ=63.2
	bromobenzene	1:2.02	P_{nma} a=16.51 b=15.74 c=15.64
Cage			Hexagonal
	m-Br-nitrobenzene	1:0.66	R3(?)
	o-Br-nitrobenzene	-	R (?) a=b=55.26 c=11.08

From I.R spectral data of a series of Werner clathrates, De Radzitzky and Hanotier[1·38] proposed the idea of charge - transfer interactions between host and guest molecules. However, up until now, none of the known crystalline structures of the clathrates shows features typical for charge - transfer molecular complexes,viz,parallelism of aromatic guest molecules and one of the aromatic ligands in the host molecule, nor some shortening of intermolecular distances with respect to the van der Waals radii. Instead the I.R spectra of the clathrates can be interpreted in terms of steric interactions only[1·39].
The term "charge - transfer" is usually given to interactions where there is weak electron pair donation. In order to cover these weak interactions, as well as stronger interactions of the same kind, the term "secondary bonding" has been introduced, which is discussed in Chapter 6. In the clathrates under study it has been found that secondary bonding does play an important role in the interaction of the iodine of the guest and the sulphur of the isothiocyanate moiety of the host.

Guarino et al[1·40] have proposed the following hypothesis: in a clathrate lattice formation one of the possible host conformational types is preferential depending on the geometry of the guest molecules enclathrated.

The propeller conformation of the host molecule is at a lower potential energy than the centrosymmetric one. However, the centrosymmetric conformation has been found in the clathrates of $Ni(NCS)_2(4\text{-}MePy)_4$ with 2-bromonaphthalene[1·37], p-terphenyl[1·41] and 2 - methylnaphthalene[1·37]. In these compounds the rise in potential energy due to the strain in the host molecule is more than compensated for by the decrease in energy due to the interaction with the guest, thus making them favourable.

The greater steric hindrance of the ligands around the metal centre in the centrosymmetric conformation also results in a lengthening of the M - N bond lengths (averaged within the molecule). Guarino[1,42] has correlated spectral differences in the visible region with the influence of non - bonded interaction on the coordination sphere at the central metal atom for the $Ni(NCS)_2(4\text{-}MePy)_4$ host. The longest M - N coordination bonds should correspond to the lowest frequency of the $^3A_{2g} \dashrightarrow {}^3T_{1g}$ band in the Ni(II) - complex d-d transitions, and this is observed. This is discussed further in Chapter 4.

Chapter 1 References

1.1 P.Cartraud, A.Cointot and A.Renaud, J. Chem. Soc., Faraday Trans. 1, 77, 1561 (1981)

1.2 J.L Flippen, J.Karle and I.L Karle, J. Am. Chem., 92, 3749 (1970)

1.3 J.L Flippen and J.Karle, J. Phys. Chem., 75, 3566 (1971)

1.4 D.D MacNicol and F.B Wilson, Chem. Comm., 786 (1971)

1.5 H.M Powell, J. Chem. Soc., 61 (1948)

1.6 M.Faraday, Quart. J. Sci., 15, 71 (1823)

1.7 C.Schafhautl, J. Prakt. Chem., 21, 129 (1841)

1.8 K.A Hoffmann and F.Kuspert, Z. Anorg. Allg. Chem., 15, 204 (1897)

1.9 E.Weber and H.P Josel, J. of Incl. Phenom., 1, 79 (1983)

1.10 C.J Pedersen, J. Am. Chem. Soc., 89, 2495 (1967)

1.11 J-M Lehn, B.Dietrich and J.P Sauvage, Tetrahedron Lett. , 2885 (1969)

1.12 R.M Kellog, Top. Curr. Chem., 11, 101 (1982)

1.13 W.Saenger, Umschau, 74, 635 (1974)

1.14 G.B Birell, A.A Lai and O.H Griffith, J. Chem. Phys., 54, 1630 (1971)

1.15 J.E.D Davies, J. Chem. Educ., 54, 536 (1977)

1.16 H.B Kagan, Chem. Technol., 510 (1976)

1.17 J.M Lalancette, G. Rollin and P. Dumas, Can J. Chem., 50, 3058 (1972)

1.18 T. Iwamoto, Isr. J. Chem., 18, 240 (1979)

1.19 W. Saenger, Angew. Chem., Int. Ed. Engl., 19, 344 (1980)

1.20 E.Weber and M.Czugler, Sec. int. symp. on clath. comp. and incl. phenom, Parma 1982

1.21 F.Vogtle,H.Sieger and W.M Muller, Top. Curr. Chem., 98, 107 (1981)

1.22 Hassel and Stromme, Acta Chem. Scand., 12, 1146 (1958)

1.23 Hassel, Mol. Phys., 1, 241 (1958)

1.24 J.M Thomas, J.M Adams, S.H Graham and D.T Tennekoon, in 'Solid state chemistry of energy conversion and storage , Advances in Chemistry series 163, Am. Chem. Soc, 1977 p. 298, Edited by J.B Goodenough and M.S Whittingham.

1.25 B.C Tofield, R.M Dell and J. Jensen, Nature, 276, 217 (1978)

1.26 J.W.H.M Uiterwyk et al, J. Chem. Soc. Chem. Comm.,200 (1982)

1.27 E. Giglio, J. Mol. Struct., 75, 39 (1981)

1.28 S.A Allison and R.M Barrer, J. Chem. Soc.,A ,1717 (1969)

1.29 W.D Schaeffer,W.S Dorsey,D.A Skinner and C.G Christian, J. Amer. Chem. Soc., 79, 5870 (1957)

1.30 W.Kemula and D.Sybilska, Nature, 185, 237 (1960)

1.31 L.R Nassimbeni and L.L Lavelle, unpublished results

1.32 J.Lipkowski,K.Suwinska,G.D.Andreetti and K.Stadnicka J. Mol. Struc, 75, 101 (1981)

1.33 J.Lipkowski and S.Majchzak.,Roczniki Chem., 49, 1655 (1975)

1.34 M.H Moore,L.R Nassimbeni and M.L Niven, J. Chem. Soc. Dalton Trans. ,2125 (1987)

1.35 J. Lipkowski, in `Inclusion Compounds`, Eds. J.L Atwood , J.E.D Davies and D.D MacNicol, Academic Press, London 1984, vol. 1, ch. 3.

1.36 H.von Hartl and T.Brudgam, Acta Crystallogr., B36 162 (1980)

1.37 J.Lipkowski,P Sagarabotti and G.D Andreetti, Acta Crystallogr., B36, 51 (1980)

1.38 P.De Radzitzky and J.Hanotier, Ind. Eng. Chem. Process design and develop., 1,10 (1962)

1.39 B.Moszynska,J.Lipkowski and A.Janowski, J. Mol. Struc. ,19, 347 (1973)

1.40 A.Guarino,G.Occhiucci,E.Possagno and R.Bassanelli, Trans. Faraday Soc., 172, 1848 (1976)

1.41 G.D Andreetti,L.Cavalca and P.Sagarabotti,
Gazz. Chim. Ital, 100, 697 (1970)

1.42 A.Guarino,G.Occhiucci,E.Possagno and R.Bassanelli,
Spectrochim. Acta, 33A, 199 (1977)

CHAPTER 2

General experimental procedure

2.1 Introduction

This chapter describes the conditions for the crystal growth of the Werner clathrates under study. Density measurements were the first step in elucidating the nature of the clathrates - this gave a good idea of the host:guest ratio. Preliminary X - ray photography of single crystals proved difficult due to the unstable nature of these crystals, although oscillation and Weissenberg photography was successful for the carbon tetrachloride and $Ni(NCS)_2(4\text{-}ViPy)_4.CHI_3$ clathrates.
TABLE 2.1 lists the structures under investigation.

2.2 Experimental

2.2.1 Preparation of $Ni(NCS)_2(4\text{-}ViPy)_4$

The host complex was prepared by the method of Schaeffer et al[2,1] as follows: Nickel isothiocyanate was prepared by dissolving 12g (.05 mol) nickel chloride in 70ml of ethanol, and then adding 9.7g (.10 mol) of KSCN. This solution was filtered to remove the KBr which forms, and then a 10% molar excess of the substituted pyridine was slowly added, in this case 24ml (.22 mol) of 4-vinylpyridine. The solution was stirred for half an hour at room temperature during which time the host forms as a blue precipitate. This was then filtered, washed with water, and vacuum dried for 24 hours.

2.2.2 Formation of $Ni(NCS)_2(4\text{-}ViPy)_4.2CH_2Cl_2$

TABLE 2.1 Structures under investigation, with the code names that refer to them.

STRUCTURE No.	COMPOSITION*	CODE NAME
I	$Ni(NCS)_2(4\text{-}ViPy)_4.2CH_2Cl_2$	VIDIC
II	$Ni(NCS)_2(4\text{-}ViPy)_4.2CCl_4$	VITET
III	$Ni(NCS)_2(4\text{-}ViPy)_4.1.8CH_2I_2$	DIODE
IV	$Ni(NCS)_2(4\text{-}ViPy)_4.CHI_3$	VICTIO
V	$[Ni(NCS)_2(4\text{-}ViPy)_4].$ $[Ni(NCS)_2(4\text{-}ViPy)_3(thf)].2CHI_3$	VICTRI

* 4-ViPy = 4-vinylpyridine

and

thf = tetrahydrofuran

A concentrated solution of the host in dichloromethane was allowed to evaporate very slowly (two to three days) which resulted in dark blue tabular crystals

2.2.3 Formation of $Ni(NCS)_2(4\text{-}ViPy)_4.2CCl_4$

2 ml of carbon tetrachloride was layered with 0.5 ml of a concentrated solution of the host in tetrahydrofuran(0.4 M). Small crystals could be seen after 2 - 3 hours and the diffusion was allowed to continue for 24 hours by which time dark blue tabular crystals had formed.

2.2.4 Formation of $Ni(NCS)_2(4\text{-}ViPy)_4.1.8CH_2I_2$

0.4 ml of CH_2I_2 (5 mmol) was dissolved in 5 ml of ethanol. 0.4g of the host (0.7 mmol) was added, the solution was heated slightly (approximately 35 °C) and the clear solution was filtered and allowed to stand for 3 - 4 hours during which time blue octahedral crystals formed. Blue needles of the α-phase also crystallised from this solution but were easily separated from the clathrate.

2.2.5 Formation of $Ni(NCS)_2(4\text{-}ViPy)_4.CHI_3$

0.6g (1 mmol) of the host was heated in 5 ml of ethanol. 0.79g (2 mmol) of CHI_3 was added to this hot solution. The solution was filtered hot and allowed to cool down over a 24 hour period, during which time yellow rectangular crystals formed.

2.2.6 Formation of $[Ni(NCS)_2(4\text{-}ViPy)_4].$
$[Ni(NCS)_2(4\text{-}ViPy)_3)(thf)].2CHI_3$

These crystals were grown in the same manner as above , except that 1 mmol of the host was dissolved in a warm mixture of 3 ml ethanol and 2 ml thf. To this warm solution

was added 2 mmol CHI_3. The solution was heated under reflux for 10 minutes, filtered and allowed to cool down over 24 hours.

2.3 Density measurements

This is by far the most accurate technique for obtaining the host:guest ratio. The flotation method was used to measure the density of these clathrates. The crystal is immersed in a liquid and a denser or less dense liquid miscible with the first is added until the crystal neither rises nor sinks in the solution. The density of the immersion liquid was then determined using an Anton Paar DMA 35 density meter.

For the carbon tetrachloride and the dichloromethane clathrates, these crystals were immersed in a saturated potassium iodide solution (1.63 g/ml) and then water was added until the crystals were suspended. For the denser iodine containing clathrates with CHI_3 and CH_2I_2 a 1.98 g/ml aqueous $ZnCl_2$ solution was used. Since compounds III, IV and V contain iodine their densities are substantially greater than that of the α-phase, which makes the determination of their host:guest ratios more accurate than when the density of the clathrate is close to that of the α-phase.

From a knowledge of the cell dimensions and the number of molecules per unit cell, Z , the experimental host:guest ratio can be calculated;

$$d = \frac{(M_{rH} + nM_{rG}) \times Z}{N_A \times V \times 10^{-24}}$$

where d = measured density of the crystal
M_{rH} = molecular weight of the host
M_{rG} = molecular weight of the guest
N_A = Avogadro's number
V = volume of the unit cell ($Å^3$)

Z = number of molecules per unit cell
n = guest:host ratio

Although this method gives accurate results errors can arise due to air bubbles clinging to the crystal. Each density measurement was repeated 3 times and the mean value was taken.

2.4 Solid state U.V spectroscopy

The reflectance spectrum of the α - phase and of each clathrate was recorded on a Beckman DK - A spectrophotometer set up for reflectance measurements. The measurements were taken as fast as possible to avoid excessive loss of guest. The crystals were crushed onto a standard silica micro - slide and the spectra were recorded between 500 - 1500 nm. These results are used to correlate host - guest interactions with the host conformation (Chapter 4).

2.5 Preliminary X - ray analysis

As mentioned earlier X - ray photography of the clathrates proved difficult due to their volatile nature. The carbon tetrachloride crystals were successfully photographed by mounting a single crystal on a glass fiber and then covering the crystal in a film of glue.The $Ni(NCS)_2(4 - ViPy)_4.CHI_3$ clathrate was air stable enough to obtain preliminary cell constants and the space - group determination.

2.6 Diffractometer data collection

The data collections for STRUCTURES I,II,IV and V were carried out at 20 °C, whereas the data collection for STRUCTURE III employed the Model XR - 85 - 1
AIR - JET™ crystal cooler and was performed at -40 °C. Small crystals of each clathrate were mounted in Lindemann

tubes which contained mother liquor. This ensured that the crystals were always in contact with the solution or its vapour, and thus prevented their deterioration in air. Accurate cell parameters were obtained by least - squares analysis of twenty five reflections measured in the range $16° < \theta < 17°$ on a Nonius CAD 4 diffractometer with graphite monochromated MoKα radiation ($\lambda = 0.7107$ Å). During the intensity data collection for each structure three reference reflections were periodically monitored to check crystal stability. The intensity data were collected in the $\underline{w} - 2\theta$ scan mode with a final acceptance limit of 20σ at 20°/min in $\underline{w}$ and a maximum recording time of 40s.

All data were corrected by a Lorentz polarisation factor and an absorption correction was applied to STRUCTURES III,IV and V. The dichloromethane and carbon tetrachloride clathrates had deteriorated too much by the end of the data collection for an absorption correction to be applied.

Crystal data and experimental details are listed in TABLES 2.2 and 2.3 .

2.7 Thermal analysis[2·2]

All thermograms were carried out on a Stanton - Redcroft thermal analyser (model STA 780) operating at a heating rate of 10 °C/min. STRUCTURES I to III and the chloroform clathrate were started at 40 °C and went up to 400 °C. STRUCTURES IV and V and pure iodoform were started at 40 °C and went up to 800 °C. During each run nitrogen was passed through the cell at a rate of 60ml/min.
The reference material used in each case was inert alumina (Al_2O_3). In the sample holder assembly each platinum crucible sits directly on top of its thermocouple; thus only the furnace temperature can be measured directly. The lag between this and the sample temperature was obtained by

TABLE 2.2 Crystal and experimental and refinement parameters for the structures

CRYSTAL DATA		
COMPOUND	I	II
MOLECULAR FORMULA	$C_{32}H_{32}N_6NiS_2Cl_4$	$C_{32}H_{28}N_6NiS_2Cl_8$
Mr/g.mol^{-1}	765.24	902.31
SPACE GROUP	$P2_1/n$	C2/c
a/Å	10.628(4)	10.112(3)
b/Å	20.30(2)	20.226(2)
c/Å	18.033(6)	20.604(6)
β/°	94.57(3)	98.25(3)
V/Å^3	3878.2	4170.5
Z	4	4
HOST:GUEST RATIO	1 : 2	1 : 2
Dm /g.cm^{-3}	1.29	1.37
Dc /g.cm^{-3}	1.29	1.40
μ (MoKα) /cm^{-1}	8.51	7.91
F (0 0 0)	1528	1832
DATA COLLECTION		
CRYSTAL DIMENSIONS /mm	.27 x .31 x .26	.25x.27x.35
TEMPERATURE /(°C)	20	20
SCAN MODE	$\underline{w}$-2Θ	$\underline{w}$-2Θ
SCAN WIDTH, $\underline{w}$/(°)	(.95 + .35tanΘ)	(.89 + .35tanΘ)
APERTURE WIDTH /mm	(1.15 + 1.05tanΘ)	(1.16 + 1.05tanΘ)
MAX. RECORDING TIME (s)	40	40
TOTAL NUMBER OF UNIQUE REFLECTIONS	1541	2591

TOTAL NUMBER OF RELECTIONS WITH Irel > 2Θ Irel	1050	1470
CRYSTAL STABILITY (%)	71.1	48.1[a]
MIN. CORRECTION FACTOR	-	1.0007
MAX. CORRECTION FACTOR	-	1.3877
AVG. CORRECTION FACTOR	-	1.1525
2Θ RANGE / (°)	2 - 50	2 - 50
FINAL REFINEMENT		
NUMBER OF VARIABLES	191	150
$R = \Sigma\|\|F_o\| - \|F_c\|\| / \Sigma\|F_o\|$	0.122	0.101
$R_w = \Sigma w^{\frac{1}{2}}\|\|F_o\| - \|F_c\|\|/\Sigma w^{\frac{1}{2}}\|F_o\|$	0.122	0.117
WEIGHTING SCHEME w	UNITY	$(\sigma^2 F)^{-1}$

[a] DECAY CORRECTION APPLIED

TABLE 2.3 Crystal data and experimental and refinement parameters for the structures

CRYSTAL DATA			
COMPOUND	III	IV	V
MOLEC. FORMULA	$C_{31.8}H_{31.6}N_6NiS_2I_{3.6}$	$C_{31}H_{29}N_6NiS_2I_3$	$C_{59}H_{59}N_{11}ONi_2S_4I_6$
Mr/g.mol^{-1}	1077.49	988.41	1944.06
SPACE GROUP	$I4_1/a$	Pbca	$P2_1/c$
a/Å	16.880(6)	15.969(4)	15.825(2)
b/Å	16.880(9)	25.417(5)	24.702(9)
c/Å	27.155(8)	19.074(6)	19.041(6)
β/ °	90	90	96.58(7)
V/Å^3	7739.2	7741.8	7394.3
Z	8	8	4
HOST:GUEST RATIO	1 : 1.8	1 : 1	1 : 2
Dm /g.cm^{-3}	1.78	1.72	1.80
Dc /g.cm^{-3}	1.78	1.70	1.75
μ (MoKα) /cm^{-1}	13.25	28.37	29.70
F (0 0 0)	4208	4144	3744
DATA COLLECTION			
CRYSTAL DIMEN./mm	.30 x .28 x .29	.25x.28x.30	.43x.45x.50
TEMPERATURE /(°C)	-40	20	20
SCAN MODE	w-2θ	w-2θ	w-2θ
SCAN WIDTH w/(°)	(.95 + .35tanθ)	(1 + .35tanθ)	(.9 + .35tanθ)
APERTURE WIDTH /mm	(1.12 + 1.05tanθ)	(1.2 + 1.05tanθ)	(1.2+1.05tanθ)
MAX. RECORDING TIME(s)	40	40	40
TOTAL NUMBER OF UNIQUE REFLECTIONS	1510	4192	4689

TOTAL NUMBER OF REFLECTIONS WITH Irel› 2Θ Irel	1193	1835	2426
CRYSTAL STABILITY /(%)	20.1[a,b]	25.7[a,b]	6.8[b]
MIN. CORRECTION FACTOR	0.8219	0.9362	0.7234
MAX. CORRECTION FACTOR	0.9995	0.9995	1.000
AVG. CORRECTION FACTOR	0.8963	0.9785	0.8719
2Θ RANGE / (°)	2 - 40	2 - 50	2 - 40
FINAL REFINEMENT			
NUMBER OF VARIABLES	137	204	436
$R = \Sigma\|\|F_o\| - \|F_c\|\| / \Sigma\|F_o\|$	0.219	0.068	0.084
$R = \Sigma w^{\frac{1}{2}}\|\|F_o\| - \|F_c\|\|/\Sigma w^{\frac{1}{2}}\|F_o\|$	0.219	0.068	0.089
WEIGHTING SCHEME W	UNITY	UNITY	$(\sigma^2 F)^{-1}$

[a] DECAY CORRECTION APPLIED
[b] ABSORPTION CORRECTION APPLIED

running a series of standard samples and plotting the furnace temperature required for melting ($T_{furnace}$) versus the known melting point (T_{melt}). Hence the sample temperature (T_s=T_{melt}) was calibrated against the furnace temperature. All temperatures quoted are sample temperatures that have been obtained from this calibration curve.

A study of the thermochemistry of these compounds gives information about their physicochemical nature. Thermal analyses were carried out in order to:

(a) Confirm the stoichiometry of the clathrates.

(b) To observe the temperature at which the guest molecules are released and

(c) to study the breakdown of the host complex.

2.8 Computer packages used for structure solving and their description

All structures were solved by the heavy - atom method and subsequent Fourier syntheses, and least - squares refinement. SHELX 76[2·3] was used for STRUCTURES I to IV. The larger number of parameters in the solution of STRUCTURE V required the use of SHELX 400.
SHELX 86 was also used in the solution of the patterson maps for the iodine containing structures.

The plotting of host molecule conformations and packing diagrams was performed using PLUTO[2·4]. ALCHEMY[2·5], a molecular modelling program system, was used to illustrate the cavities in the different clathrates.

EENY[2,6] was used to map out the cavities in the crystal lattice. A hydrogen atom is placed in the lattice as a probe and systematically moved around the unit cell. The potential energy is calculated at each point and in this way a potential energy profile of the clathrate was obtained.

OPEC[2,7] was also used to map out the cavities by assigning each atom a suitable van der Waals radius and calculating where regions of empty space exist in the clathrate. Both EENY and OPEC are discussed further in Chapter 4.

Chapter 2 References

2.1 W.D Schaeffer, W.S Dorsey, D.A Skinner and J. Christian, J Am. Chem. Soc., 79, 5870 (1957)

2.2 M.E Brown, 'Getting started in thermal analysis',1985, Rhodes University, South Africa

2.3 G.M Sheldrick, SHEL - 76 program system in 'Computing in Crystallography', edited by H.Schenk, R.Olthof-Hazekamp, H.van Koningsveld, G.C Bassi; Delft Univ. Press,1978,34

2.4 W.D.S Motherwell; PLUTO program for plotting molecular and crystal structures, Cambridge Univ., England, unpublished.

2.5 ALCHEMY, Tripos Associates Inc., 6548 Clayton Road, St. Louis, Missouri, 63117

2.6 W.D.S Motherwell; 'EENY potential energy program' Univ. Chem. Laboraties, Cambridge,1974

2.7 A. Gavezzotti; 'OPEC organic packing energy calculations program', J. Am. Chem. Soc., 105, No16, 5220 (1983)

CHAPTER 3

Structure solutions

3.1 Introduction

This chapter describes how each structure was solved and lists tables of fractional atomic coordinates as well as isotropic or anisotropic temperature factors for each one.

The heavy atoms i.e Ni, I, S and Cl were treated anisotropically, except for STRUCTURE I, where the smaller number of reflections precluded the chlorine atoms from being treated anisotropically. The carbon, hydrogen, nitrogen and oxygen atoms were treated isotropically.
The hydrogen atoms were fixed at 1.00 Å from their parent carbon atoms and were assigned a common temperature factor.

Bond lengths involving several of the vinyl carbon atoms are outside the usually quoted limits. The isotropic temperature factors of these atoms are consistently higher than those in the aromatic rings, which indicates some disorder in these vinyl groups.

All the crystals studied decayed to varying extents during their data collections. In compounds II to V this decay was isotropic and so a decay correction could be applied, whereas in compound I this decay was anisotropic and therefore no decay correction was applied.

3.1.1 STRUCTURE 1 (VIDIC) $Ni(NCS)_2(4\text{-}ViPy)_4.2CH_2Cl_2$

($P2_1/n$ Z=4 a=10.628Å b=20.300Å c= 18.033Å β=94.57°)

After approximately 12 hours on the diffractometer, 1800 reflections out of the total 4000 reflections had been collected, when there was a sharp drop in intensity of the three reference reflections used to check crystal stability. The data collection was repeated and again there was this sharp fall off in intensity. In both cases the crystal was still surrounded in mother liquor and so it appeared as if the X - ray interaction with the crystal was causing its decay. The first set of reflections was considered the best, and the reflections up until this decrease in intensity were used for the structure solution.

From the conditions on h k l, shown below, the space - group was determined to be $P2_1/n$.

h k l :	no conditions
h 0 l :	h + l even
0 k 0 :	k even

The peaks expected in the three - dimensional patterson map are shown in the grid below:

	x,y,z	$-x+\frac{1}{2},y+\frac{1}{2},-z+\frac{1}{2}$	-x,-y,-z	$x+\frac{1}{2},-y+\frac{1}{2},z+\frac{1}{2}$
x,y,z	0	$-2x+\frac{1}{2},\frac{1}{2},-2z+\frac{1}{2}$	-2x,-2y,-2z	$\frac{1}{2},-2y+\frac{1}{2},\frac{1}{2}$
$-x+\frac{1}{2},y+\frac{1}{2},-z+\frac{1}{2}$	$2x+\frac{1}{2},\frac{1}{2},2z+\frac{1}{2}$	0	$\frac{1}{2},-2y+\frac{1}{2},\frac{1}{2}$	2x,-2y,2z
-x,-y,-z	2x,2y,2z	$\frac{1}{2},2y+\frac{1}{2},\frac{1}{2}$	0	$2x+\frac{1}{2},\frac{1}{2},2z+\frac{1}{2}$
$x+\frac{1}{2},-y+\frac{1}{2},z+\frac{1}{2}$	$\frac{1}{2},2y+\frac{1}{2},\frac{1}{2}$	-2x,2y,-2z	$-2x+\frac{1}{2},\frac{1}{2},-2z+\frac{1}{2}$	0

$P2_1/n$

Multiplicity	Vector	Corresponding Ni-Ni peak from patterson map
4	0,0,0	0,0,0
2	$\frac{1}{2},2y+\frac{1}{2},\frac{1}{2}$	$\frac{1}{2}$,0.967,$\frac{1}{2}$
2	$\frac{1}{2},-2y+\frac{1}{2},\frac{1}{2}$	$\frac{1}{2}$,0.033,$\frac{1}{2}$
2	$2x+\frac{1}{2},\frac{1}{2},2z+\frac{1}{2}$	0.565,$\frac{1}{2}$,0.822
2	$-2x+\frac{1}{2},\frac{1}{2},-2z+\frac{1}{2}$	0.435,$\frac{1}{2}$,0.178
1	2x,2y,2z	.065,.467,.322
1	-2x,-2y,-2z	-.065,-.467,-.322
1	2x,-2y,2z	.065,-.467,.322
1	-2x,2y,-2z	-.065,.467,-.322

The Patterson peaks were scaled such that $\Sigma Z_3^2 = 999$ at the origin of the Patterson map. On this scale, a single Ni - Ni vector has a calculated peak height of 199 and a double Ni - Ni vector of height 398. Analysis of the three - dimensional Patterson map showed a peak of height 299 at $\frac{1}{2}, 0.967, \frac{1}{2}$ which was identified as the satellite peak at $\frac{1}{2}, 2y+\frac{1}{2}, \frac{1}{2}$ yielding $2y=0.467$. The peak of height 283 at $0.565, \frac{1}{2}, 0.822$ was identified as the satellite peak at $2x+\frac{1}{2}, \frac{1}{2}, 2z+\frac{1}{2}$ yielding $2x=0.065$ and $2z=0.322$. The inversion peak corresponding to $2x, 2y, 2z$ was found at $0.065, 0.467, 0.322$ with a height of 189. We also found all the symmetry related peaks shown in the grid above. The nickel was therefore located at the general position $x=0.032$ $y=0.233$ $z=0.161$, which was used for the calculation of structure factors, from which the first difference electron density map was obtained. After three least squares refinements two pyridine rings had been located and the residual R value stood at 0.35. Four large peaks corresponding to two independent CH_2Cl_2 guest molecules were located. Inclusion of these peaks into the model brought the R value down to 0.21. Subsequent difference fourier maps yielded the remainder of the host molecule. After addition of the hydrogens the final R value stood at 0.122. Nowhere was the electron density greater than 0.5 $e^-/Å^3$. The high temperature factors of the chlorine atoms is an indication of the high degree of thermal motion of the guest molecules. TABLE 3.1 lists the fractional atomic coordinates and temperature factors for STRUCTURE 1.

3.1.2 STRUCTURE II (VITET) $Ni(NCS)_2(4\text{-}ViPy)_4.2CCl_4$

(C2/c Z=4 a=10.112Å b=20.226Å c=20.604Å β=98.25°)

Oscillation and Weissenberg photography revealed a monoclinic space - group with approximate cell dimensions;

TABLE 3.1 Fractional atomic coordinates (x 10**4) and Thermal Parameters (A**2 x 10**3) with e.s.d. s in parentheses for STRUCTURE I

Atom	x/a	y/b	z/c	Uiso/Uequiv(*)
Ni(1)	323(4)	2333(2)	1611(11)	104(10) *
S(1)	3995(9)	1017(5)	2309(10)	96(14) *
S(2)	-3079(10)	3830(5)	941(12)	165(15) *
N(1)	1940(22)	1755(12)	1795(25)	79(9)
N(2)	-1272(24)	2910(13)	1363(27)	93(10)
N(11)	1469(23)	3209(13)	1477(25)	85(9)
N(21)	394(25)	2172(18)	462(26)	77(13)
N(31)	-789(24)	1466(13)	1699(27)	85(10)
N(41)	286(33)	2507(17)	2789(26)	104(17)
C(1)	2778(30)	1451(16)	2038(33)	87(12)
C(2)	-2006(29)	3280(16)	1173(32)	82(11)
C(12)	2558(27)	3139(16)	1222(29)	80(11)
C(13)	3286(34)	3665(17)	1058(33)	116(15)
C(14)	2818(37)	4307(19)	1374(37)	117(15)
C(15)	1753(31)	4342(18)	1677(33)	98(13)
C(16)	1078(28)	3795(15)	1752(30)	80(11)
C(17)	3753(43)	4990(22)	1014(38)	161(21)
C(18)	3304(51)	5476(30)	1366(46)	220(29)
C(22)	54(30)	2705(19)	-82(32)	88(16)
C(23)	132(31)	2521(22)	-853(32)	97(17)
C(24)	531(39)	1951(26)	-1286(37)	102(19)
C(25)	762(38)	1571(25)	-635(37)	120(22)
C(26)	701(32)	1593(22)	124(35)	96(18)
C(27)	562(35)	1962(20)	-2130(40)	157(23)
C(28)	531(**)	1380(**)	-2501(**)	97(24)
C(32)	-1914(34)	1406(19)	1250(34)	113(15)
C(33)	-2661(37)	846(21)	1348(38)	130(17)
C(34)	-2368(37)	347(20)	1887(40)	115(15)
C(35)	-1212(35)	427(19)	2318(35)	120(15)
C(36)	-501(32)	966(17)	2160(33)	97(13)
C(37)	-3103(35)	-286(20)	2051(36)	123(16)
C(38)	-3891(43)	-405(22)	1522(41)	157(20)
C(42)	-827(28)	2611(14)	3209(31)	65(11)
C(43)	-762(45)	2718(22)	3990(31)	135(24)
C(44)	275(33)	2690(19)	4550(37)	75(13)
C(45)	1270(55)	2551(24)	4120(32)	161(30)
C(46)	1366(32)	2507(15)	3335(32)	86(13)
C(47)	67(52)	2930(26)	5218(49)	157(29)
C(48)	-629(39)	3200(21)	5417(41)	129(19)
C(0A)	6463(53)	471(25)	3940(47)	190(25)
Cl(1A)	7731(19)	1062(10)	4030(17)	192(11)
Cl(2A)	5370(21)	583(10)	4369(16)	202(12)
C(0B)	7338(37)	154(19)	9368(33)	187(23)
Cl(1B)	8760(21)	110(52)	8940(31)	201(20)
Cl(2B)	7440(19)	980(32)	8830(16)	171(26)

Anisotropic atoms have thermal parameters (A**2 x 10**3) of the form :

EXP(-2*PI**2(U11*H**2*(A*)**2+...+2*U12*H*K*(A*)*(B*)+...)

Atom	U11	U22	U33	U23	U13	U12
Ni(1)	69(3)	84(3)	158(30)	-17(8)	8(6)	11(2)
S(1)	112(7)	119(8)	57(38)	50(13)	1(11)	33(6)
S(2)	112(8)	109(9)	268(44)	46(14)	-32(13)	21(6)

a= 10.9Å b= 19.98Å c=19.07Å and β= 96.78°.

From the reflection conditions on h k l,viz;

h k l: h + k = 2n
h 0 l: h,l = 2n
and 0 k 0: k = 2n

the space - group could of been either Cc (no.9) or C2/c (no.15). From the density measurement the number of host molecules per unit cell was determined to be four, and therefore the nickel atoms would have to fall on a special position in the centric space - group, which would coincide with a general position of the acentric space - group Cc. Therefore the expected patterson map for the Ni-Ni vectors would be identical for both space- groups, and could not be used to determine whether the structure was centric or not. A grid of the vectors expected in C2/c was drawn up in a similar manner to that used in STRUCTURE I. Analysis of the various satellite and inversion peaks was carried out as before. From the patterson map the Ni atom was found to lie on the 2 - fold axis at 0 0.307 0.25 (Wyckoff position e). The crystal structure is reported with respect to cell choice 1, unique axis b with the origin at $\bar{1}$. A difference fourier map was calculated with the Ni atom at site occupancy factor 0.5. As the host molecule was located it became evident that two trans 4 - vinylpyridine moieties were lying along the diad. Consequently the vinyl groups of these trans substituted pyridine rings were disordered around the diad and so the terminal carbon atoms of the vinyl groups were given a site occupancy factor of 0.5. The carbon tetrachloride guest molecules were easily located and refined, although the U_{equiv} values for the chlorine atoms were generally higher than for atoms in the host which indicates a fair degree of thermal motion in the guest molecules. A final R value of 0.101 was obtained. After the

final refinement nowhere was the electron density greater than 0.6 e-/Å^3.

As mentioned earlier, from the conditions on h k l and the Patterson map, there was ambiguity as to whether the correct space - group was C2/c or Cc. This uncertainty was resolved in the following manner[3·1]:

The Cc space - group is a subset of C2/c, the two - fold rotation and screw axes as well as the inversion centres being absent in Cc. Cc, however, retains the diagonal and axial glide planes present in C2/c. The structure was solved in Cc, and since the diad is absent in this space - group, the complete host molecule and the two carbon tetrachloride guest molecules related by the diad in C2/c, were required for the model, from which the structure factors were calculated. Atoms for one half of the host molecule at positions x,y,z have their equivalent positions, related by the diad, at $-x,y,\frac{1}{2}-z$ in C2/c.

Since for the structure solution in Cc there are almost twice as many parameters as the model in the centrosymmetric C2/c space - group, better agreement between the observed and calculated structure factors was obtained (reflected in a lower R value for the Cc solution). In C2/c the atom P at $x \pm \sigma x$, $y \pm \sigma y$, $z \pm \sigma z$ has its equivalent position in Cc, P', at $x' \pm \sigma x'$, $y' \pm \sigma y'$, $z' \pm \sigma z'$. The absolute difference in each positional parameter i.e $\triangle x = |x-x'|, \triangle y = |y-y'|, \triangle z = |z-z'|$, on going from C2/c to Cc, was then compared with the average standard deviation of that parameter i.e $(\sigma x + \sigma x')/2$, $(\sigma y + \sigma y')/2$ and $(\sigma z + \sigma z')/2$.
If the differences in x,y,z on going from C2/c to Cc for each atom is less than ten times the average standard deviation i.e if

$$\triangle x < 10(\sigma x + \sigma x')/2$$
$$\triangle y < 10(\sigma x + \sigma x')/2$$

and $\triangle z < 10(\sigma x + \sigma x')/2$

then it can be assumed, with a high degree of confidence, that C2/c is the correct space - group. Each host atom in Cc was compared in this manner with its equivalent atom in C2/c and these values are listed in APPENDIX A. The guest molecules were excluded from this analysis since the error in determining the positions of these atoms is generally larger than in the host molecule due to their greater thermal motion. Very few of the parameters were outside the limits described above and so the correct space - group was assumed to be C2/c. Unfortunately the structure solution in Cc did not refine as well as in C2/c and so many of the $\sigma x'$,$\sigma y'$ and $\sigma z'$ values are higher than the corresponding values in C2/c, but even if the analysis is performed with only the lower standard deviation values of the C2/c solution, the majority of the $\triangle$ values are less than ten times their corresponding $\bar{\sigma}$ values.

There was extensive correlation in the least - squares matrix for the Cc solution, whereas little correlation was observed for the C2/c solution, which also indicated that C2/c was the correct space - group.

Fractional atomic coordinates and thermal parameters for STRUCTURE II are given in TABLE 3.2

3.1.3 STRUCTURE III (DIODE) $Ni(NCS)_2(4\text{-}ViPy)_4.1.8CH_2I_2$

($I4_1/a$ Z=8 a=b=16.880Å c=27.150Å)

From the first data collection at 25 °C, the heaviest atom found from the patterson map was found to be lying on the diad, Wyckoff position e, at 0.50 0.25 0.540. This is the usual position for a Ni atom in the β - phase clathrates of

TABLE 3.2 Fractional atomic coordinates (x 10**4)
and Thermal Parameters (A**2 x 10**3)
with e.s.d. s in parentheses for STRUCTURE II

Atom	x/a	y/b	z/c	Uiso/Uequiv(*)
NI(1)	0(0)	3075(1)	2500(0)	66(1) *
N(21)	0(0)	4138(8)	2500(0)	78(5)
N(41)	0(0)	2037(8)	2500(0)	71(5)
N(11)	694(11)	3099(6)	1557(6)	73(3)
N(1)	1951(12)	3090(6)	2947(6)	77(3)
C(12)	1794(15)	3445(7)	1458(8)	79(4)
C(13)	2149(16)	3528(7)	871(8)	77(4)
C(14)	1449(15)	3247(7)	328(8)	80(4)
C(15)	315(17)	2864(8)	433(9)	91(5)
C(16)	23(15)	2795(7)	1056(8)	75(4)
C(17)	1786(22)	3324(11)	-342(11)	119(6)
C(18)	2732(25)	3678(12)	-509(13)	125(7)
C(22)	490(16)	4472(8)	3002(9)	89(5)
C(23)	507(16)	5161(8)	3062(9)	90(5)
C(24)	0(0)	5499(12)	2500(0)	91(7)
C(27)	0(0)	6281(18)	2500(0)	132(11)
C(28)	271(40)	6684(22)	2806(19)	104(12)
C(42)	1042(16)	1671(9)	2375(8)	89(5)
C(43)	1101(16)	1018(8)	2368(8)	89(5)
C(44)	0(0)	614(15)	2500(0)	110(8)
C(47)	0(0)	-108(18)	2500(0)	127(10)
C(48)	551(54)	-514(26)	2340(30)	106(19)
C(1)	2989(14)	3049(7)	3236(7)	75(4)
C(0)	2332(36)	800(17)	4600(18)	168(11)
CL(1)	1063(11)	268(5)	4202(5)	211(6) *
CL(2)	3693(12)	340(5)	4904(7)	218(6) *
CL(3)	2782(12)	1400(5)	4096(5)	203(6) *
CL(4)	1698(9)	1167(5)	5236(5)	189(5) *
S(1)	4473(5)	3018(4)	3649(3)	154(3) *

Anisotropic atoms have thermal parameters (A**2 x 10**3) of the form :

EXP(-2*PI**2(U11*H**2*(A*)**2+...+2*U12*H*K*(A*)*(B*)+...)

Atom	U11	U22	U33	U23	U13	U12
NI(1)	45(1)	57(1)	90(2)	0(0)	-9(1)	0(0)
CL(1)	214(10)	201(9)	193(10)	-45(7)	-59(8)	21(7)
CL(2)	174(8)	186(9)	273(13)	34(8)	-36(8)	42(7)
CL(3)	241(11)	176(9)	189(9)	36(7)	15(8)	24(8)
CL(4)	158(7)	220(10)	185(9)	-32(7)	13(6)	10(7)
S(1)	73(3)	223(8)	149(5)	28(5)	-42(3)	11(4)

$Ni(NCS)_2(4\text{-}ViPy)_4$ (the cell dimensions are also very similar).Since the iodine atoms of the guest were not revealed as the heaviest atoms in the patterson, although iodine has almost twice as many electrons as nickel, it appeared as if there was some disorder of the diiodomethane guest molecules. The measured density of 1.78 $g.cm^{-3}$ gave a host:guest ratio of 1 : 1.8 , which indicated that the guest molecules were located in the general positions , although not quite stoichiometrically.

The host molecule was located which resulted in a residual R value of 0.30, with still a lot of electron density in the region of the four - fold inversion centre,Wyckoff position b. The CH_2I_2 molecules appeared to be severely disordered around this centre and so it was decided to repeat the data collection at a lower temperature,using the AIR - JET low - temperature cooling device.

The reflections were collected at -20 °C, but there was no noticeable increase in intensities of the reflections compared to the corresponding ones at 25 °C. This structure solution still revealed disorder in the guest molecules, although there appeared to be fewer peaks in this region, but more concentrated regions of electron density. Although an R value of 0.12 was obtained by including fragments of iodine peaks into the structure solution, no sensible chemical model could be found from these peaks. It was decided to attempt yet a third data collection, this time at -40 °C. For each data collection the required equivalencies for tetragonal 4/m symmetry viz; $F(h\ k\ l) = F(\bar{h}\ \bar{k}\ l)$ $F(\bar{k}\ h\ l) = F(k\ \bar{h}\ l) = F(\bar{h}\ \bar{k}\ \bar{l}) = F(h\ k\ \bar{l}) = F(k\ \bar{h}\ \bar{l})$ $F(\bar{k}\ h\ \bar{l})$, were checked. The structure is reported with respect to the second origin choice at $\bar{1}$.

There appeared to be more stronger reflections at this lower temperature. The percentage of reflections with

Irel > 2σ Irel out of the total number of reflections was 66%, as opposed to 26% at -20 °C and 24% at 25 °C. This gave some indication that the iodines were less vibrant, although these values also depend on the crystal quality. The host molecule was found as before, and structure factors calculated. The ensuing difference electron density map was carefully scanned in the $\bar{4}$ region (0 0.25 0.375). Five reasonably strong peaks were located (5 $e^-/Å^3$ to 2 $e^-/Å^3$) in this region around which a tentative model could be proposed to explain this disorder problem. This is shown in Fig 3.1.

Peak I1 is located on the diad (Wyckoff position e), 2.7Å from I2, which is in a general position. This short distance would suggest that one iodine of the CH_2I_2 is disordered between I1 and I2. These two peaks are well defined in the electron density map which indicates a statistical disorder, rather than a thermal one were we would expect peaks I1 and I2 to be smeared out and to merge into one another.

The second iodine atom appears as peaks I3, I4 and I5 which do merge into one another and thus indicates either thermal or positional disorder of this iodine, even at -40 °C. The distances from I1 and I2 to I3, I4, and I5 are given below. The normal iodine to iodine distance in a molecule of diiodomethane is about 3.6Å.

I1 - I3	3.89Å	I2 - I3	3.79Å
I1 - I4	4.70Å	I2 - I4	3.59Å
I1 I5	3.87Å	I2 - I4	3.78Å

In fig 3.1(a) four diiodomethane molecules are shown around the $\bar{4}$ centre, with I2 in the general position and I3, I4 and I5 making up the other iodine. This iodine has a complex motion and appears to follow an "L - shaped" path, which may be a result of the shape of the cavity in which it finds

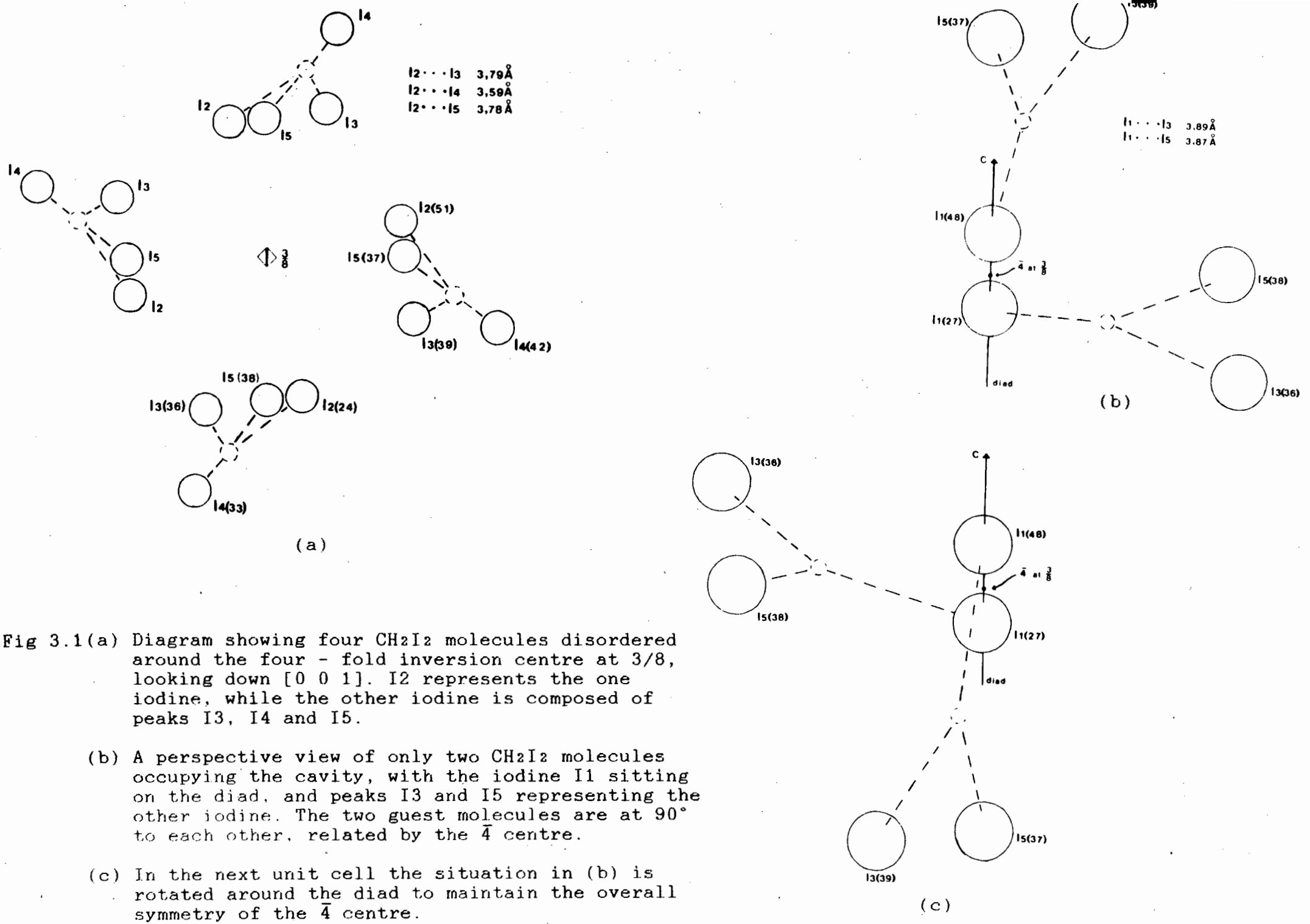

Fig 3.1(a) Diagram showing four CH_2I_2 molecules disordered around the four - fold inversion centre at 3/8, looking down [0 0 1]. I2 represents the one iodine, while the other iodine is composed of peaks I3, I4 and I5.

(b) A perspective view of only two CH_2I_2 molecules occupying the cavity, with the iodine I1 sitting on the diad, and peaks I3 and I5 representing the other iodine. The two guest molecules are at 90° to each other, related by the $\bar{4}$ centre.

(c) In the next unit cell the situation in (b) is rotated around the diad to maintain the overall symmetry of the $\bar{4}$ centre.

itself. This is explored further in Chapter 4. In the next unit cell, fig 3.1(b) ,I2 has now moved onto the diad, to become I1. Although the carbon atom of the guest was not located, the C-I bonds are represented as dashed lines. Only the two guest molecules related by the $\bar{4}$ centre at 90° to each other are possible if I1 sits on the diad. In order to maintain the overall symmetry of the four - fold inversion centre, in the next unit cell the situation in (b) is rotated around the diad, fig 3.1(c).

If cases (a), (b) and (c) occur equally then at the three $\bar{4}$ centres shown there is a total of 8 guest molecules i.e 32 guest molecules over the three unit cells, there being four such $\bar{4}$ centres per cell. This means a host : guest ratio of 1 : 1.33 (d = 1.63 $g.cm^{-3}$) since there are eight host molecules per unit cell.

However, the measured density is 1.78 $g.cm^{-3}$ i.e a host : guest ratio of 1.8, which suggests that the situation in fig3.1(a) predominates. From the study in Chapter 4, the volume of the cavity seems barely sufficient to accomodate four CH_2I_2 molecules, so that every now and then two of the guest molecules are "left out" to relieve the congestion, and the two remaining molecules rearrange to give the situation in fig 3.1 (b) and (c).

The disorder of the iodines is so severe that it made the assignment of site occupation factors difficult. These values were assigned by adding the electron density of these five peaks from the electron density map, and then the site occupation of each iodine fragment was taken as the electron density of the iodine peak/total electron density of the five peaks. The site occupation factor of I1 was taken as half of this value since it sits on the diad.

Inclusion of these five peaks into the structure solution yielded a final R value of 0.219. Although the iodines were treated anisotropically obviously this ellipsoidal model of their motion is an oversimplified one.

TABLE 3.3 lists fractional atomic coordinates and temperature factors for STRUCTURE III.

3.1.4 STRUCTURE IV (VICTIO) $Ni(NCS)_2(4\text{-}ViPy)_4.CHI_3$

(Pbca Z=8 a=15.969Å b=25.417Å c=19.074Å)

The oscillation photograph of a single crystal revealed m_x symmetry which indicated an orthorhombic space - group. Two mirrored axis 90° apart were also found in the Weissenberg photography.

From the Weissenberg photographs the reflection conditions on h k l were found to be;

0 k l	l = 2n
h 0 l	h = 2n
h k 0	k = 2n
h 0 0	h = 2n
0 k 0	k = 2n
0 0 l	l = 2n

which uniquely defines the space - group as Pcab.

However, it is customary to report the structures in the space - group Pbca, and so the reflection indices were transformed by applying the matrix shown below;

TABLE 3.3 Fractional atomic coordinates (x 10**4) and Thermal Parameters (A**2 x 10**3) with e.s.d. s in parentheses for STRUCTURE III

Atom	x/a	y/b	z/c	Uiso/Uequiv(*)
Ni(1)	5000(0)	2500(0)	5383(3)	74(3) *
N(1)	4054(26)	1721(24)	5346(15)	95(14)
C(1)	3398(29)	1607(28)	5376(17)	75(14)
S(1)	2447(12)	1318(11)	5284(7)	146(10) *
N(11)	5586(21)	1805(22)	4829(14)	75(12)
N(21)	5527(21)	1824(20)	5935(13)	65(10)
C(12)	5468(27)	1013(28)	4855(18)	79(15)
C(13)	5842(21)	553(23)	4433(14)	49(11)
C(14)	6284(23)	961(24)	4063(16)	58(12)
C(15)	6287(28)	1749(29)	4076(19)	84(15)
C(16)	5960(24)	2157(26)	4453(16)	65(13)
C(17)	6605(33)	441(33)	3605(20)	106(19)
C(18)	7049(27)	268(34)	3295(55)	130(39)
C(22)	6297(28)	1674(27)	5986(18)	76(14)
C(23)	6636(27)	1291(25)	6345(17)	68(14)
C(24)	6146(20)	888(19)	6704(13)	35(10)
C(25)	5416(24)	1047(22)	6671(15)	55(12)
C(26)	5024(28)	1437(25)	6270(17)	73(14)
C(27)	6599(24)	510(23)	7132(16)	59(12)
C(28)	6169(36)	267(34)	7515(28)	131(23)
I(1)	0(0)	2500(0)	5191(6)	207(8) *
I(2)	411(6)	1034(8)	4888(4)	150(6) *
I(3)	-635(8)	884(10)	6127(5)	131(7) *
I(4)	-751(9)	6(15)	5790(7)	154(11) *
I(5)	33(33)	987(17)	6269(12)	203(25) *

Anisotropic atoms have thermal parameters (A**2 x 10**3) of the form :

EXP(-2*PI**2(U11*H**2*(A*)**2+...+2*U12*H*K*(A*)*(B*)+...)

Atom	U11	U22	U33	U23	U13	U12
Ni(1)	81(4)	81(4)	61(7)	0(0)	0(0)	0(0)
S(1)	169(18)	117(14)	153(19)	4(13)	-57(14)	-53(13)
I(1)	264(15)	264(15)	93(14)	0(0)	0(0)	0(0)
I(2)	92(7)	235(13)	125(10)	87(9)	-7(6)	-37(8)
I(3)	123(10)	173(14)	96(10)	-16(9)	-13(8)	-25(9)
I(4)	62(10)	261(25)	139(18)	140(18)	0(10)	60(13)
I(5)	404(66)	98(20)	107(28)	24(18)	52(35)	104(34)

$$\begin{pmatrix} h \\ l \\ -k \end{pmatrix} = \begin{pmatrix} 1 & 0 & 0 \\ 0 & 0 & 1 \\ 0 & -1 & 0 \end{pmatrix} \begin{pmatrix} h \\ k \\ l \end{pmatrix}$$

The patterson map was complicated since not only did it involve peaks corresponding to the vectors between symmetry related iodines, but also peaks representing vectors between independent iodines. Two iodine atoms on an iodoform molecule were located from some of the highest peaks in the patterson map, shown below:

multiplicity	I to I vector	Corresponding peak found in patterson map for:	
		I1	I2
4	$2x+\frac{1}{2},\frac{1}{2},0$	$0.896,\frac{1}{2},0$	$0.500,\frac{1}{2},0$
4	$-2x+\frac{1}{2},\frac{1}{2},0$	$0.104,\frac{1}{2},0$	$0.500,\frac{1}{2},0$
4	$0,2y+\frac{1}{2},\frac{1}{2}$	$0,0.614,\frac{1}{2}$	$0,0.640,\frac{1}{2}$
4	$0,-2y+\frac{1}{2},\frac{1}{2}$	$0,0.386,\frac{1}{2}$	$0,0.360,\frac{1}{2}$
4	$\frac{1}{2},0,2z+\frac{1}{2}$	$\frac{1}{2},0,0.887$	$\frac{1}{2},0,0.732$
4	$\frac{1}{2},0,-2z+\frac{1}{2}$	$\frac{1}{2},0,0.113$	$\frac{1}{2},0,0.268$

From these peaks the tentative positions of I1 and I2 were found to be 0.198,0.057,0.194 and 0.000,0.070,0.116 , respectively. These two iodines were used to calculate structure factors, from which a difference electron density map yielded the third iodoform iodine atom (R=0.334). The Ni atom was also located, as well as the six coordinated nitrogens and a few carbons. Both the host and guest molecules were found to be lying in general positions, resulting in a host : guest ratio of 1 : 1, agreeing with the density measurement. These atomic positions were used in a structure factor calculation from which a third difference fourier map was calculated, bringing the R value down to 0.255. After three more refinements the host molecule had been located and the residual value,R stood at 0.069. Hydrogen atoms were placed on the host and after the final refinement the R value was 0.068. Nowhere was the electron density greater than 0.4 $e^{-}/Å^{3}$. TABLE 3.4 lists the fractional atomic coordinates and temperature factors for STRUCTURE IV.

3.1.5 STRUCTURE V (VICTRI) $[Ni(NCS)_2(4\text{-}ViPy)_4]$. $[Ni(NCS)_2(4\text{-}ViPy)_3(thf)].2CHI_3$

($P2_1/c$ Z=4 a=15.825Å b=24.702Å c=19.041Å β=96.58°)

From the intensity data collection the space - group was found to be monoclinic with the cell dimensions given above. The reflection conditions were;

h k l:	no conditions
h 0 l:	l = 2n
0 k 0:	k = 2n

which defines the space - group as $P2_1/c$.

TABLE 3.4 Fractional atomic coordinates (x 10**4) and Thermal Parameters (A**2 x 10**3) with e.s.d. s in parentheses for STRUCTURE IV

Atom	x/a	y/b	z/c	Uiso/Uequiv(*)
I(1)	1984(2)	572(1)	1937(2)	98(1) *
I(2)	4(2)	701(1)	1162(2)	113(1) *
I(3)	1746(2)	504(1)	70(2)	106(1) *
C(0)	1233(25)	849(15)	1008(22)	105(14)
Ni(1)	2302(3)	3392(2)	-6(3)	87(2) *
N(11)	3409(19)	3515(13)	564(16)	88(10)
N(21)	1733(23)	4043(15)	526(21)	117(12)
N(31)	1184(20)	3280(12)	-581(17)	90(10)
N(41)	2811(19)	2756(12)	-548(17)	96(11)
N(1)	2752(17)	3911(11)	-769(14)	74(9)
N(2)	1849(18)	2886(11)	774(15)	80(9)
S(1)	2917(7)	4816(4)	-1538(6)	98(5) *
S(2)	1320(9)	2185(5)	1721(7)	134(7) *
C(1)	2828(18)	4290(12)	-1117(17)	61(9)
C(2)	1649(19)	2584(13)	1184(18)	63(10)
C(12)	3806(27)	3134(18)	921(22)	106(15)
C(13)	4490(27)	3148(18)	1304(23)	112(15)
C(14)	4987(28)	3652(17)	1331(22)	103(13)
C(15)	4585(25)	4041(17)	976(21)	104(14)
C(16)	3680(26)	3995(17)	611(21)	103(14)
C(17)	5712(27)	3777(18)	1710(22)	108(15)
C(18)	6111(28)	3405(18)	2057(23)	118(16)
C(22)	1711(30)	4070(19)	1216(27)	138(18)
C(23)	1188(29)	4475(20)	1581(27)	133(18)
C(24)	921(28)	4847(19)	1250(26)	107(15)
C(25)	949(26)	4820(18)	591(25)	103(14)
C(26)	1279(27)	4439(19)	195(25)	123(16)
C(27)	289(35)	5240(21)	1698(31)	156(22)
C(28)	-362(49)	5498(30)	1680(40)	240(35)
C(32)	408(26)	3319(15)	-239(22)	99(14)
C(33)	-337(23)	3240(14)	-611(20)	81(12)
C(34)	-388(24)	3220(15)	-1319(21)	82(12)
C(35)	394(25)	3278(15)	-1662(21)	95(14)
C(36)	1136(25)	3286(14)	-1282(21)	92(13)
C(37)	-1205(29)	3238(16)	-1695(24)	111(15)
C(38)	-1296(32)	3251(20)	-2380(31)	149(19)
C(42)	2414(26)	2259(15)	-550(21)	95(13)
C(43)	2837(24)	1831(17)	-899(20)	103(14)
C(44)	3689(27)	1895(18)	-1226(23)	104(14)
C(45)	4039(24)	2368(16)	-1206(21)	93(13)
C(46)	3707(26)	2784(17)	-849(20)	103(14)
C(47)	3966(39)	1425(23)	-1624(30)	182(25)
C(48)	3465(36)	939(23)	-1663(30)	176(24)

Anisotropic atoms have thermal parameters (A**2 x 10**3) of the form

EXP(-2*PI**2(U11*H**2*(A*)**2+...+2*U12*H*K*(A*)*(B*)+...)

Atom	U11	U22	U33	U23	U13	U12
I(1)	81(2)	104(2)	109(2)	0(2)	-12(2)	13(2)
I(2)	73(2)	150(3)	116(2)	-18(2)	-5(2)	25(2)
I(3)	107(2)	106(2)	104(2)	18(2)	23(2)	16(2)
Ni(1)	97(4)	72(3)	93(4)	15(3)	13(3)	-8(3)
S(1)	103(9)	101(8)	89(8)	28(7)	-16(7)	-40(7)
S(2)	146(12)	114(10)	143(13)	43(10)	51(10)	14(9)

From the density measurement and cell dimensions eight host and eight guest molecules were present in the unit cell. $P2_1/c$, however can only accommodate 4 molecules in the general positions, or else 2 molecules at each of the four inversion centres (Wyckoff positions a,b,c and d). The only way that eight host molecules can arrange themselves is if all the special positions are occupied, or the four general positions and two of the special positions or else all eight at general positions but with two independent sets of four host molecules. This latter case was found to be true. The eight guest molecules were also found to be lying in general positions. Using the SHEL86 Patterson subroutine four iodine atoms were located. The remaining two iodine atoms were located from the first difference map. Thus these six iodines comprised the two independent iodoform guests.

SHEL400 was used for the difference fourier synthesis since it can handle a maximum of 500 parameters as opposed to SHEL76 which can only manage 228. After five difference fourier maps the R value stood at 0.097. One complete host molecule had been located and for the second host molecule the nickel, three 4-vinylpyridine and the two isothiocyanate ligands had been found. The remaining 4-vinylpyridine moiety could not be found at the sixth coordination site, and it became apparent that this site was in fact occupied by a tetrahydrofuran(thf) molecule, coordinated through the oxygen.

There was some uncertainty as to whether there was disorder at this coordination site. The possibility existed for this site to be occupied by thf in 80%, say , of these host molecules and the remainder being occupied by the 4-vinylpyridine, so that we were observing an average situation. In order to check this, electron density maps were studied in the region of this coordination site to see

if there was any smearing of the peaks for the thf ligand. The para- carbon atom of the pyridine ligand, as well as the carbon atoms of the vinyl group would also be expected to give distinguishable peaks. These maps are shown in fig 3.2. They are in layers of x, from 0.00 to 0.16 in increments of 0.02. No smearing of the thf peaks was observed and neither were there any discernible peaks to indicate the presence of a pyridine ligand in this region.

Thus this structure represents a ternary crystal system with two different crystallographically independent host molecules enclathrating the iodoform molecules.

The fractional atomic coordinates and temperature factors for STRUCTURE V are listed in TABLE 3.5.

Chapter 3 References

3.1 F. Herbstein, Private communication.

X = .06

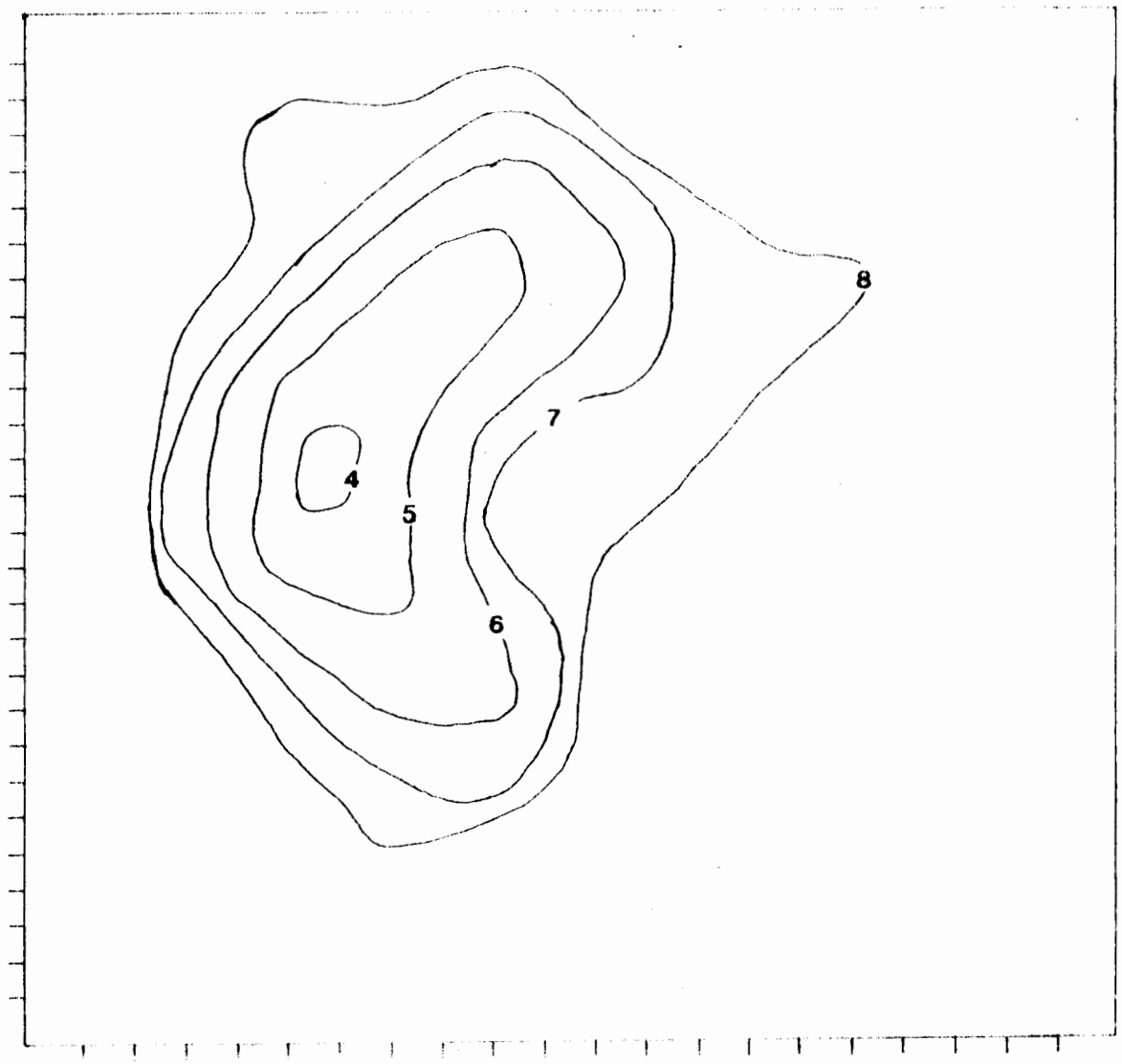

X= .04

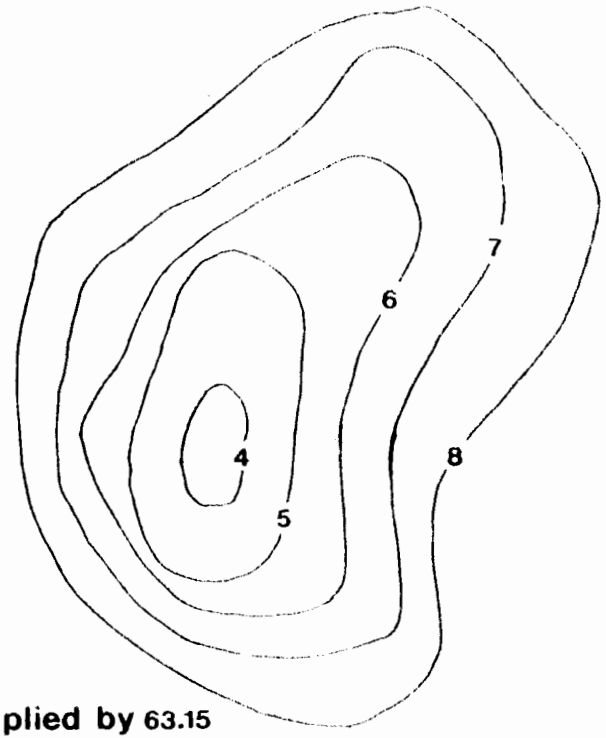

multiplied by 63.15

CONTOUR KEY	
1	160 — 180
2	140 — 160
3	120 — 140
4	100 — 120
5	80 — 100
6	60 — 80
7	40 — 60
8	20 — 40

Y across

Z down

X = .08

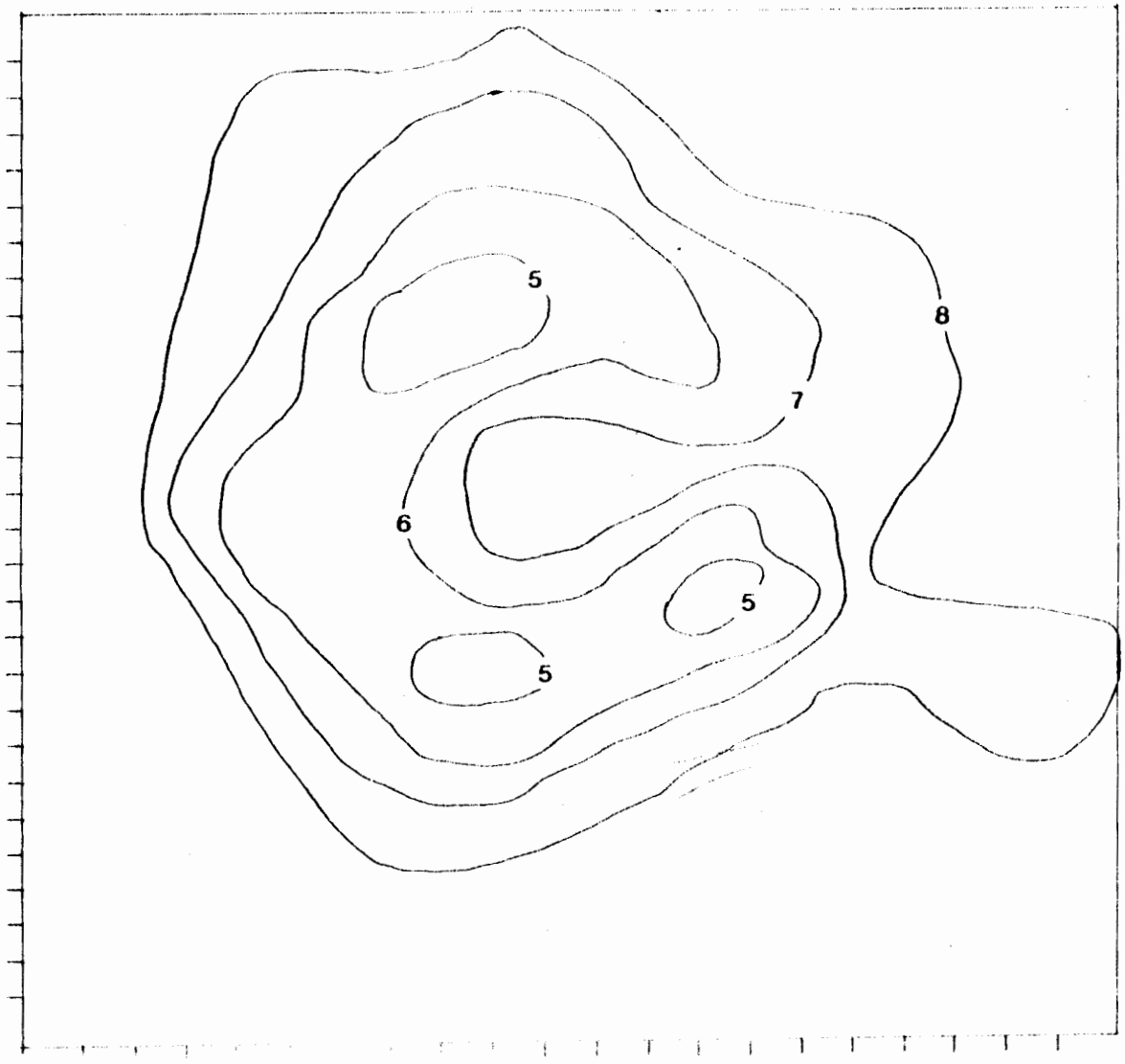

X = .10

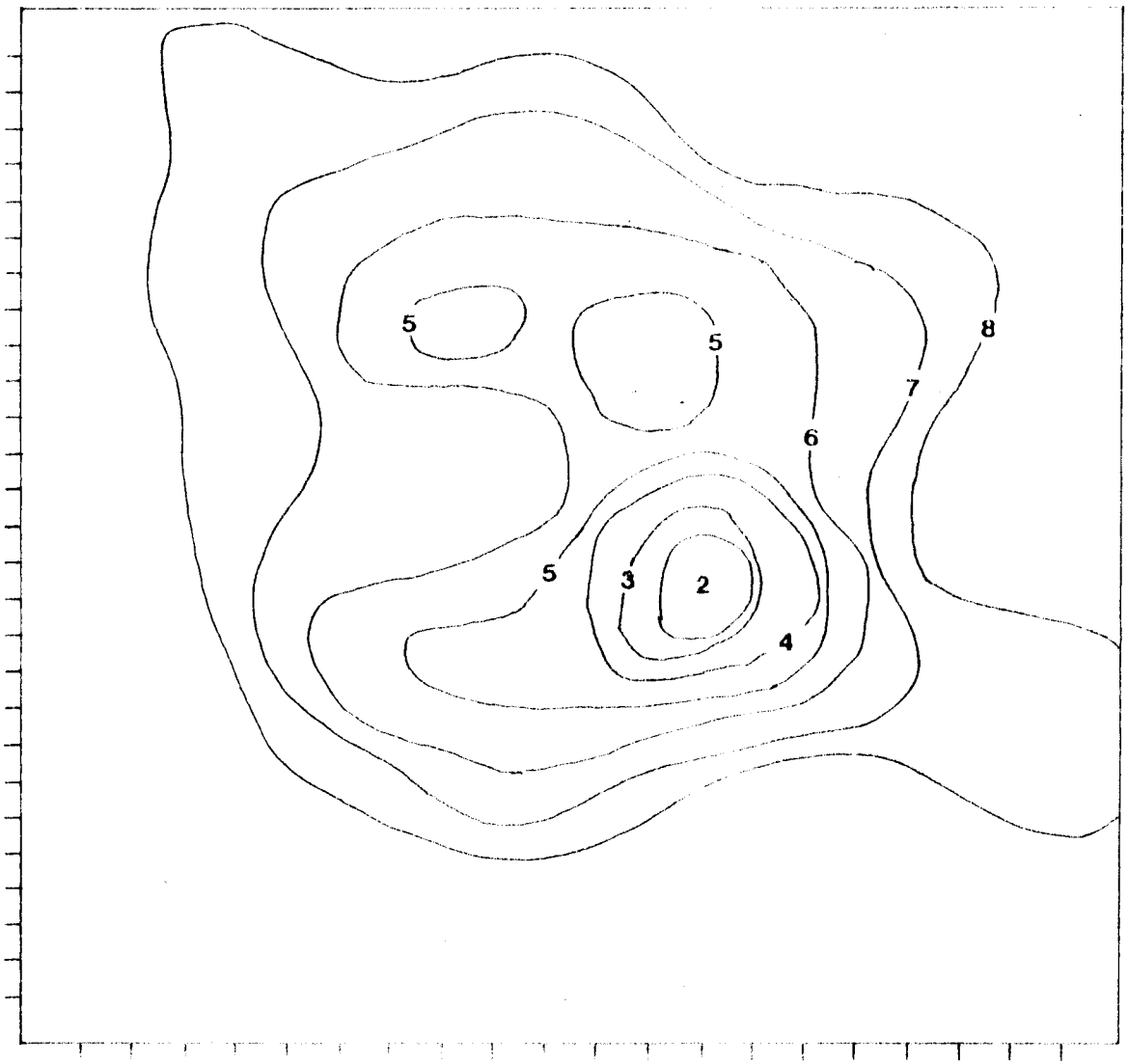

X=.12

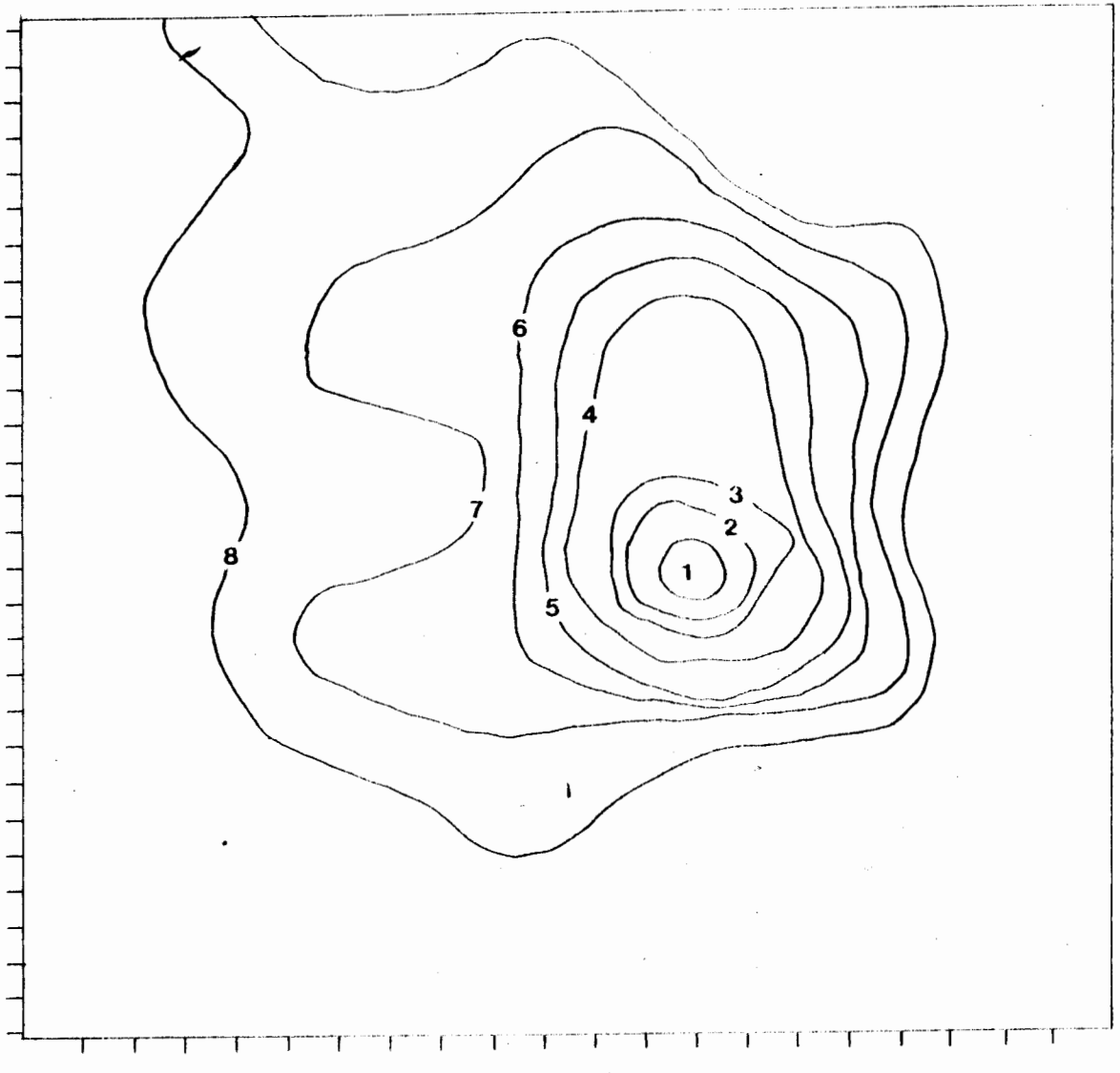

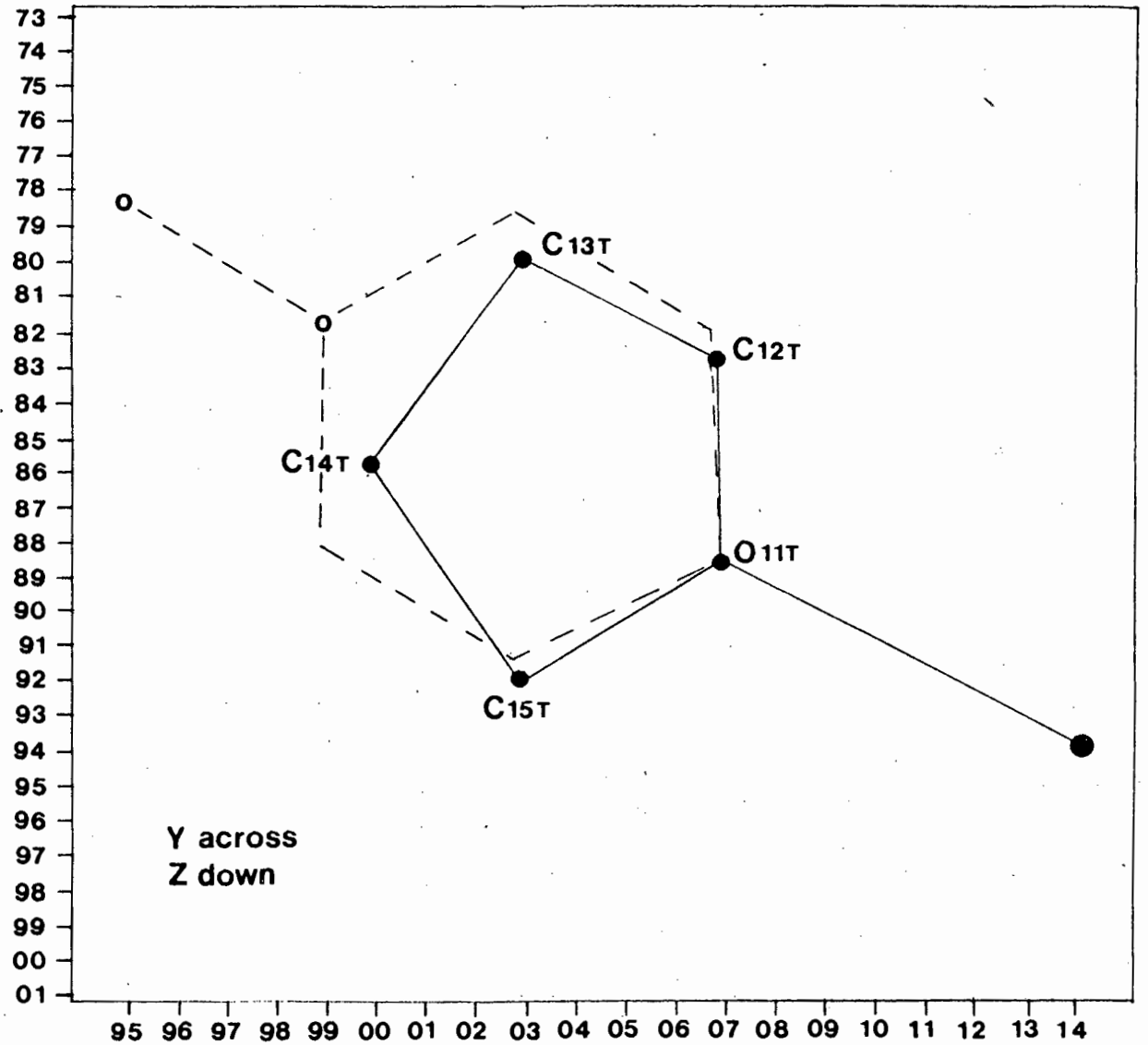

Fig 3.2 Electron density cross - sections in the region of the coordinated thf ligand, from x=.04 to x=.12 in increments of .02.

TABLE 3.5 Fractional atomic coordinates (x 10**4) and Thermal Parameters (A**2 x 10**3) with e.s.d. s in parentheses for STRUCTURE V

Atom	x/a	y/b	z/c	Uiso/Uequiv(*)	
C(0A)	3874(31)	9122(22)	8862(25)	91(17)	
C(0B)	1167(39)	810(27)	3696(31)	131(24)	
I(1B)	1739(3)	485(2)	4697(2)	114(2)	*
I(1A)	3396(3)	9341(1)	9852(2)	83(2)	*
I(2A)	3207(2)	9434(1)	7971(2)	71(1)	*
I(3A)	5223(2)	9293(2)	8923(2)	101(2)	*
I(2B)	1689(3)	485(2)	2806(2)	102(2)	*
I(3B)	-202(3)	597(2)	3623(2)	106(2)	*
Ni(1A)	1873(4)	1421(2)	-279(3)	62(3)	*
Ni(1B)	7252(4)	1678(2)	4884(3)	69(3)	*
S(1A)	2681(12)	-8(6)	1351(8)	108(9)	*
S(2A)	905(10)	2806(6)	-1923(9)	105(8)	*
S(1B)	7717(11)	106(5)	3557(8)	102(8)	*
S(2B)	6256(11)	2703(6)	6736(8)	98(8)	*
N(1A)	2377(21)	898(14)	479(18)	55(11)	
N(11A)	815(22)	1511(13)	268(19)	51(10)	
N(2B)	6890(22)	2244(14)	5621(20)	66(11)	
N(2A)	1324(24)	1934(15)	-1029(20)	71(12)	
N(11B)	6066(24)	1747(15)	4320(20)	71(12)	
N(21B)	6763(23)	1024(14)	5525(21)	62(11)	
N(1B)	7551(26)	1086(18)	4134(22)	88(14)	
N(31B)	7717(24)	2322(14)	4266(18)	58(11)	
N(41A)	2567(27)	2056(16)	291(20)	80(13)	
N(31A)	2877(23)	1309(15)	-869(19)	63(11)	
N(41B)	8454(22)	1569(14)	5415(18)	59(11)	
C(1A)	2525(23)	514(16)	838(20)	38(11)	
C(2A)	1144(26)	2306(17)	-1422(22)	48(12)	
C(1B)	7612(34)	687(23)	3902(27)	90(18)	
C(32A)	3368(38)	886(24)	-859(29)	94(19)	
C(33A)	4129(34)	871(22)	-1169(26)	84(17)	
C(34A)	4479(31)	1261(19)	-1523(25)	70(15)	
C(35A)	3889(34)	1763(21)	-1546(27)	87(17)	
C(36A)	3181(36)	1702(23)	-1211(27)	90(18)	
C(37A)	5265(31)	1182(20)	-1853(25)	68(15)	
C(38A)	5652(41)	1519(28)	-2118(27)	116(23)	
C(12A)	895(29)	1513(17)	963(25)	62(13)	
C(13A)	148(31)	1544(18)	1407(26)	74(15)	
C(14A)	-669(25)	1536(14)	1048(22)	38(12)	
C(15A)	-719(30)	1523(17)	388(26)	66(14)	
C(16A)	10(28)	1490(16)	-21(23)	54(12)	
C(17A)	-1337(30)	1582(17)	1466(26)	71(15)	
C(18A)	-1395(35)	1656(22)	2084(33)	103(19)	
C(42A)	2167(31)	2578(19)	290(23)	66(14)	
C(43A)	2721(35)	3024(21)	583(27)	86(18)	
C(44A)	3442(29)	2978(17)	855(23)	53(13)	
C(45A)	3808(34)	2427(21)	861(26)	87(17)	
C(46A)	3319(29)	2009(17)	561(22)	61(13)	
C(47A)	4063(50)	3366(29)	1239(37)	146(27)	
C(48A)	3830(49)	3867(35)	1198(43)	174(33)	
C(2B)	6643(27)	2432(17)	6118(24)	52(13)	
C(32B)	8368(30)	2250(19)	3916(24)	65(14)	
C(33B)	8643(38)	2657(24)	3590(29)	107(20)	
C(34B)	8258(32)	3185(19)	3445(26)	67(15)	

TABLE 3.5 (CONT')

C(35B)	7656(31)	3181(19)	3837(25)	72(15)
C(36B)	7304(28)	2815(18)	4235(23)	60(14)
C(37B)	8480(37)	3722(24)	3007(29)	108(20)
C(38B)	9065(45)	3687(31)	2661(37)	180(34)
C(12B)	5298(39)	1774(21)	4591(31)	99(19)
C(13B)	4552(37)	1810(21)	4222(30)	101(19)
C(14B)	4424(28)	1806(17)	3491(24)	56(13)
C(15B)	5160(29)	1740(17)	3207(24)	61(14)
C(16B)	5943(28)	1768(16)	3603(23)	47(12)
C(17B)	3537(35)	1812(20)	3125(29)	89(18)
C(18B)	3286(48)	1776(32)	2441(46)	186(36)
C(22B)	6931(30)	1081(20)	6213(27)	74(16)
C(23B)	6627(39)	641(25)	6595(35)	127(21)
C(24B)	6133(37)	268(23)	6243(34)	95(19)
C(25B)	6014(43)	294(28)	5574(39)	133(24)
C(26B)	6348(35)	643(24)	5156(31)	106(19)
C(27B)	5784(50)	-145(28)	6803(39)	153(28)
C(28B)	5166(63)	-343(29)	6767(44)	194(35)
C(42B)	8879(33)	1993(21)	5782(27)	87(17)
C(43B)	9742(36)	1959(22)	6105(28)	94(18)
C(44B)	10108(30)	1445(19)	6191(24)	68(14)
C(45B)	9644(32)	1025(19)	5835(25)	77(16)
C(46B)	8871(31)	1084(19)	5473(24)	74(15)
C(47B)	11027(41)	1349(25)	6565(31)	116(22)
C(48B)	11445(58)	1669(33)	6913(43)	179(34)
O(11T)	1256(20)	772(13)	-848(18)	84(10)
C(12T)	1185(43)	696(25)	-1587(33)	132(23)
C(13T)	679(49)	202(32)	-1840(40)	176(31)
C(14T)	471(36)	-34(23)	-1212(30)	104(19)
C(15T)	870(43)	222(27)	-581(34)	149(26)

Anisotropic atoms have thermal parameters (A**2 x 10**3) of the form :

EXP(-2*PI**2(U11*H**2*(A*)**2+...+2*U12*H*K*(A*)*(B*)+...)

Atom	U11	U22	U33	U23	U13	U12
I(1B)	136(4)	79(3)	119(4)	-12(2)	-19(3)	12(3)
I(1A)	116(3)	58(2)	75(3)	12(2)	17(2)	1(2)
I(2A)	81(3)	63(2)	69(3)	-1(2)	7(2)	-2(2)
I(3A)	77(3)	98(3)	125(4)	-5(3)	6(3)	24(2)
I(2B)	112(3)	85(3)	111(3)	11(2)	22(3)	12(3)
I(3B)	101(3)	105(3)	111(3)	-5(3)	7(3)	17(3)
Ni(1A)	75(5)	38(4)	73(5)	8(3)	5(4)	7(3)
Ni(1B)	85(5)	51(4)	74(5)	-11(3)	26(4)	-3(4)
S(1A)	165(17)	68(11)	95(13)	32(9)	37(12)	30(10)
S(2A)	99(13)	73(11)	139(15)	34(10)	-2(11)	13(9)
S(1B)	159(16)	28(8)	111(13)	-10(7)	-13(12)	10(9)
S(2B)	127(14)	69(10)	109(13)	-17(9)	53(11)	8(9)

CHAPTER 4

Host conformation and molecular packing in structures I to V

4.1 Introduction

This chapter describes the conformation of the host molecule in the various clathrates and the molecular packing in these crystals, paying particular attention to the shape and size of the cavity in which the guest molecules reside. The types of cavities formed by $[Ni(NCS)_2(4\text{-ViPy})_4]$ in these clathrates shows the versatility of this host for enclathrating different guest molecules. The carbon tetrachloride and dichloromethane molecules occupy channels running the length of the unit cell, the iodoform molecules occupy elongated cages and the diiodomethane clathrate has the typical β-phase zeolitic structure. The cavities were mapped with the use of EENY (potential energy profile of the crystal) and OPEC (van der Waals profile). These two approaches are discussed later on.

4.2 Host conformation

In all five structures the Ni atom has an irregular octahedral coordination, being surrounded by 6 nitrogen atoms, except in STRUCTURE V where every second host molecule has had a substituted pyridine moiety replaced by a thf ligand. The Ni atom lies in the plane defined by the four pyridine nitrogen atoms (or three nitrogens and one oxygen) and the isothiocyanate ligands are always found to be lying trans to one another. The environment of the Ni atom, with bond lengths and angles for STRUCTURE IV is shown in fig 4.1.

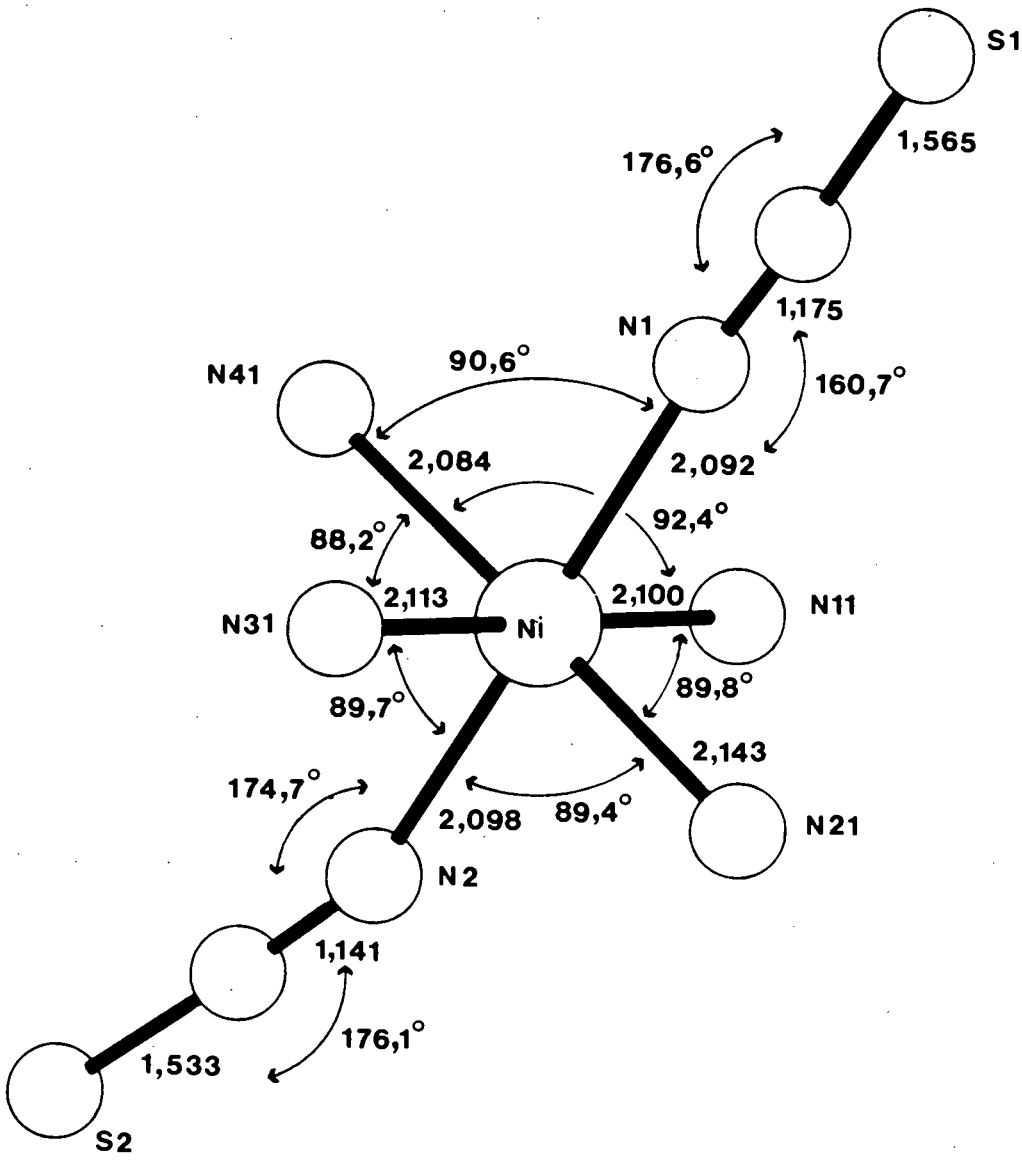

Fig 4.1 The environment of the nickel atom in STRUCTURE IV showing bond lengths (Å) and angles.

Fig 4.2(a) shows the conformation of the host molecule found in STRUCTURE II, with atomic nomenclature. The disordered vinyl groups are shown as dashed lines. The conformation of the host molecule with the coordinated thf base is shown in fig 4.2(b). There appears to be no significant trans effect of the Ni-N bond opposite the thf ligand.

Full tables of bond lengths and bond angles are given in APPENDIX B. TABLE 4.1 lists the average bond length found for each type of bond in STRUCTURES I - V.

As previously observed in complexes of this type[4.1,4.2] there is a significant difference not only between the Ni - N bond distances of the isothiocyanate and pyridine ligands (0.06 Å difference) but also between those of symmetrically independent isothiocyanate (0.03 Å variation in Ni - N_{cs} distance) and pyridine (0.16 Å variation in Ni - N_{py} length) ligands. On average, however, the Ni - N_{py} distances are .04 Å longer than those of Ni - N_{cs}.

The NCS group plays a significant role in determining the overall conformation of the host molecule, and the flexibility of this ligand is revealed in the variation of bond angles, with the Ni - N - C angle ranging from 149° (STRUCTURE III) to 174° (STRUCTURE IV) and the N - C - S angle spanning 165° (STRUCTURE III) to 179° (STRUCTURE V).

In all the clathrates the isothiocyanate groups have the arrangement seen in fig 4.2(a) and (b), illustrated below:

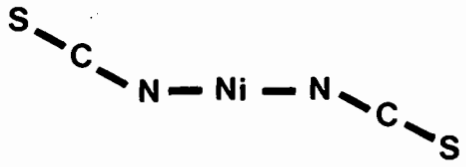

as opposed to both the sulphur atoms lying on the same side of the Ni atom found in the non - clathrated α - phase of $[Ni(NCS)_2(4\text{-ViPy})_4]$, shown below:

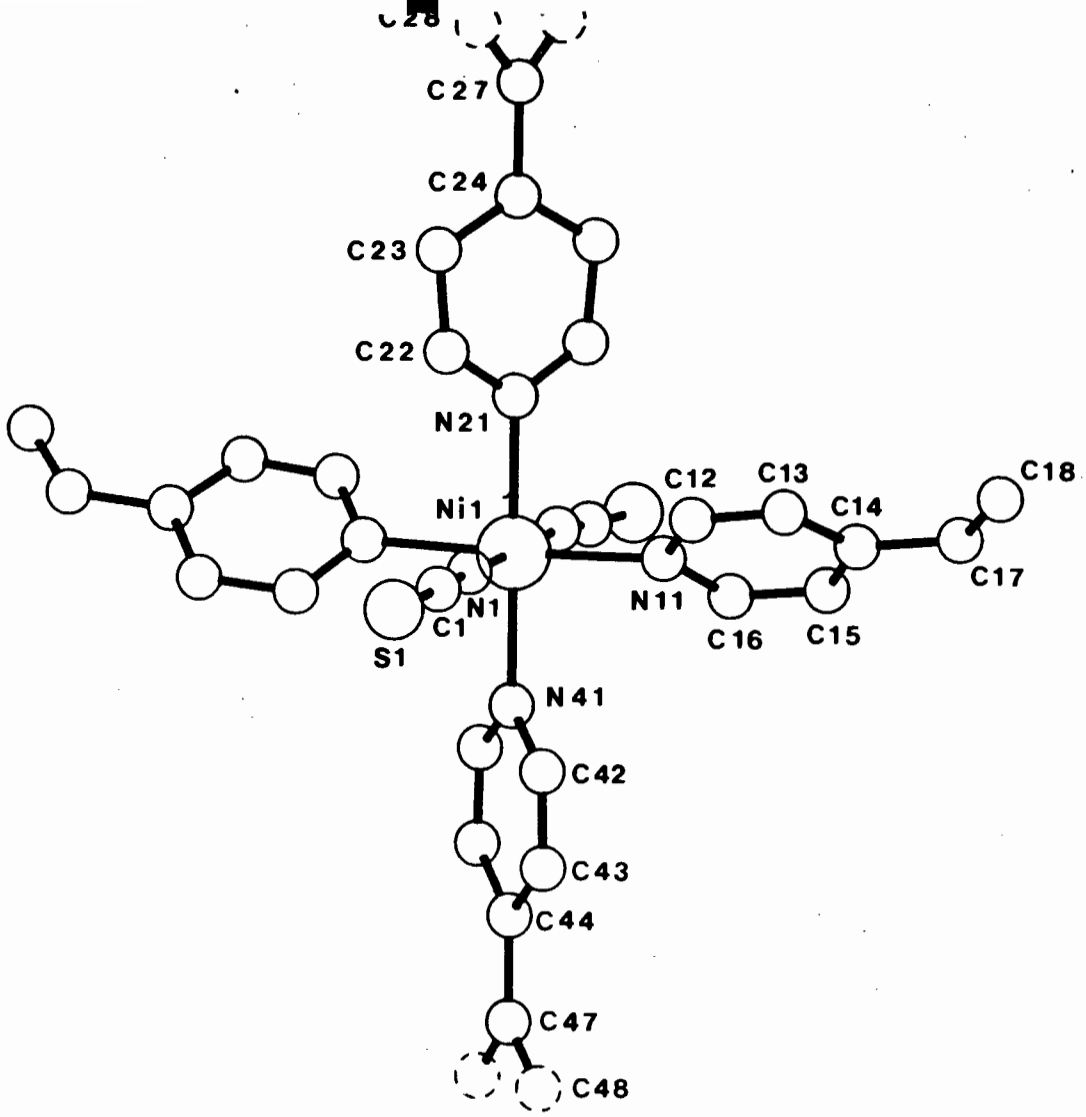

Fig 4.2(a) Perspective view of the host molecule conformation in STRUCTURE II, showing the disordered vinyl groups.

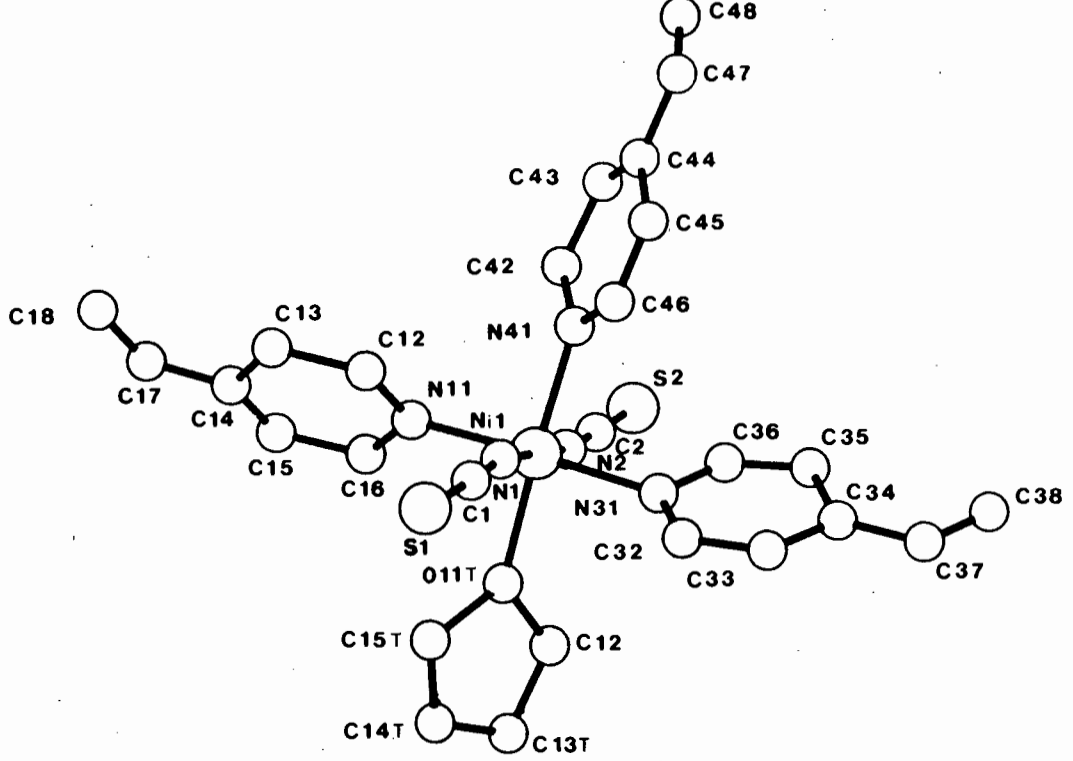

Fig 4.2(b) Perspective view of the thf substituted host molecule conformation in STRUCTURE V.

TABLE 4.1 Average bond lengths for the host molecules in STRUCTURES I to V

BOND TYPE	MIN. LENGTH[a]	MAX. LENGTH[a]	AVG. LENGTH
Ni - N_{py}	2.061 (V)	2.220 (V)	2.12(4)
Ni - N_{cs}	2.029 (V)	2.135 (V)	2.08(3)
N_{cs} - C_{s}	1.090 (V)	1.200 (V)	1.15(3)
C_{s} - S	1.533 (IV)	1.694 (III)	1.60(5)
N_{py} - C_{py} C_{py} - C_{py}	1.250 (V)	1.503 (IV)	1.36(7)
C_{ring} - C_{vin}	1.265 (III)	1.609[b] (IV)	1.42(9)
C_{vin} - C_{vin}	1.140 (I)	1.336 (III)	1.22(9)
Ni - O	STRUCTURE V		2.11
O - C_{thf}	" "		1.51(7)
C_{thf} - C_{thf}	" "		1.45(4)

(a) Number in brackets refers to the STRUCTURE

(b) Unusually long due to disorder

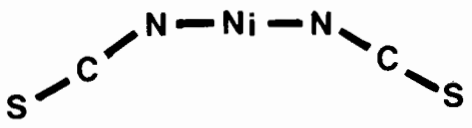

If the Ni atom were coordinated only to four aromatic bases, in the absence of the NCS groups, then we would expect the adopted conformation to be the most relaxed one, with the pyridine ligands perpendicular to the nitrogen - nickel molecular plane. This is indeed the case, as exhibited by crystals of tetrakis(3,4-dimethylpyridine)Nickel(II) perchlorate[4.3], where the Ni has square planar coordination. Introduction of the trans NCS groups into this coordination sphere introduces repulsive non - bonded interactions and the most favourable conformation of the pyridine ligands around the M - N coordination bonds corresponds to the "propeller" shaped molecule.

Conformational studies of the MX_2A_4 molecules[4.4] have shown that this propeller conformation is of lowest energy, but there is another conformation of higher energy possible which corresponds to the centrosymmetric conformation. One pair of pyridine ligands are almost coplanar with the NCS groups, so that the steric repulsion is greater than for the other pair of pyridine ligands with the two NCS units. The overall Ni - N bond lengths, averaged within the molecule, are longer for the centrosymmetric than for the propeller conformation and Guarino et al have shown that it is possible to observe this spectrally[4.5]. The $^3A_{2g}$ --> $^3T_{1g}$ band in the Ni d - d transition is seen to occur at lower frequency for host molecules in the centrosymmetric conformation relative to the α - MX_2A_4 solid and at higher frequency for host molecules in the propeller conformation.

Some of the values obtained for clathrates of $Ni(NCS)_2(4\text{-}MePy)_4$ are shown in TABLE 4.2. This table also shows the values for α - $[Ni(NCS)_2(4\text{-}ViPy)_4]$ and compounds I to IV. Their U.V - visible reflectance spectra were recorded

TABLE 4.2 $^3A_{2g}$ --> $^3T_{1g}$ band shifts ($\Delta\underline{v}$) observed in $[Ni(NCS)_2(4\text{-}MePy)_4]$ and $[Ni(NCS)_2(4\text{-}ViPy)_4]$ inclusion componds with reference to the visible spectra of their α-phase solids.

COMPOUND	$^3A_{2g}$ -> $^3T_{1g}$ trans.(cm^{-1})	$\Delta\underline{v}$	type of conformation and symmetry of the host molecule
α-$[Ni(NCS)_2(4\text{-}MePy)_4]$	17 301	-	Propeller,C_2
.1-bromonaphthalene	17 483	+182	Propeller,C_1
.p-xylene	17 361	+60	Propeller,C_2
.p-dibromobenzene	17 422	+121	Propeller,C_2
.2-bromonaphthalene	17 241	-60	C_1
.p-terphenyl	17 241	-60	C_1
α-$[Ni(NCS)_2(4\text{-}ViPy)_4]$	17 544	-	Propeller,C_1
.2CH_2Cl_2	17 550	+6	Propeller,C_1
.2CCl_4	17 730	+186	Propeller,C_2
.2CH_2I_2	17 689	+145	Propeller,C_2
.CHI_3	17 786	+242	Propeller,C_1

on a Beckman DK - A spectrophotometer set in reflectance mode.

For the crystals under study there is little change at the coordination octahedron e.g the Ni-N bond lengths for STRUCTURE IV are 2.098, 2.092, 2.143, 2.113, 2.100 and 2.084 compared to those for the α-phase complex of 2.055, 2.025, 2.113, 2.113, 2.145 and 2.076. Only a distortion of the ligands due to the accommodation of the guest molecules occurs. This perturbation of the crystalline field around the central Ni(II) ions results in shifts of the d-d transitions.

No splitting is observed in the spin - allowed $^3A_{2g} \dashrightarrow {}^3T_{1g}$ transition, which confirms the absence of any severe tetragonal distortion of the Ni coordination sphere i.e the coordination is practically octahedral. We can see that just from such an observation is it possible to predict the conformational type of the MX_2A_4 host in the crystalline state.

The versatility of this class of compounds has been ascribed to their rotational freedom around the Ni - N bonds. This supposedly allows adjustment of the substituted pyridines to accommodate the various guest molecules, differing in size and shape. As already discussed, the rotational freedom of the ligands is restricted. The torsional configuration of the 4-vinylpyridines is given by the torsion angles N1 - Ni - N(x1) - C(x2) with x=1(γ_1), 2(γ_2), 3(γ_3), 4(γ_4). TABLE 4.3(a) lists the torsion angles for each structure. From a conformational potential energy study of the $Ni(NCS)_2(3,5\text{-diMePy})_4$ complex[4-6] it has been shown that the conformation of the substituted pyridines is governed by the ortho - hydrogen atoms; therefore asymmetry imposed by the substituent at the para position may be ignored. This would give two - fold axial symmetry to the pyridines and

TABLE 4.3 (a) Comparison of selected torsion angles in the host molecules.

STRUCTURE	I	II	III	IV	V	
					Host A	Host B
γ_1	35.7	35.8	36.1	43.0	36.4	43.2
γ_2	44.9	44.9	33.8	44.9	-	38.6
γ_3	35.8	35.8	36.1	33.2	25.0	35.2
γ_4	39.5	39.5	33.8	44.6	42.7	35.2
γ_5*	-	-	-	-	32.7	-

N1 - Ni - N(X1) - C(X2)

with x = 1(γ_1),2(γ_2),3(γ_3),4(γ_4)

* γ_5 = N1A - NiA - O1T - C12T for the thf ligand in the $Ni(NCS)_2(4\text{-}ViPy)_3(thf)$ host molecule

TABLE 4.3 (b) Comparison of the above torsion angles with those of the α-phase host molecule.

STRUCTURE	α phase	I	II	III	IV	V
						Host B
γ_1	43.1	44.9	44.9	36.1	44.6	43.2
γ_2	35.6	35.8	35.8	33.8	43.0	38.6
γ_3	40.0	39.5	39.5	36.1	44.9	35.2
γ_4	37.6	35.7	35.8	33.8	33.2	35.2

therefore 180° can be added to or subtracted from the torsion angles. The torsion angles shown in TABLE 4.3 (a) are those calculated from the refined positions of the atoms in the five structures. In each structure, the labelling of the pyridine ligands was carried out cyclically, and each compound was initially arbitrarily labelled. However, in order to carry out meaningful comparison of the structures, the combination of torsion angles [γ_1 γ_2 γ_3 γ_4] was systematically searched for which yielded the minimum in the sum of the squares of their differences. The torsion angles of the host in its α-phase clathrate was also included in this analysis for comparison. The result is shown in TABLE 4.3(b). If the incorporation of guest molecules into the host lattice had no effect on the host conformation, then we would expect no difference between the torsion angles of the two conformations. However, as can be seen from TABLE 4.3(b), the inclusion of guest molecules does influence the host conformation, relative to that in the α-phase, and although these differences in the torsion angles are not greater than 8°, even this small variation is sufficient to allow the host to accommodate guests of varying shapes and sizes.

4.3 Molecular packing

The size and topologies of the cavities in the clathrates were mapped out with the use of EENY and OPEC.

4.3.1 EENY

Semi - empirical potential functions describing van der Waals interactions between pairs of non - bonded atoms have been used in the study of the molecular environment of guest molecules in crystals. The shape of the van der Waals potential function is characterised by the depth of the

potential well, the corresponding equilibrium distance between the atoms and the steepness of the curve arising from repulsion at short distances.

EENY uses the atom - atom potential function shown below:

$$U(r) = a.\exp(-br)/r^6 - c/r^6$$

where r is the distance between any pair of atoms and the coefficients a, b, c and d are those given by Giglio[4.7]. These potential energy curves were derived primarily to give good agreement for calculations of molecular positions in crystal structures. No account is taken of partial atomic charges or dipole interactions, and the energy values derived mean little in an absolute sense. Giglio's force field has been used successfully in a number of problems, including the intermolecular energy calculations in deoxycholic acid clathrates[4.8,4.9], the intramolecular conformations of a variety of compounds such as vitamin U hydrochloride[4.10], conformation patterns in cholanic acids[4.11] and the study of rotational motion of disordered perchlorate ions[4.12].

The shapes of the cavities in the clathrates under study were described by placing a hydrogen probe atom in the crystal structure, built up of host molecules(guest excluded) and then systematically moving the hydrogen atom through the unit cell and calculating the potential energy at each point, so that in this way an intermolecular energy profile is mapped. The unit cell was sliced into 10 sections along an axis and at each interval two - dimensional energy maps were evaluated. The zero - potential energy surface was drawn with the use of ALCHEMY. The positions of the guest molecules from the crystal structure were found to be close to the position of minimum energy calculated by EENY.

4.3.2 OPEC

Each type of atom in the crystal structure is regarded as a hard sphere and assigned a van der Waals radius of $R_{m,i}$. Although the neighbourhood of an atom in the crystal structure may affect its shape and size, radii considered to be representative of most crystalline environments for the atoms are used by OPEC[4-13]. This sphere may interpenetrate with spheres associated to other atoms on the same molecule, bound to or not bound to atom m,i. It may also interpenetrate with spheres associated with atoms on neighbouring molecules.

The packing analysis is performed by describing each point in the unit cell by a vector, $\underline{s}$ which can be inside one or more of the atomic spheres i.e inside the host molecule or outside. The element of volume d_v centred at $\underline{s}$ is accordingly labelled as either occupied or free. By sampling the cell space by systematic variation of $\underline{s}$, all the points in the cell either have a value of 0, which indicates an unoccupied volume, or else a finite number which represents the packing density in that zone. In this way the "empty space" in the clathrates can be studied.

4.3.3 Molecular packing of STRUCTURES I and II
$Ni(NCS)_2(4\text{-}ViPy)_4.2G$ where $G=CH_2Cl_2$ (I) or CCl_4 (II)

These two clathrates have a similar packing arrangement. As mentioned, the carbon tetrachloride clathrate packs in the space - group C2/c with a host : guest ratio of 1 : 2. The host molecules lie on the diad running parallel to $\underline{y}$ (Wyckoff position e), with Ni, N21, C24, C27, N41, C44 and C47 lying on the diad, fig.4.2(a). Thus there are two bands of pyridine rings running along the diads at Z = .25 and Z = .75. These bands of ligands are stacked on top of one

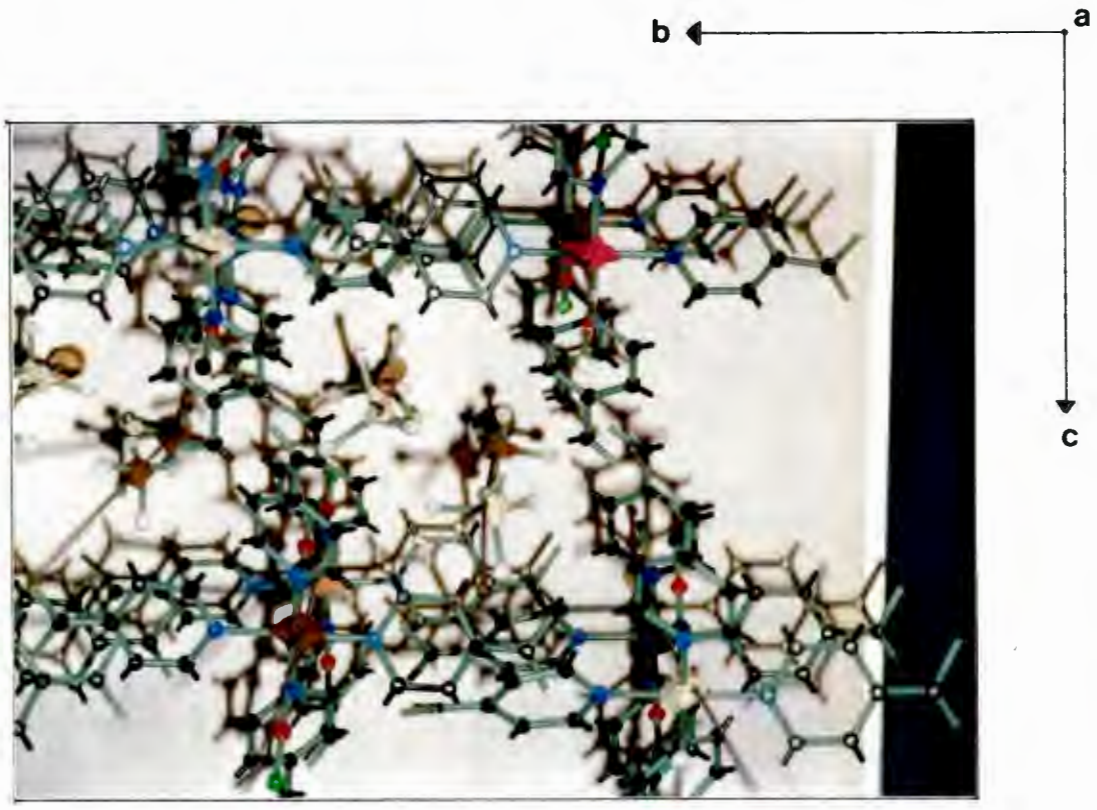

Fig 4.3 Photograph of the model of STRUCTURE II looking in the [1 0 0] direction. The centre channel runs parallel to x,½,½ and to the left of this is the channel at x,1,½. The guest molecules are shown in the channels.

another going up x, which forms the two opposite "walls" of a channel running parallel to x. By virtue of the fact that two pyridine ligands lie on the diad, the other two trans pyridine and isothiocyanate ligands are confined to lie perpendicular to the two - fold rotation axis, inclined to the XY plane at about 65°. These ligands form the other two sides of the channel as the host molecules pack along the x- axis. A model of this packing arrangement is shown in the photograph in fig 4.3 ,which reveals two parallel channels, with the guest molecules located in them.

The channel centred on the line $x,\frac{1}{2},\frac{1}{2}$ can be clearly seen and to the right of this is the identical symmetry related channel centred at $x,1,\frac{1}{2}$ which lags behind the former channel by a/2 Å. This is due to the symmetry of C2/c and is illustrated below for an hypothetical example with the figure 7 representing the host molecules (heights alongside).

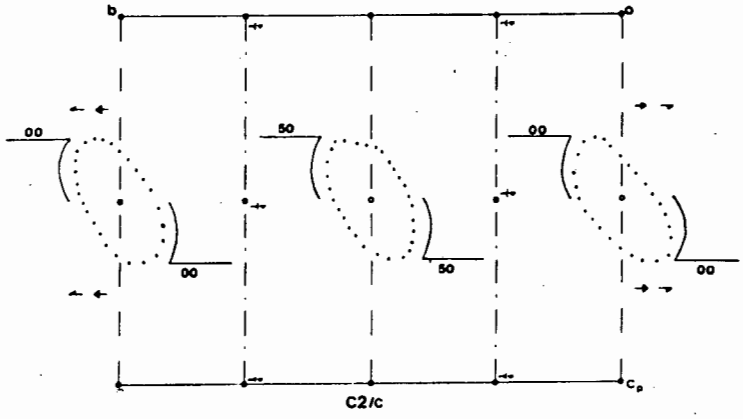

The above case may be compared with the $Ni(NCS)_2(4\text{-phenylpyridine})_4.4DMSO$ clathrate which has $P\bar{1}$ symmetry[4.15]. In this case the guest molecules lie in two distinct and crystallographically nonequivalent channels which are parallel to the z - axis. This is illustrated below:

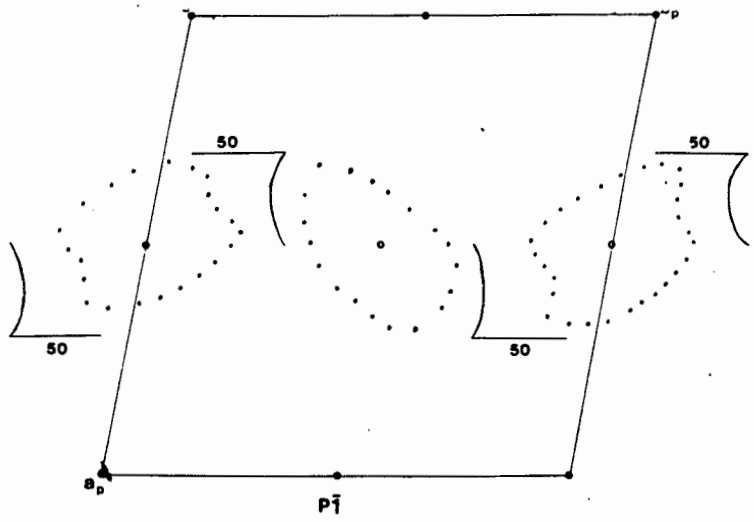

The $Ni(NCS)_2(4\text{-}ViPy)_4.2CH_2Cl_2$ clathrate, although it packs in the space - group $P2_1/n$, has a similar structure to that of the carbon tetrachloride clathrate. This similarity is revealed by comparing the packing diagrams, viewed down [1 0 0] , of both structures, fig 4.4. The Ni atoms lie in general positions, and although the substituted pyridines are not constrained to lie along a diad , one pair of trans pyridines have orientated themselves to lie approximately parallel to the y - axis. The guest molecules also occupy similar positions in the unit cell.

The dichloromethane clathrate is isomorphous with the chloroform clathrate[4,18] ($P2_1/n$, a=10.435 b=19.787 c=19.82 β=99.10). This similarity of the CH_2Cl_2 and $CHCl_3$ clathrates with the CCl_4 clathrate is illustrated in Chapter 6 (fig 6.1). The type of packing exhibited by these three clathrates has been termed the δ-phase.

The voids in the crystal structure of this inclusion compound were explored with the use of EENY and OPEC. For both models the unit cell length `a` was sliced into 10 sections and the two - dimensional maps were calculated for each layer. Fig 4.5 shows the contour of the channels at each cross-section (from OPEC). This revealed the channels running parallel to $x,\frac{1}{2},\frac{1}{2}$ and $x,\frac{1}{2},1$, described earlier. The cross - sectional circumference of the carbon tetrachloride molecules are shown at each layer. The channels reach their widest between x=.70 to .80 with a cross-section of about

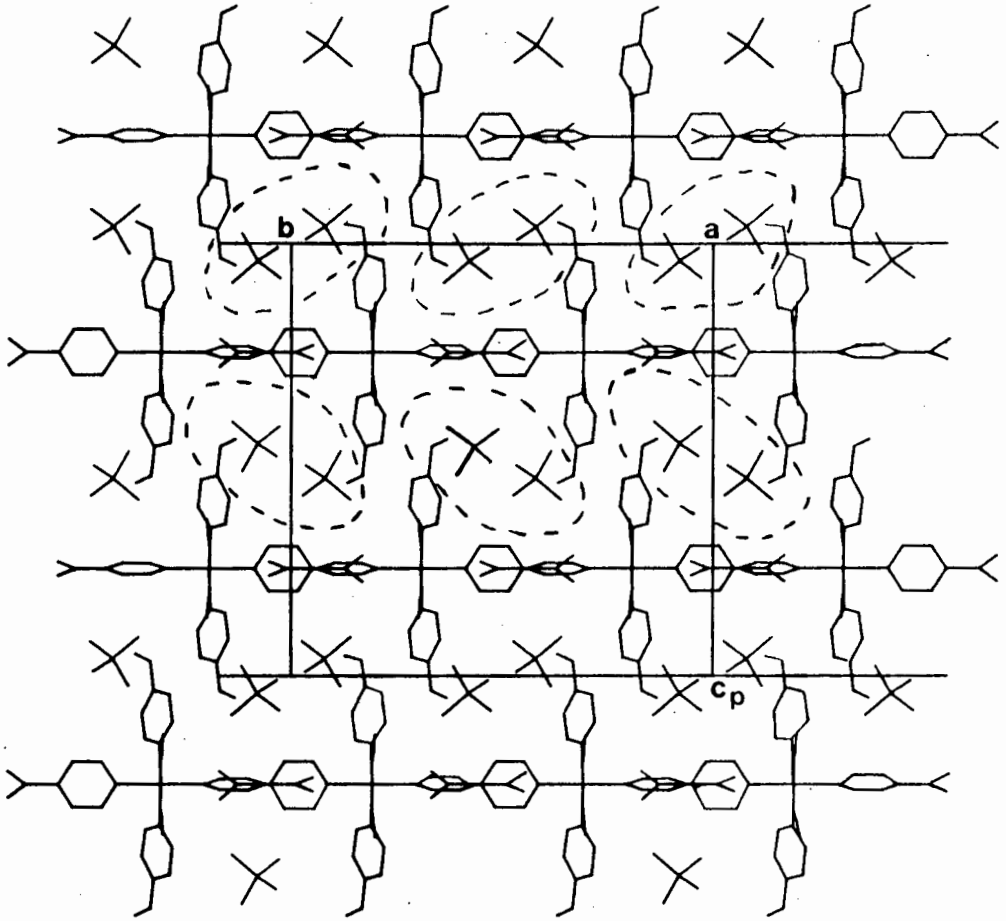

STRUCTURE II
C2/c

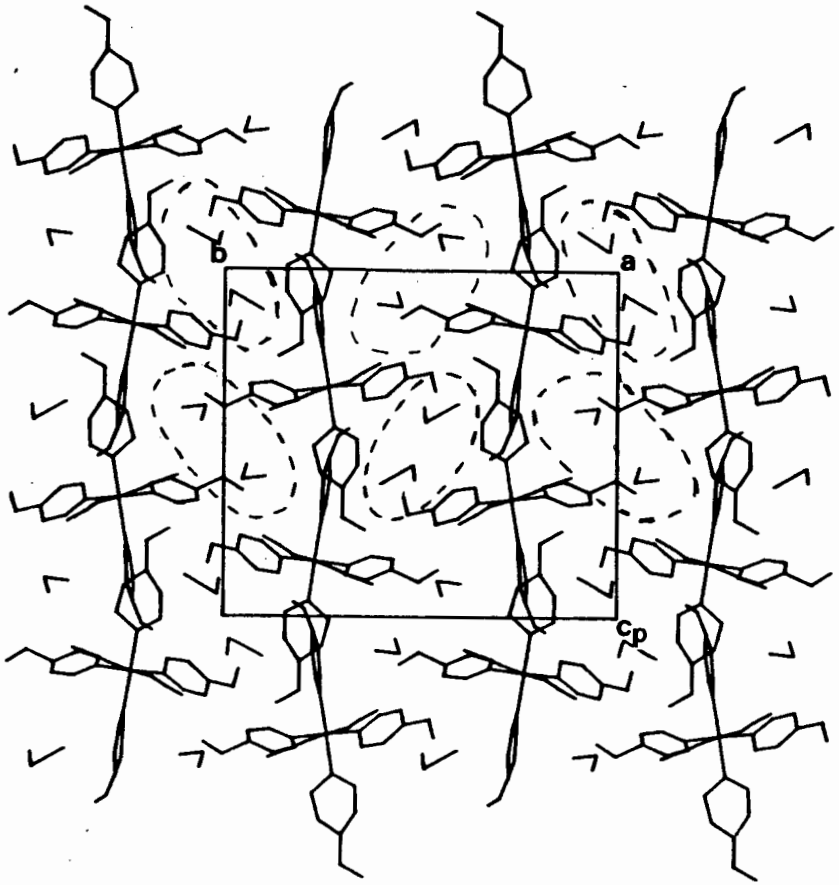

STRUCTURE I
$P2_1/c$

Fig 4.4 Packing diagrams looking down [1 0 0] of STRUCTURES I and II showing their similar packing arrangement. The channel cross - sections are shown as dashed lines.

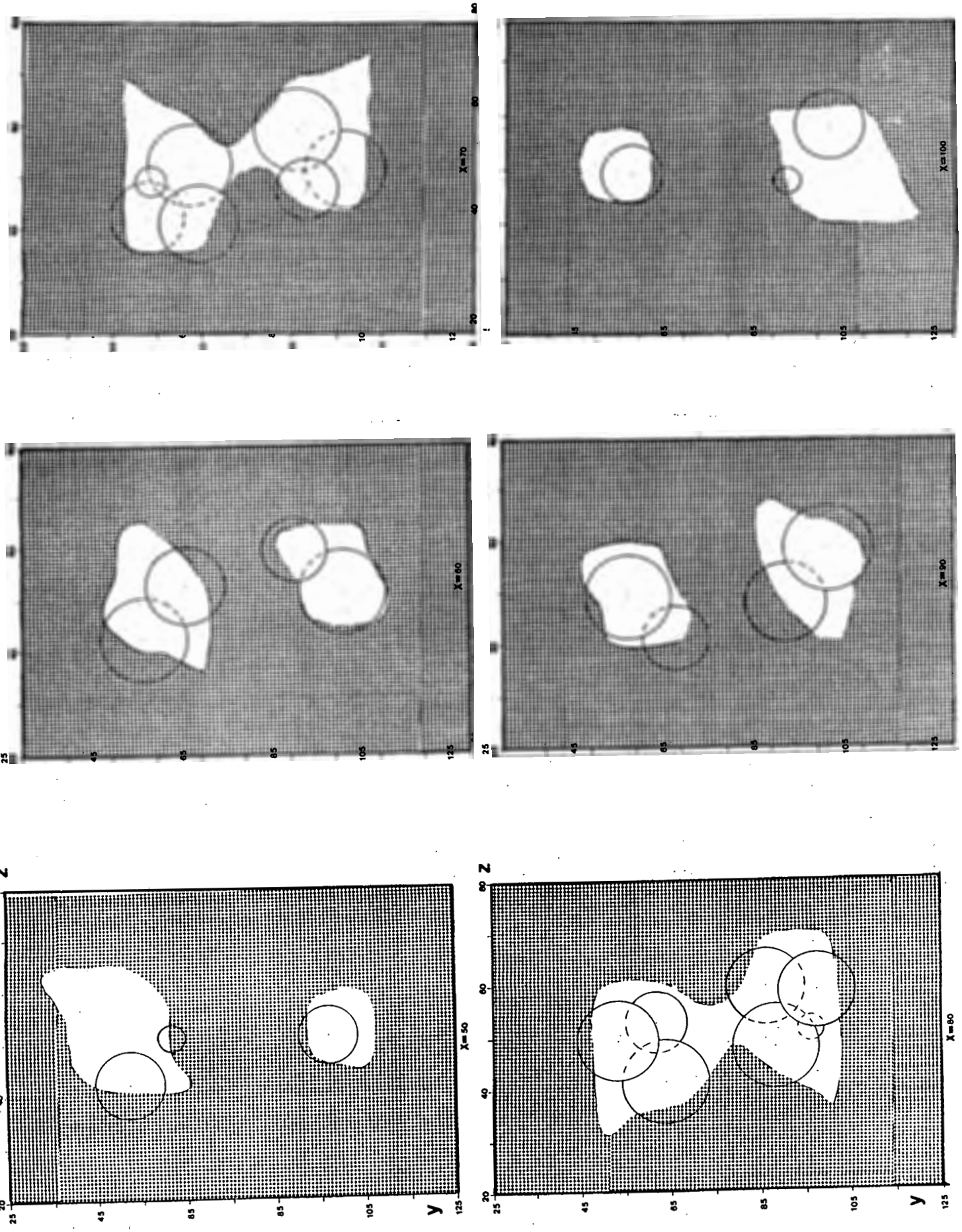

Fig 4.5 Cross - sections from x=.50 to x=1.0 of STRUCTURE II (OPEC).

5.3Å x 5.3Å into which the carbon tetrachloride molecules fit snugly .

The relation of the channels with respect to the host molecules are shown in the stereographic drawing, fig 4.6, which is calculated from OPEC. The channels zig - zag parallel to x, with every second segment being wide enough to accommodate 2 guest molecules. This constriction in the channel confines the carbon tetrachloride molecules and probably accounts for the thermal stability of this clathrate. At 25 °C there is very little weight loss after 6-7 hours exposure to the atmosphere.

From OPEC it can be seen that the two channels are in fact connected by a narrow passage which runs between the isothiocyanate groups. This is not seen with EENY, probably because the passage is too narrow to allow a hydrogen molecule to pass through without a steep rise in potential energy.

4.3.4 STRUCTURE III

$Ni(NCS)_2(4\text{-}ViPy)_4.1.8CH_2I_2$ (III)

The diiodomethane clathrate crystallises in the $I4_1/a$ space - group. Although the nickel atoms of the host molecules sit at the normal position found for the β-phase clathrates, it was noticed that the NCS group of STRUCTURE III was slewed by 90° relative to the NCS groups reported for the chloroform and xylene clathrates of the same host. For the Ni atom at 0.500 0.250 0.540 the sulphur atom is at 0.248 0.373 0.553 in the chloroform and xylene clathrates, and is located at 0.245 0.132 0.528 in STRUCTURE III. The atomic coordinates of the host reported here can be transformed to those of the host molecule in its chloroform and xylene clathrates by applying the matrix below:

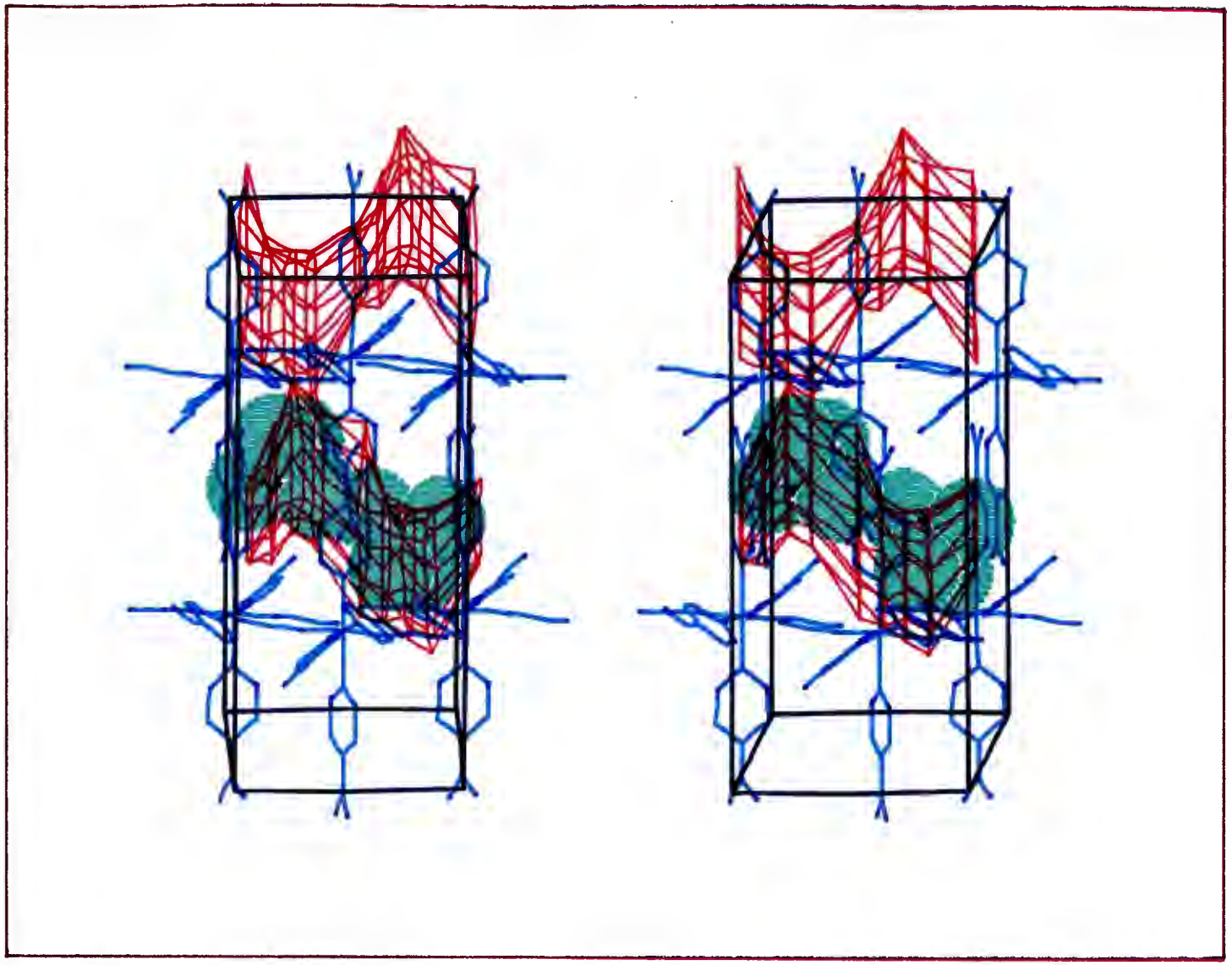

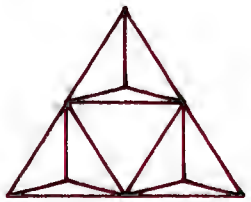

Alchemy

TRIPOS Associates

St. Louis, Mo.

$$\begin{pmatrix} x' \\ y' \\ z' \end{pmatrix} = \begin{pmatrix} 1 & 0 & 0 \\ 0 & -1 & 0 \\ 0 & 0 & 1 \end{pmatrix} \begin{pmatrix} x \\ y \\ z \end{pmatrix} + \begin{pmatrix} 0 \\ \frac{1}{2} \\ 0 \end{pmatrix}$$

where x,y,z are the coordinates of an atom in STRUCTURE III and x',y',z' are the coordinates of that atom reported in the xylene and chloroform clathrates of $[Ni(NCS)_2(4\text{-ViPy})_4]$. This is illustrated in fig 4.7(a).

It is necessary to take the inverse transpose of the above matrix to see what affect it has on the cell parameters. As it works out the above matrix is the inverse transpose of itself, and so we obtain:

$$\begin{pmatrix} a' \\ b' \\ c' \end{pmatrix} = \begin{pmatrix} 1 & 0 & 0 \\ 0 & -1 & 0 \\ 0 & 0 & 1 \end{pmatrix} \begin{pmatrix} a \\ b \\ c \end{pmatrix} + \begin{pmatrix} 0 \\ \frac{1}{2} \\ 0 \end{pmatrix}$$

where a,b,c are the cell parameters in STRUCTURE III and a',b',c' are those in the usually reported clathrates. Therefore this transformation is effectively moving the origin to $0,\frac{1}{2},0$ and then reversing the direction of b, which transforms the cell reported here to that usually reported for the β-phase clathrates of $[Ni(NCS)_2(4\text{-ViPy})_4]$. The view down [0 0 1] is shown in fig 4.7(b).

The potential energy study of the channels in this structure reveal that they are very similar to that found in the unsolvated β-phase clathrate of the same host[4,16].

Potential energy cross - sections in layers of z, at .05 intervals revealed the channel network of this crystal structure. It is criss - crossed by channels running parallel to the x and y axes. The channels at y=.75 (.25 along c), x=.00 (.50 along c) and y=.25 (.75 along c) are

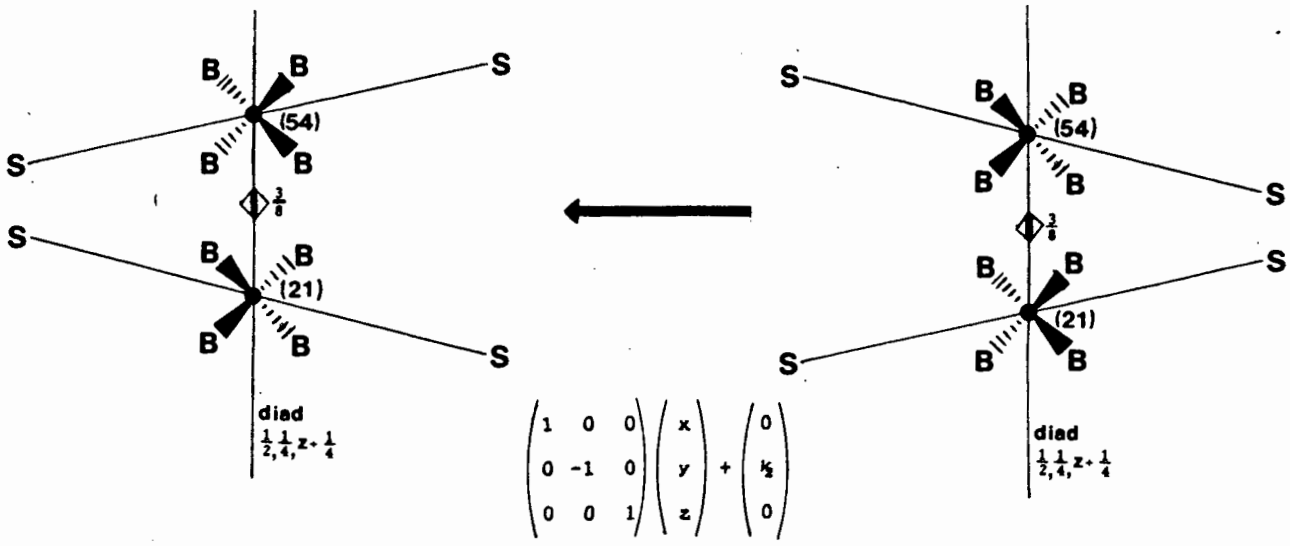

Fig 4.7(a) Schematic diagram of the orientation of the host molecules in STRUCTURE III (on the right), which can be transformed to that usually reported for the ß-phase clathrates of $Ni(NCS)_2(4\text{-}ViPy)_4$[4.17] by applying the above matrix.

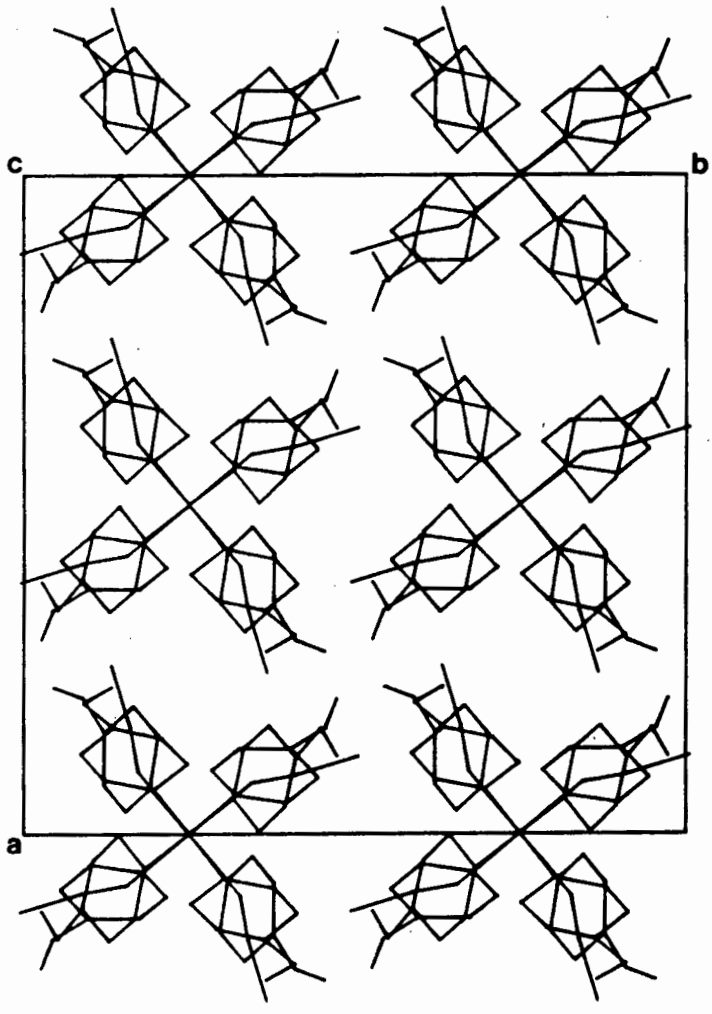

Fig 4.7(b) Packing diagram of STRUCTURE III looking down [0 0 1]. (guest excluded)

shown as dashed lines in fig 4.8. Only two of the disordered CH_2I_2 molecules have been shown for the sake of clarity. These layers are shown in fig 4.9 ,from z=.25 to z=.50. On inspection of these sections the channels are seen to be composed of a string of cavities of irregular cross - section, zig - zagging in the general direction of $\underline{x}$, and linked together by narrow tunnels running through the centres of symmetry. In the majority of β-phase clathrates the guest molecules have been located in these tunnels, at the inversion centres called by Wyckoff position d.

However, in this clathrate the diiodomethane molecules are found in the large cavities which encompass the $\bar{4}$ centres, Wyckoff position b. The one iodine composed of peaks I1 and I2 appears to be sitting mainly in the channel while the other iodine(peaks I3, I4 and I5) sits entirely in the cavity. Between z=.25 and z=.50 the cavity must twist by 90° as a consequence of the four - fold inversion centres and the four - fold screw axes and we can see that this occurs quite sharply between z=.35 and z=.40 i.e in the space of 1.36Å. This change in direction of the cavity places this iodine in a region of high potential energy, and so the shape of the cavity is probably a contributing factor in the disorder of this atom. If one looks at the diagrams of the cross-sections for the carbon-tetrachloride and iodoform clathrates, figs 4.5 and 4.11, respectively, it is seen that the guest molecules fit nicely into the cavities, extending out of their cavities in places. The cavity for the diiodomethane molecules has a cross-section of approximately 4.5Å x 11.0Å, and it appears that this void formed by the host molecules is too large to accommodate four CH_2I_2 molecules so that they are effectively held in position.

4.3.5 STRUCTURES IV and V

$Ni(NCS)_2(4\text{-}ViPy)_4.CHI_3$ **(IV)** and

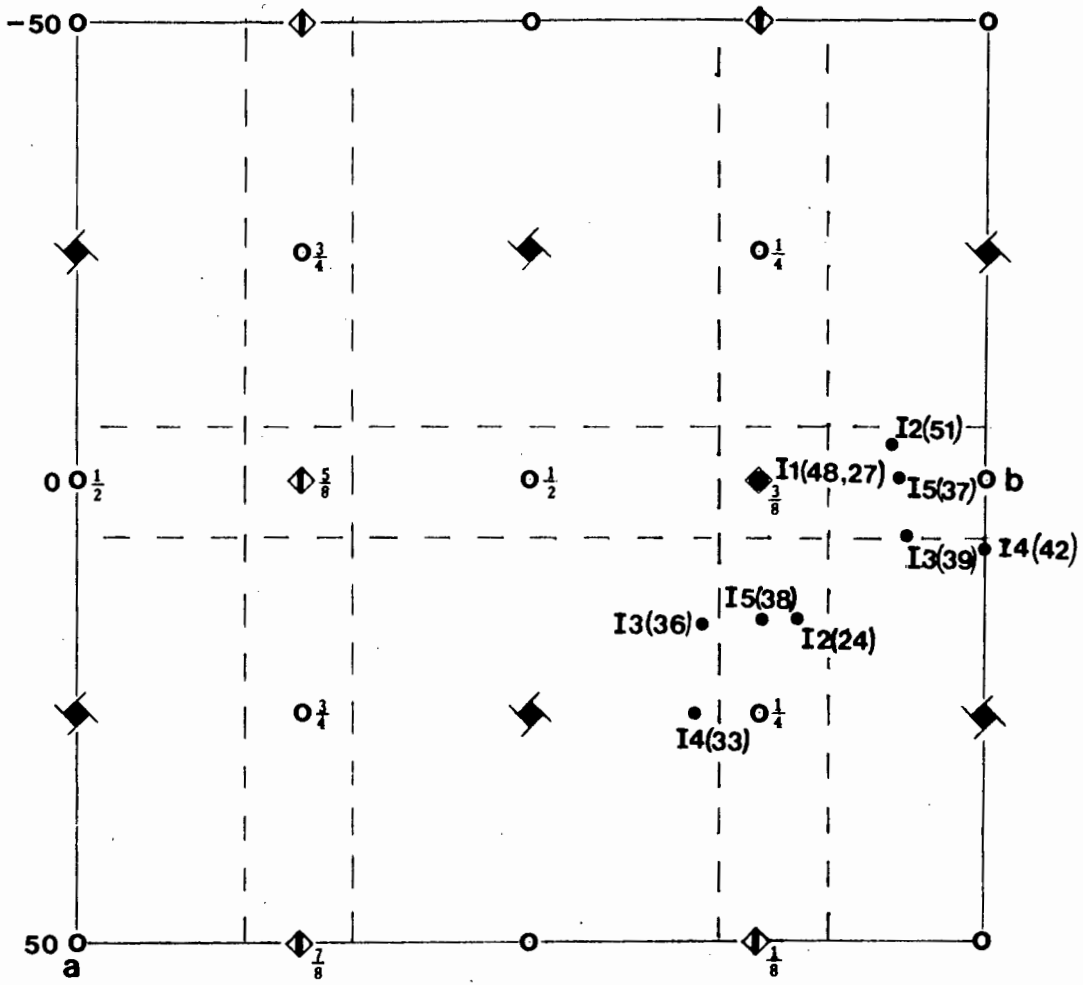

Fig 4.8 Channel pattern in STRUCTURE III. The dashed lines show the channel system passing through the inversion centres at the heights indicated. Two of the disordered guest molecules are shown around the 4 centre at 3/8 along c.

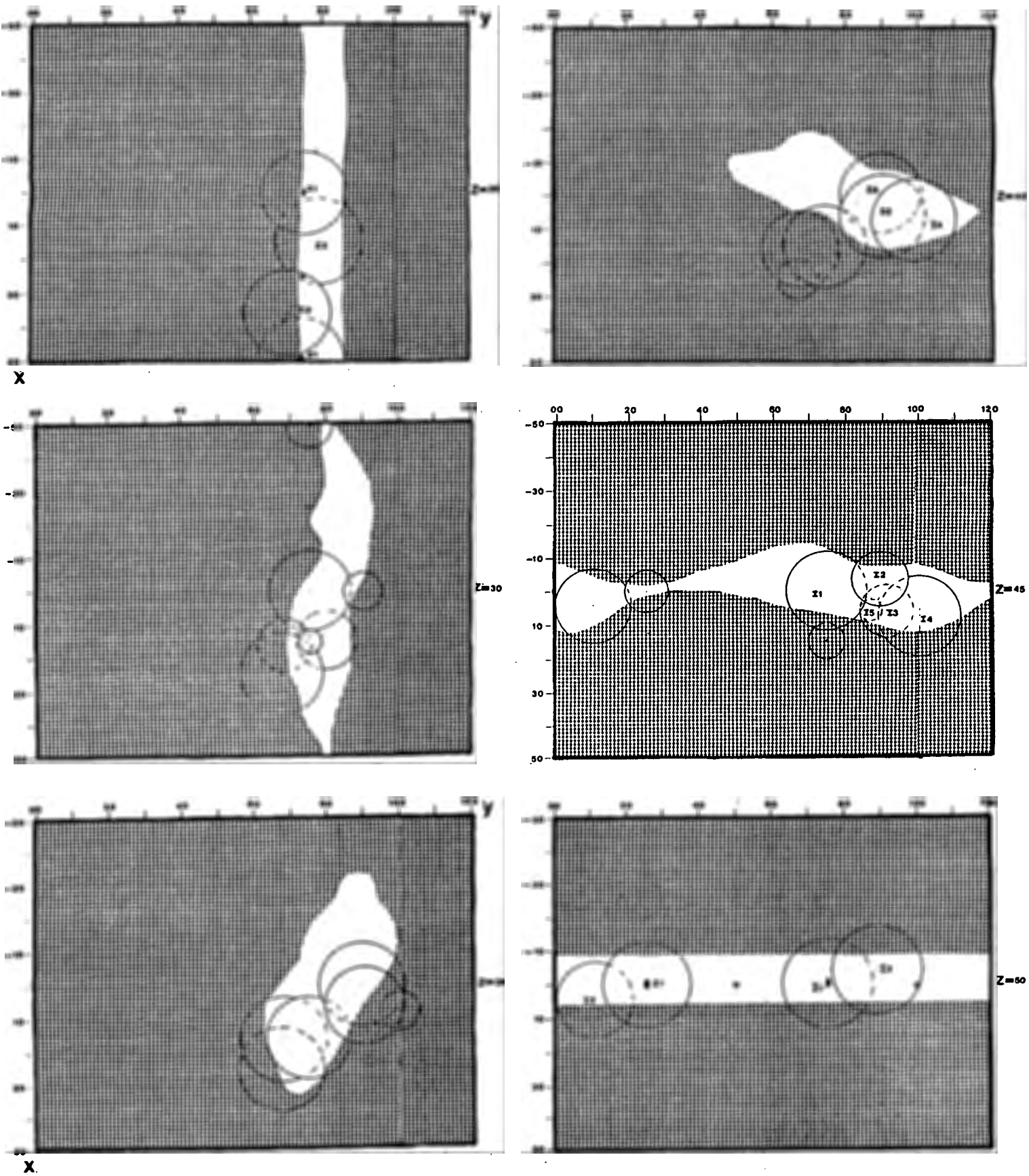

Fig 4.9 Cross - sections from z=.25 to z=.50 of STRUCTURE III(EENY). The two disordered CH_2I_2 molecules areshown in the cavity around the $\bar{4}$ centre at 3/8 along c.

$[Ni(NCS)_2(4\text{-}ViPy)_4].[Ni(NCS)_2(4\text{-}ViPy)_3(thf)].2CHI_3$ **(V)**

The $Ni(NCS)_2(4\text{-}ViPy)_4.CHI_3$ compound has Pbca symmetry and the $[Ni(NCS)_2(4\text{-}Vipy)_4][Ni(NCS)_2(4\text{-}ViPy)_3(thf)].2CHI_3$ compound has $P2_1/c$ symmetry. These two structures, however, display a very similar packing arrangement. Fig 4.10 shows a projection down [1 0 0] for both structures, which reveals this similarity. The replacement of every eighth 4-vinylpyridine ligand in STRUCTURE IV by a thf moiety has served to skew the packing arrangement, with β going from 90° to 96.58°. There is also a loss of symmetry on going from Pbca to $P2_1/c$. This is discussed further in Chapter 6.

EENY and OPEC were used to map out the cavities in STRUCTURE IV. The unit cell was studied in layers of $\underline{x}$. Elongated, S - shaped cages, running parallel to $\underline{x}$ and narrowing at both ends were revealed. The contour of two of these cavities at each cross - section, calculated from OPEC, and centred at $x,\frac{1}{2},\frac{1}{2}$ and $x,0,\frac{1}{2}$ are shown in fig 4.11. The iodoform molecules are shown in each layer. The cage at $x,\frac{1}{2},0$ runs more or less between x=.10 and .90 and so spans about 12.8Å. At x=.50 the channel has a width of approximately 10Å, although there is a constriction in the middle of the cavity in this layer which has confined one of the iodoform iodines to lie on one side of the void. The stereographic drawing, fig 4.12, shows the channels in relation to the host molecules, calculated from EENY.

The shape and size of the channels using EENY is again very similar to those obtained with OPEC. As can be seen from figs 4.6 and 4.12, in certain regions the space - filled guest molecules protrude an appreciable amount from their zero potential energy and van der Waals contoured channels. This would appear to indicate a certain degree of host - guest interaction between certain constituents of the host molecules and the guest. This is particularly so for the

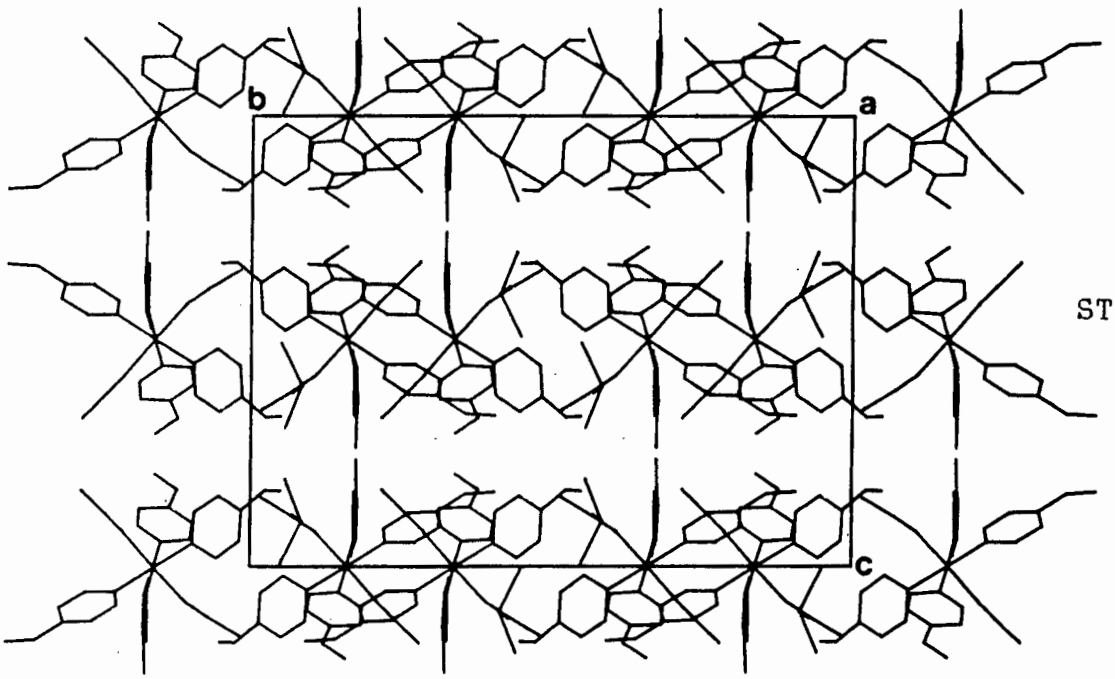

STRUCTURE IV
Pbca

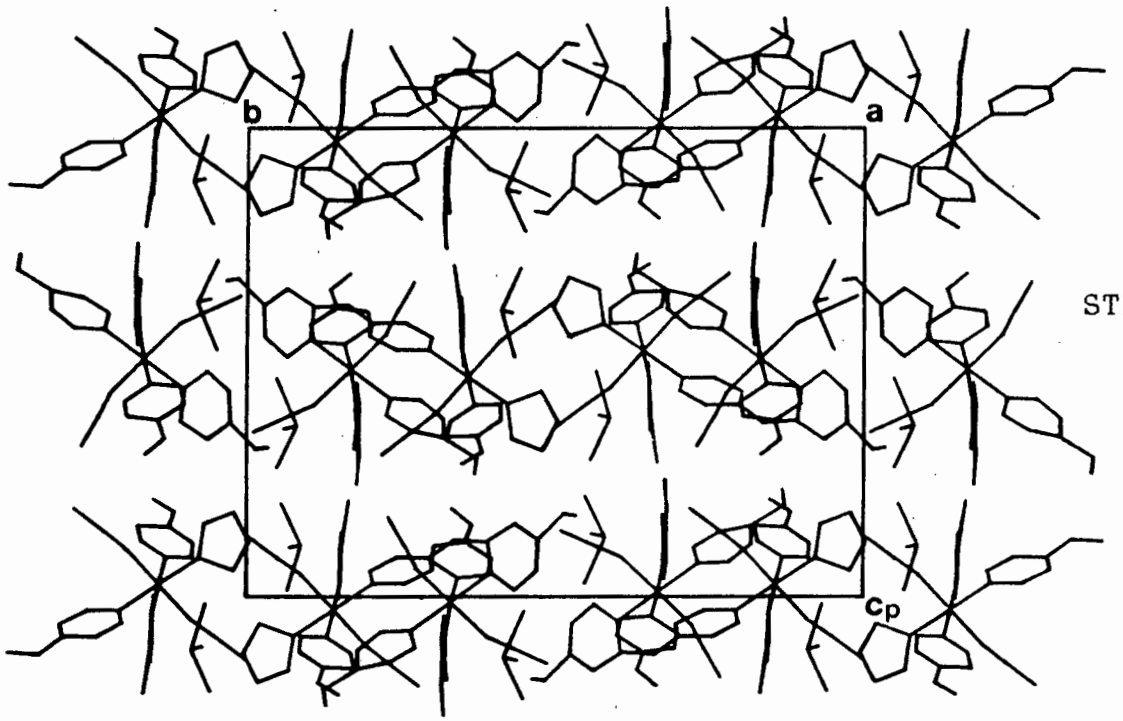

STRUCTURE V
P2₁/c

Fig 4.10 Packing diagrams of STRUCTURES IV and V looking down [1 0 0]. ß in STRUCTURE V has been 6.58°skewed from 90°.

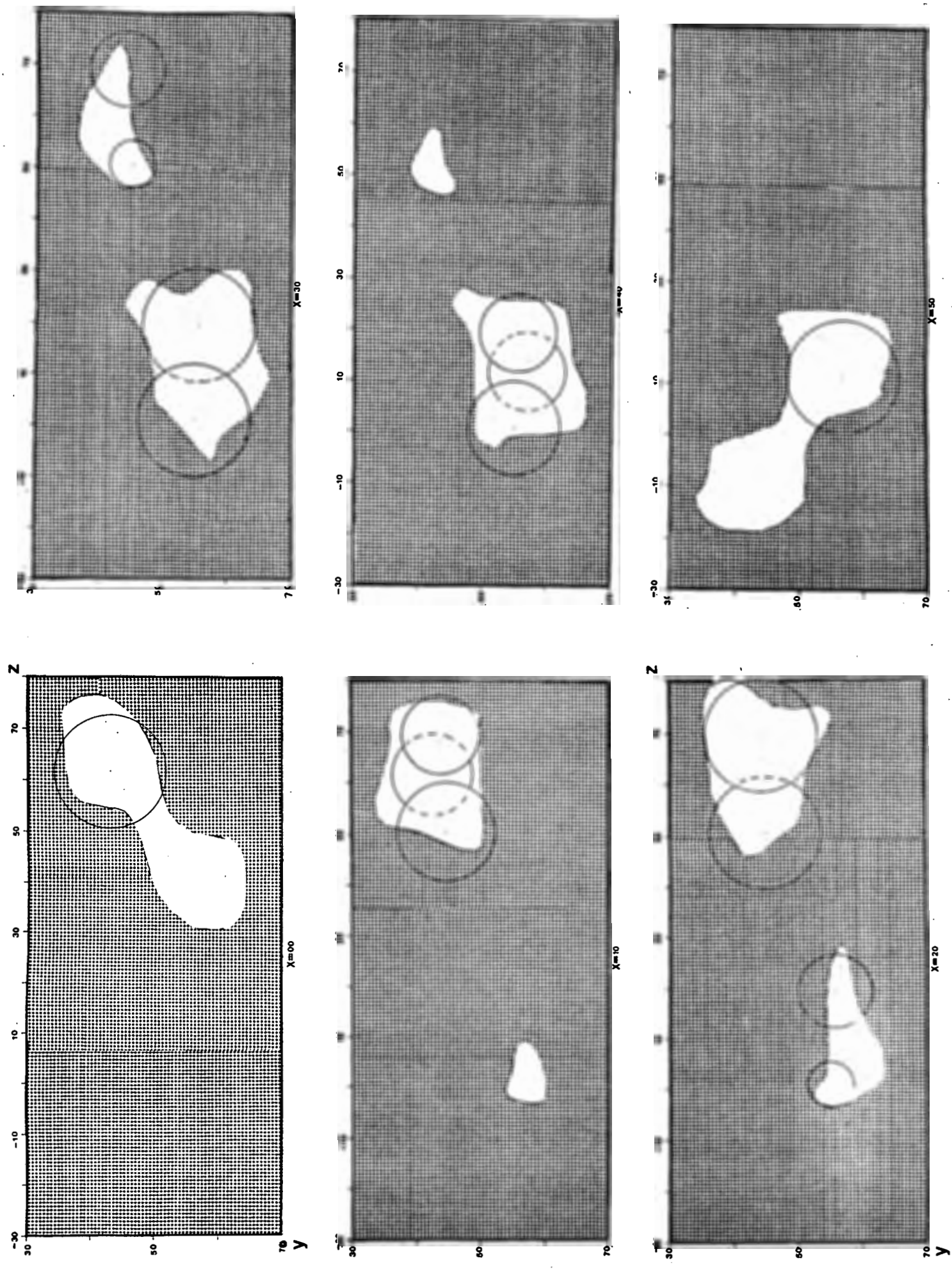

Fig 4.11 Cross - sections from z=.00 to z=.50 of STRUCTURE IV (OPEC).

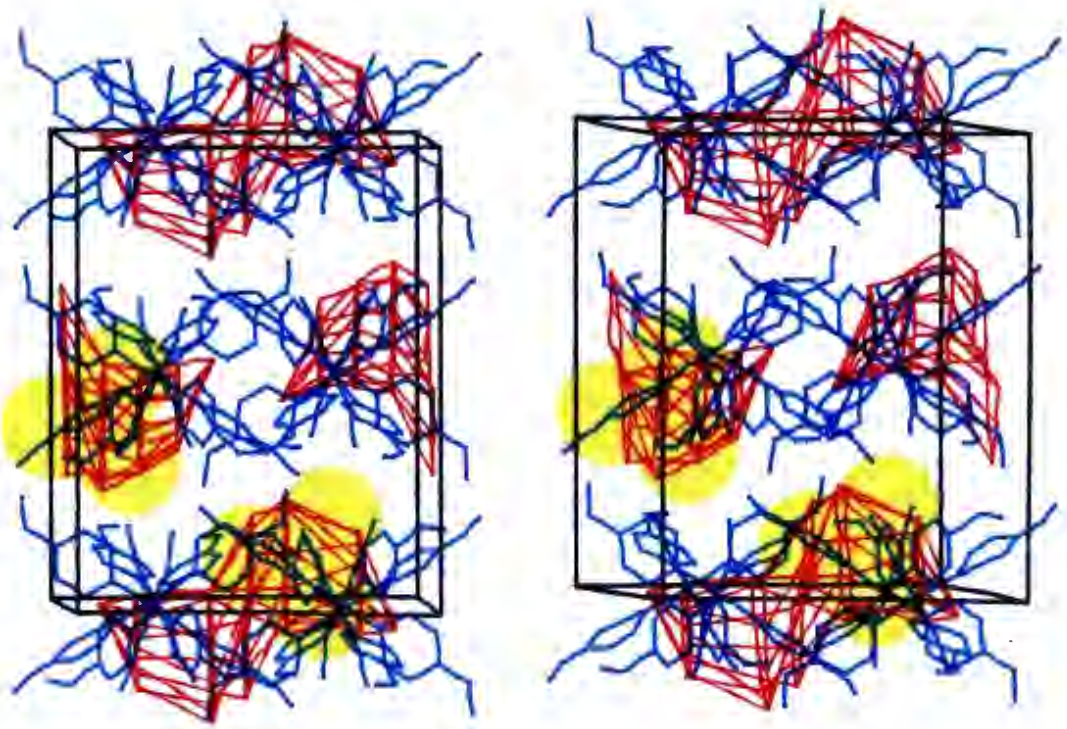

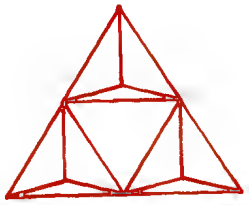

Alchemy

TRIPOS Associates

St. Louis, Mo.

iodoform clathrates, where the sulphur atom interacts considerably with the iodines to form a secondary bond, discussed further in Chapter 6.

4.4 Packing densities and volume comparisons

4.4.1 Packing densities

The packing density is expressed as the volume per non - hydrogen atom and the values for each structure are given in TABLE 4.4. The values for the α-phase[4.17], p-xylene[4.17] and $CHCl_3$[4.18] clathrates are also included for comparison.

We can see that the δ-phase clathrates of CH_2Cl_2, $CHCl_3$ and CCl_4 have a similar packing efficiency, with the CCl_4 clathrate being just a bit more efficiently packed than the other two. This corresponds to lower temperature factors for the chlorine atoms of the carbon tetrachloride guest molecules compared to those of the dichloromethane and chloroform molecules i.e less thermal disorder for the CCl_4 molecules.

In the β-phase clathrate of $Ni(NCS)_2(4\text{-}ViPy)_4$.p-xylene, the guest is well - ordered and this clathrate packs more efficiently than the α-phase (packing density of 19.7). Even for the β-phase clathrates of m- and o-xylene, where the guest is disordered around the centre of inversion (packing densities of 20.1 and 20.3 respectively), are these clathrates better packed than for the $I4_1/a$ clathrate of CH_2I_2, which has a packing density of 21.8. This would also appear to indicate disordering of the CH_2I_2 molecules,and possibly that occupation of the cavity around the $\bar{4}$ centre results in less efficient packing than when the guest molecules sit in the channels around the inversion centres.

TABLE 4.4 Packing densities (volume per non - hydrogen atom)

COMPOUNDS*	SPACE - GROUP	TYPE OF CAVITY	VOLUME/NON-HYDROGEN ATOM
H(α-phase)	Pbca	-	19.9
H.2CH_2Cl_2	$P2_1/n$	Channel	21.5
H.2$CHCl_3$	$P2_1/n$	Channel	21.5
H.2CCl_4	C2/c	Channel	21.3
H.1.8CH_2I_2	$I4_1/a$	crossed - channels	21.8
H.p-xylene	$I4_1/a$	crossed - channels	19.7
H.CHI_3	Pbca	Cage	22.5
H.H'.2CHI_3	$P2_1/c$	Cage	22.3

* H = $Ni(NCS)_2(4\text{-ViPy})_4$

and

H' = $Ni(NCS)_2(4\text{-ViPy})_3(thf)$

The iodoform clathrates are found to have very similar packing efficiencies,with the thf substituted compound being slightly better packed.

4.4.2 Volume comparisons

An interesting approach to calculate the theoretical volume occupied by each guest molecule is to assume that the volume of a host molecule, taken as $V_\alpha/8$ where V_α is the volume of the α-phase, remains constant in each structure. The total volume occupied by the guest molecules is then

$(V_{clath} - Z\ V_\alpha/8)$, and dividing this by the number of guest molecules in the unit cell gives a theoretical volume occupied by each guest molecule. These values are given in TABLE 4.5 , as well as the theoretical volume of each type of guest molecule calculated from Kitaigorodsky[4.19]. An approximate value of the cavity volume/number of guests in the cavity determined from OPEC is also given.

For the CH_2Cl_2, $CHCl_3$ and CCl_4 clathrates the theoretical volume occupied increases as the size of the guest molecule increases. This increase is linear, and by extrapolating back to a guest molecule with zero volume, the volume occupied by this point in space is 48.6Å (fig 4.13). This may well correspond to the β_o structure discussed in Chapter 1, and the total volume of this proposed intermediate is 3486.2Å (4 host molecules plus 8 volumes of 48.6Å each). A possible way of checking this would be to find the volume of the clathrate of the 4-vinylpyridine host with a small molecule e.g methanol, which would approximate that of the β_o structure, and to see how it compares with the one calculated above. If this is the case then the empty β_o structure swells by as much as 11% for the CH_2Cl_2 clathrate and 20% for the CCl_4 clathrate as the guest molecules enter

TABLE 4.5 Volume comparisons

$V_\alpha/8 = 774.4$ Å^3

COMPOUND*	$V_{theor.}$ occupied by guest molecule (Å^3)	$V_{theor.}$ of guest (Å^3)	V of cavity/no. of guests in the cavity(OPEC) (Å^3)
H.2CH_2Cl_2	97.6	49	-
H.2$CHCl_3$	117.9	67	-
H.2CCl_4	134.1	85	110
H.1.8CH_2I_2	96.5	85	80
H.CHI_3	193.4	121	200
H.H'.2CHI_3	149.9	121	-

*

H = $Ni(NCS)_2(4\text{-ViPy})_4$

and

H' = $Ni(NCS)_2(4\text{-ViPy})_3(thf)$

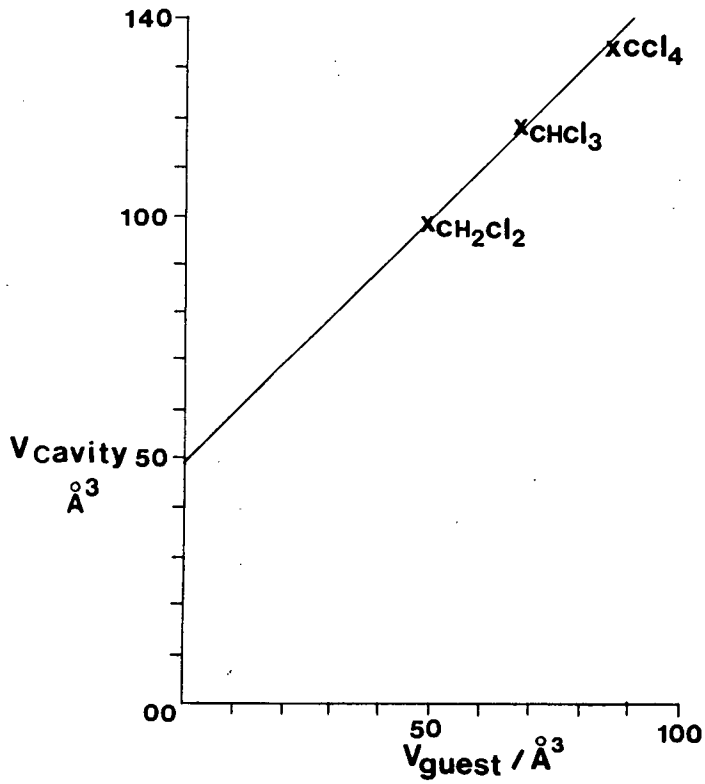

Fig 4.13 Graph of the volume of the guest molecules(Å^3) versus the theoretical volume occupied by each guest for the $Ni(NCS)_2(4\text{-ViPy})_4$ clathrates of CH_2Cl_2, $CHCl_3$ and CCl_4.

its pores. The theoretical volume occupied by the guest is 1.6 - 2.0 times larger than the actual volume of the guest molecules which is an indication of the porous nature of these clathrates.

On the other hand in the case of STRUCTURE III the volume occupied by the CH_2I_2 molecule, both from the theoretical approach (96.5Å^3) and calculated from OPEC (80Å^3), agree closely with the volume of CH_2I_2 (85Å^3). This substantiates the picture of four diiodomethane molecules packed closely in the cavity with very little space to spare.

In STRUCTURES IV and V it appears as if the substitution of every eighth 4-vinylpyridine ring by a thf ligand has resulted in quite a large decrease in the volume available for the iodoform molecules.

Chapter 4 References

4.1 J. Lipkowski; in 'Inclusion Compounds', edited by J.L Atwood, J.E.D Davis, D.D Macnicol; Academic Press; New York, vol. 1, Chapter3 (1981)

4.2 D.R Bond, G.E Jackson and L.R Nassimbeni, S. Afr. J. Chem., 36, 19 (1983)

4.3 F. Madaule - Aubry, W.R Busing and G.M Brown, Acta Cryst., B24, 754 (1968)

4.4 J. Lipkowski, J. Mol. Struct., 75, 13 (1981)

4.5 A. Guarino, G. Occhiucci, E. Possagno and R. Bassanelli, Spectrochimica Acta, 33A, 199 (1977)

4.6 L.R Nassimbeni, S. Papanicolaou and M.H Moore, J. Incl. Phenom., 4, 31 (1986)

4.7 E. Giglio, Nature, 222, 339 (1969)

4.8 S. Candelero De Sanctis and E. Giglio, Acta Cryst., B35, 2650 (1979)

4.9 E. Giglio, J. Mol. Struct., 75, 39 (1981)

4.10 G. Del Re, E. Gavuzzo, E. Giglio, F. Leij, F. Mazzo and V. Zappia, Acta Cryst., B33, 3289 (1977)

4.11 E. Giglio and C. Quagliata, Acta Cryst., B31, 743 (1975)

4.12 W. Fedeli, F. Mazza, E. Giglio, C. Quagliata and N. Scarcelli, Acta Cryst., B32, 878 (1976)

4.13 A. Gavezzotti, OPEC organic packing energy calculations program, J. Am. Chem. Soc., 105, 5220 (1983)

4.14 K. Mirsky, in 'Computing in Crystallography, Proceedings of an International Summer school on Crystallographic computing'; Delft, Univ. Press: Twente, 1978, p 169.

4.15 L.R Nassimbeni, S. Papanicolaou and M.H Moore, J. Incl. Phenom., 4, 31 (1986)

4.16 E. Rodulfo de Gil and I.S Kerr, J. Appl. Cryst., 10, 315 (1977)

4.17 M.H Moore, L.R Nassimbeni, M.L Niven and M.W Taylor, Inorg. Chim. Acta, 115, 211 (1986)

4.18 M.H Moore, L.R Nassimbeni and M.L Niven, Inorg. Chim.

Acta, 131, 45 (1987)

4.19 A.I Kitaigorodsky,'Molecular Crystals and molecules', Academic Press, New York, 1973, Chap. 1.

CHAPTER 5

Thermal analysis - a thermogravimetric and differential thermal analysis study of compounds I to V

5.1 Introduction

Thermogravimetry(TG) involves measuring the mass of a sample as its temperature is increased. A plot of mass versus temperature permits evaluation of the thermal stability of the sample. The thermal decomposition of Werner clathrates involves a mass loss which occurs in a number of steps, the first stage being the loss of guest, accompanied by or followed soon after by the decomposition of the host. Thermogravimetry proves useful since these mass changes are directly related to the specific stoichiometries of the clathrates. As a consequence this method can often be used to verify the guest content in the clathrate (although some guest may be lost during sample preparation).

Differential thermal analysis is the monitoring of the difference in temperature between a sample and a reference compound as a function of temperature. Differences in temperature between the sample and an inert reference substance will be observed when changes that involve a finite heat of reaction, such as chemical reaction or structural changes, occur in the sample. If $\triangle H$ is positive (endothermic reaction), the temperature of the sample lags behind that of the reference. If $\triangle H$ is negative (exothermic reaction), then the sample temperature exceeds that of the reference. Fig 5.1 shows a DTA curve for these two cases. An important aspect of DTA is that the area under the peak is proportional to the heat of reaction and the amount of material present, and thus permits quantitative analysis. This is discussed later on.

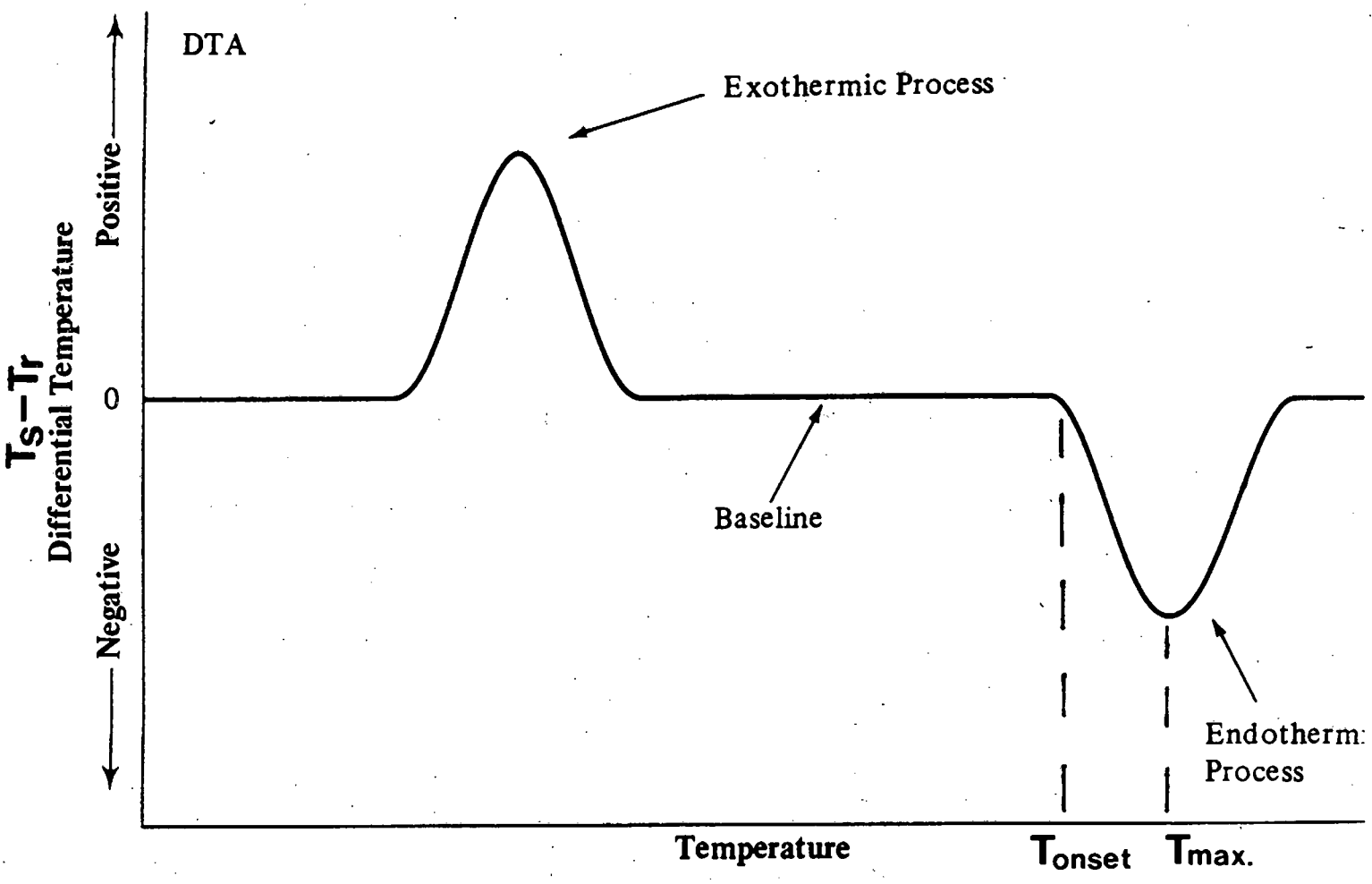

Fig 5.1 Illustration of a differential thermal analysis (DTA) curve, showing peaks corresponding to exothermic and endothermic events.

The reference material used should have the following characteristics:

(a) It should undergo no thermal events over the operating temperature range.
(b) It should not react with the sample holder or the thermocouple.
(c) Its thermal conductivity and heat capacity should be similar to those of the sample.

The reference used in this study was alumina, Al_2O_3. The samples were heated in an inert nitrogen atmosphere (flow rate was 60ml/min.)

5.2 Thermal analysis of Werner clathrates

Quantitative thermal measurements on $[MX_2B_4]$ complexes have been reported since the mid 1960's[5.1-5.3]. The course of their thermal decomposition cannot be given a simple general description. Thermogravimetric curves have shown that dissociation of the four bases may proceed in four, three or two steps[5.4-5.8]. Casellato and Casu[5.8] have classified clathrates of $[MX_2B_4]$ complexes as either thermally stable or unstable. Clathrates which dissociate into host and guest before thermal decomposition of the host begins are regarded as thermally unstable, whereas in the decomposition of stable clathrates chemical destruction of the host accompanies escape of the guest component. Fig 5.2 shows the TG and DTA curves for the $[Ni(NCS)_2(4\text{-}MePy)_4]$ clathrates of benzene and p-xylene. $[Ni(NCS)_2(4\text{-}MePy)_4].C_6H_6$ is an example of a thermally unstable compound since the first step in the TG analysis curve corresponds to the loss of one benzene guest molecule per host molecule. The analogous step in the TG curve of $[Ni(NCS)_2(4\text{-}MePy)_4]$.p-xylene corresponds to concurrent partial destruction of the host molecule and removal of the guest, and thus is considered thermally stable.

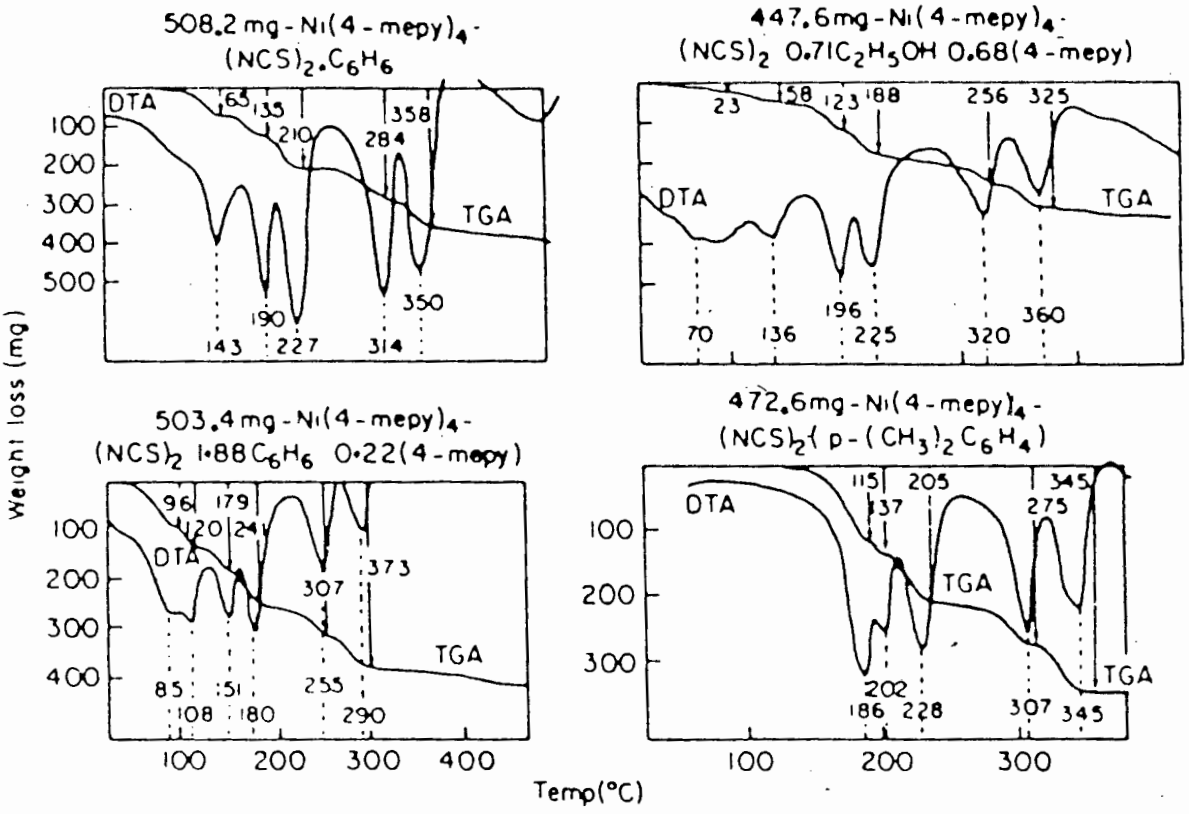

Fig 5.2 TG and DTA curves for some clathrates of the [Ni(NCS)2(4-MePy)4] complex[5.9].

Inclusion compounds having high guest:host molar ratios, corresponding to layer-type structures, are generally less thermally stable than the zeolite-like β-phases[5-8]. Fig 5.2 illustrates the thermal analysis of two different benzene inclusion compounds of $[Ni(NCS)_2(4\text{-}MePy)_4]$ having approximate 1:1 and 2:1 benzene:host molar ratios. Maxima in DTA curves, corresponding to desorption of the guest are observed at about 143 °C for the 1:1 clathrate and 108 °C for the 2:1 clathrate.

5.3 Determination of enthalpy changes for a thermal event in DTA

During an endothermic event the temperature of the sample, T_s, lags behind the temperature of the reference, T_r, which follows the heating programme. For an exothermic event the sample temperature is greater than that of the reference. If $\triangle T$ $(=T_s-T_r)$ is recorded against T_r(or the furnace temperature, $T_f=T_r$) then of course an exothermic process will have a positive value of $\triangle T$, and an endothermic process a negative value, shown in Fig 5.1. Every event is characterised by its onset temperature (T_{onset} in Fig 5.1) which is quoted as the sample temperature, T_s, in Table 5.1 and marked by arrows on the abscissae of each compound in the DTA curves of Compounds I to V, fig's 5.3 and 5.4.

The temperature at which the recorder response is at its maximum distance from the baseline (T_{max} in fig5.1) is not reported here because it is very dependent upon the heating rate used in the temperature programme and factors such as sample size and thermocouple position. The DTA peak areas are assumed to be proportional to the heat of reaction and upon the amount of material, and are related by the equation

$$A_s K = \triangle Hm_s \qquad \text{eqn. 1}$$

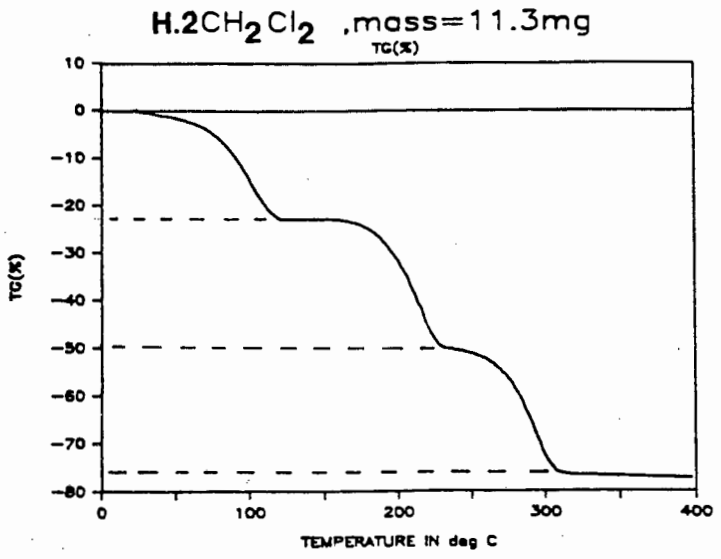

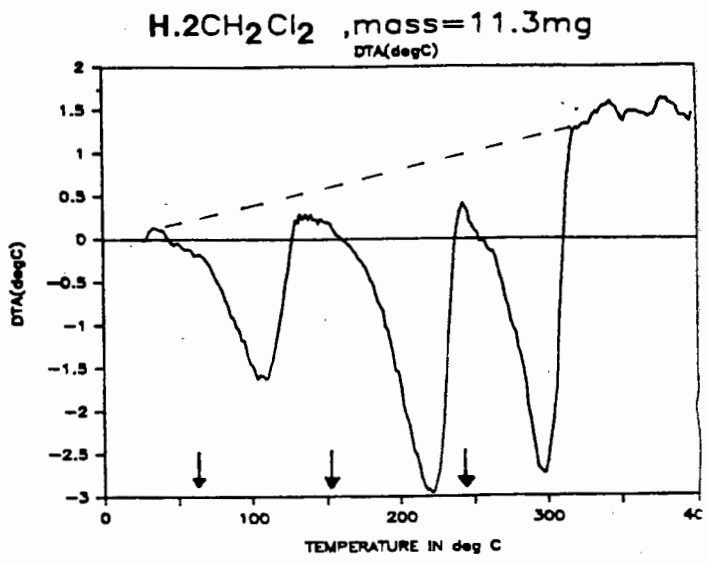

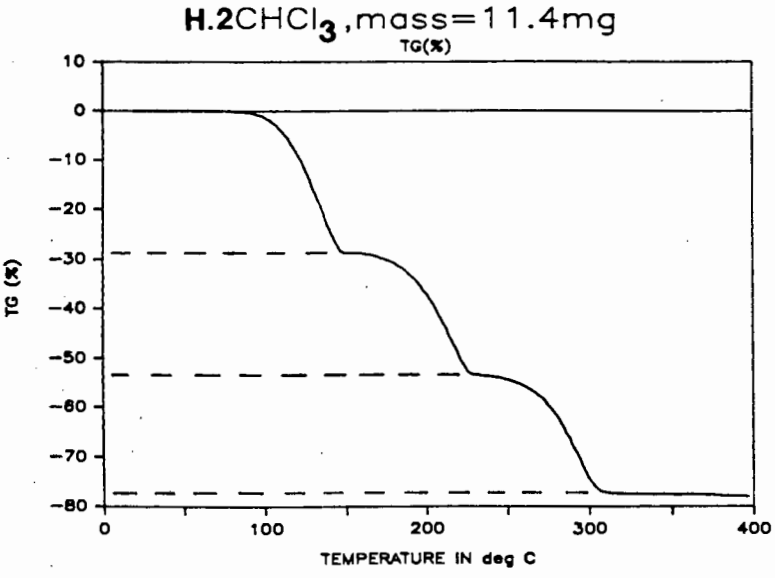

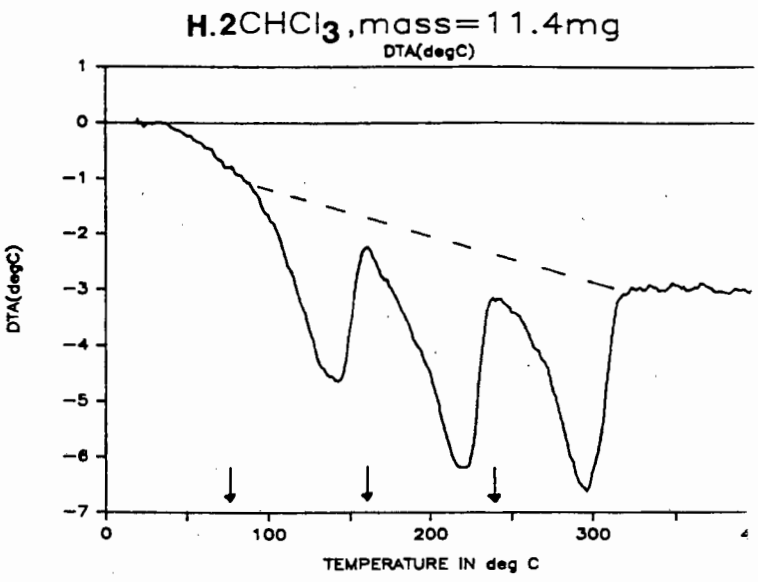

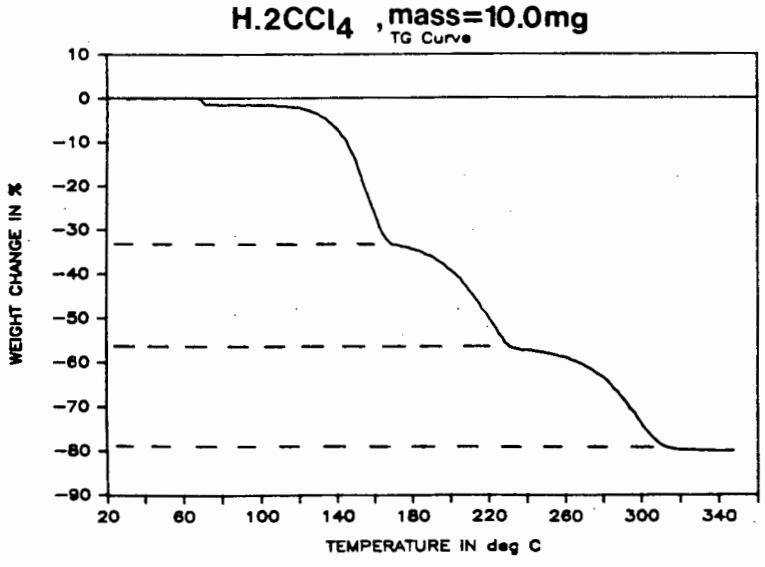

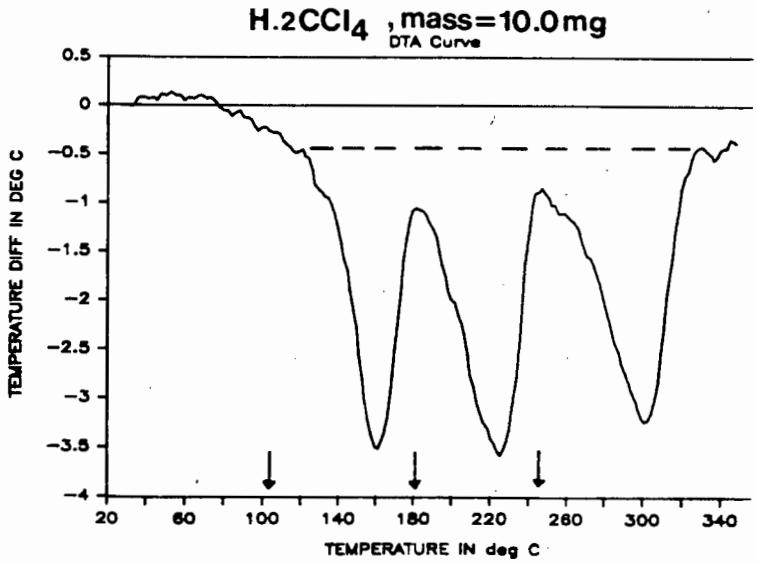

Fig 5.3 TG curves (on the left) and DTA curves(on the right) for the $Ni(NCS)_2(4\text{-}ViPy)_4.2G$ clathrates, where G = CH_2Cl_2, $CHCl_3$ or CCl_4.

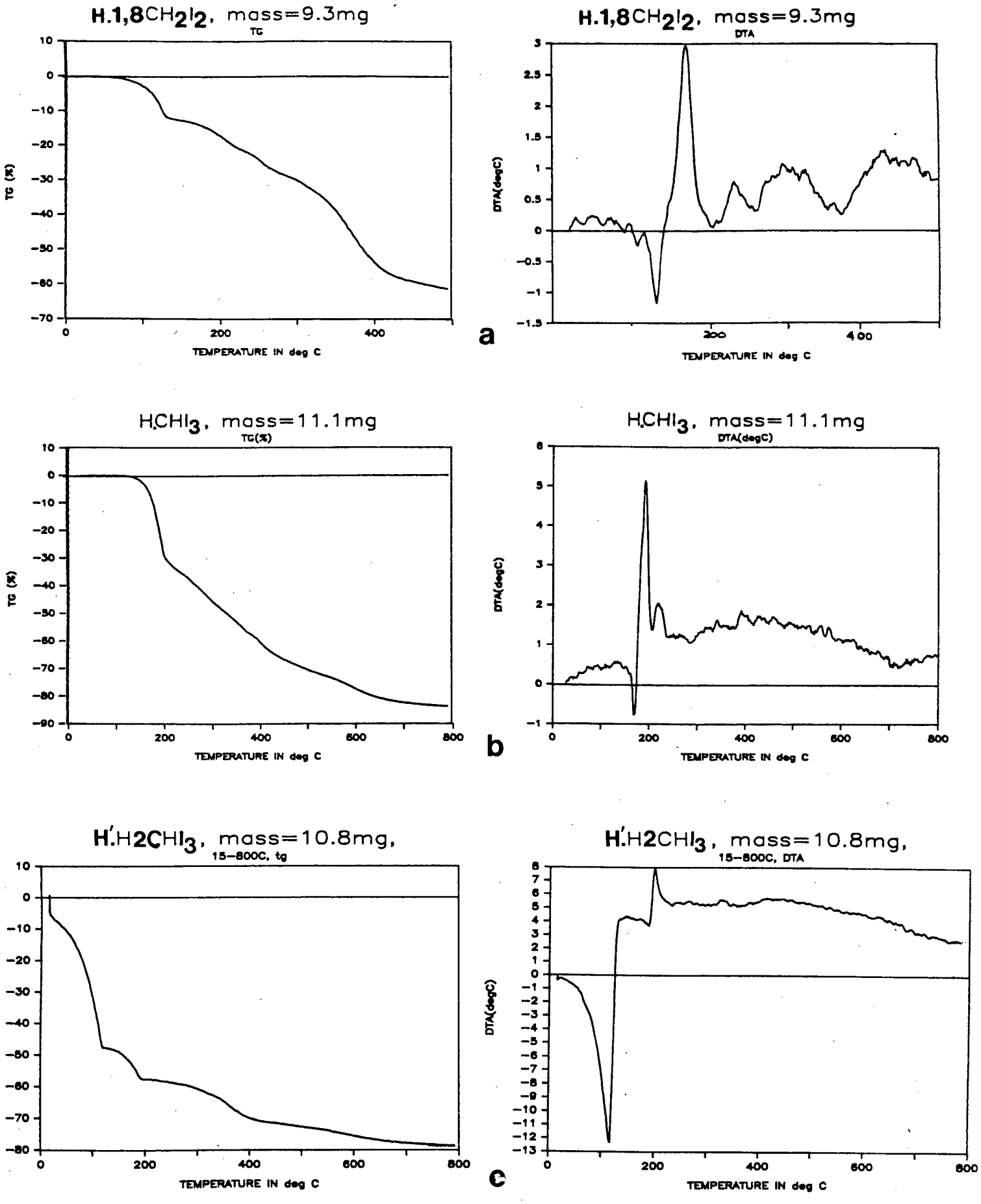

Fig 5.4 TG curves (on the left) and DTA curves(on the right) for (a) $Ni(NCS)_2(4\text{-}ViPy)_4.1.8CH_2I_2$ (b) $Ni(NCS)_2(4\text{-}ViPy)_4.CHI_3$ and (c) $[Ni(NCS)_2(4\text{-}ViPy)_4].[Ni(NCS)_2(4\text{-}ViPy)_3(thf)].2CHI_3$.

where m_s is the amount of sample (moles) and K is an empirical conversion factor. This factor was determined by relating the known enthalpy change for the melting of pure naphthalene ($\triangle H_{m,naphthalene}$ = 18.992 $kJ.mol^{-1}$) to the measured peak area of this enthalpy change. The procedure used to obtain the enthalpy change for a process occurring in the sample, $\triangle H_s$, was firstly to determine

$$K = \triangle H_{melting,naph.} \times \frac{\text{no. of moles naphth.}}{A}$$

then to use this value (0.319 J/cm^2) in eqn. 1.

The constant K is temperature dependent and so ideally calibrations should be carried out over the temperature range being studied, by using standards which melt at different temperatures in this range. The enthalpy change for the endothermic guest release reaction in the CH_2Cl_2, $CHCl_3$ and CCl_4 clathrates of $[Ni(NCS)_2(4\text{-}ViPy)_4]$ is of main interest and this occurs from about 60 - 110 °C. Naphthalene melts at 80-81 °C and thus the K value obtained from the $\triangle H_m$ of naphthalene falls in this range.

In DTA curves thermal events in the sample are detected by deviations of the signal from the baseline, which is not always easy to establish. It may initially be displaced from zero as a result of mismatching in thermal properties of the sample and reference material and asymmetry in the construction of the sample and reference holders. After decomposition was complete the response did not return to its original position because the thermal properties of the residue are different from those of the original clathrate.

There is some error in determining the baseline, and therefore only large differences in enthalpy change values obtained can be considered significant. When two thermal events overlapped in the DTA curve the areas were estimated

by extrapolation of the steepest slope to the baseline. Measurement of the chosen areas was carried out by the 'cutting and weighing' method, the values obtained, $A_m(cm^2)$, are listed in TABLE 5.1.

5.4 Results and discussion

5.4.1 Thermal decomposition of $Ni(NCS)_2(4\text{-}ViPy)_4.2G$ where G = CH_2Cl_2, $CHCl_3$ or CCL_4

The TG and DTA curves of these clathrates are shown in fig 5.3. From the shape of the TG curves it can be seen that each clathrate decomposes on heating in three distinct stages, illustrated below:

$$Ni(NCS)_2(4\text{-}ViPy)_4.2G$$

(a) $\downarrow$ $-2\ G$

$$Ni(NCS)_2(4\text{-}ViPy)_4$$

(b) $\downarrow$ $-2\ (4\text{-}ViPy)$

$$Ni(NCS)_2(4\text{-}ViPy)_2$$

(c) $\downarrow$ $-2\ (4\text{-}ViPy)$

$$Ni(NCS)_2$$

These clathrates are classed as thermally unstable, since the first step involves loss of the guest, to leave the host molecule intact, which then decomposes to $Ni(NCS)_2(4\text{-}ViPy)_2$ via the loss of two pyridine bases (step b), which further decomposes to $Ni(NCS)_2$ with the loss of the remaining two substituted pyridines (step c). The percentage weight loss obtained in each case from the TG curves (values are reported in TABLE 5.1) shows excellent agreement between

TABLE 5.1 Thermal analysis data for $Ni(NCS)_2(4\text{-ViPy})_4.2G$ where $G=CH_2Cl_2$, $CHCl_3$ or CCl_4.

X = NCS and B = 4-vinylpyridine	%wght loss		sample temp., T_m (°C)	Area (cm^2)	$\triangle H$ (kJ/mol)
	calc.	meas.			
$NiX_2B_4.2CH_2Cl_2$ ----> NiX_2B_4 + $2CH_2Cl_2$	22.2	22.6	67	4.12	89
NiX_2B_4 ----> NiX_2B_2 + 2B	49.7	49.5	155	7.74	167
NiX_2B_2 ----> NiX_2 + 2B	77.2	77.4	245	6.87	148
$NiX_2B_4.2CHCl_3$ ----> NiX_2B_4 + $2CHCl_3$	28.6	28.9	77	5.15	102
NiX_2B_4 ----> NiX_2B_2 + 2B	53.8	53.0	162	7.09	165
NiX_2B_2 ----> NiX_2 + 2B	79.1	78.0	240	5.84	136
$NiX_2B_4.2CCl_4$ ----> NiX_2B_4 + $2CCl_4$	34.1	34.2	105	3.99	115
NiX_2B_4 ----> NiX_2B_2 + 2B	57.4	57.3	182	5.16	149
NiX_2B_2 ----> NiX_2 + 2B	80.7	80.1	246	4.58	132

experimental and theoretical values, never differing by more than 1%.

This thermal decomposition of the CH_2Cl_2, $CHCl_3$ and CCl_4 clathrates of $[Ni(NCS)_2(4\text{-ViPy})_4]$ follows the same mechanism as the decomposition of its thf, 4-ViPy, o-xylene and p-xylene clathrates[5,10]. The structure of the thermal decomposition intermediates of the $[Ni(NCS)_2(NH_3)_4]$ complex[5,10] have been established, and the first step involves loss of an ammonia ligand to form $[Ni(NCS)_2(NH_3)_3]$, which then loses a second NH_3, followed by a third step which results in the loss of the last two ammonia ligands to leave a polymer of $Ni(NCS)_2$. The dark yellowish - brown powder left remaining at the end of each thermal analysis performed in this study resembled that described for $[Ni(NCS)_2]$ in this publication[5,11].

The order in the different temperatures at which the guests are released from the $[Ni(NCS)_2(4\text{-ViPy})_4]$ lattice corresponds to observations made while handling single crystals of these clathrates in the atmosphere;

$$CH_2Cl_2 < CHCl_3 < CCl_4$$
$$67°C \quad 77°C \quad 105°C$$

The cracking of the clathrate crystals of dichloromethane and chloroform as the guest escaped was seen to occur only after a few minutes exposure to the air, while the faces of the carbon tetrachloride crystals were still shiny after 6-7 hours exposure and they were still capable of extinguishing plane polarised light after this time.

This guest release reaction represents the release of gaseous (because its molecules are kept separate within the host structure) solvent molecules from the host lattice. The enthalpy change associated with this reaction therefore gives information concerning the energy of host lattice - guest molecule interactions. A summary of these enthalpy

values together with their temperatures as well as the structural data of the clathrates is listed in TABLE 5.2.

Each of the three guests comes off at a higher temperature than their respective boiling points, and the energy required to release the guest molecules increases as the volume of the guest increases. As described in Chapter 4, the guest molecules are located in channels, and it is the constrictions in these channels which confines the 'trapped' molecules. It is possible that as the size of the cavity containing these molecules increases, i.e from CH_2Cl_2 to $CHCl_3$ to CCl_4, then the diameter of the constrictions in the channels remains the same or becomes narrower, thereby making it most difficult for the bulkier CCl_4 guest molecules to escape.

The carbon tetrachloride clathrate is also more efficiently packed than the chloroform or dichloromethane clathrates, and in the light of these results it is understandable that a higher temperature must be attained for the CCl_4 molecules to break through the well - ordered host lattice. It is interesting to compare the thermal properties of the $Ni(NCS)_2(4\text{-}EtPy)_4.2CCl_4$ clathrate[5,12] with the $Ni(NCS)_2(4\text{-}ViPy)_4.2CCl_4$ clathrate. In the former clathrate the CCl_4 guest molecules escape at 55°C (21°C below their boiling point) and the $\triangle H$ value obtained for the guest release reaction is 80 kJ/mol. This clathrate also exhibits the same mode of packing as in the δ-phase clathrates of CH_2Cl_2, $CHCl_3$ and CCl_4, but has a packing efficiency of 22.2 $Å^3$/non hydrogen atom compared to that of 21.3 $Å^3$/non hydrogen atom for the $Ni(NCS)_2(4\text{-}ViPy)_4.2CCl_4$ clathrate. The less efficient packing in the $[Ni(NCS)_2(4\text{-}EtPy)_4]$ host lattice must play an important role in the weaker retentive forces of this clathrate.

TABLE 5.2 Summary of information obtained on the environment of CH_2Cl_2, $CHCl_3$ and CCl_4 in their $[Ni(NCS)_2(4\text{-ViPy})_4]$ clathrates.

Guest	CH_2Cl_2	$CHCl_3$	CCl_4
Packing efficiency vol / non H atom (Å^3)	21.5	21.5	21.3
Volume of the cavity/ guest molecule (Å^3)	97.6	117.9	134.1
T_{onset}(°C) of guest release reaction	67	77	105
$\triangle$H(kJ/mol) of guest release reaction	89	102	115
$\triangle H_{vap}$(kJ/mol)	28.22	29.70	30.00
Boiling point (°C) of the solvent	40.2	62	76

The $[Ni(NCS)_2(4\text{-}ViPy)_4]$ host complex decomposes at significantly lower temperatures than the $[Ni(NCS)_2(4\text{-}MePy)_4]$ complex. The highest temperature attained for the removal of the first two bases is for the carbon tetrachloride clathrate (182°C), the lowest temperature being found for the dichloromethane compound (155°C). The variation in the removal of the last two pyridine bases is not as marked (approximately 245°C). Hence once the first two base ligands have been removed the $[Ni(NCS)_2(4\text{-}ViPy)_2]$ structures appear to be rendered very similar.

For all three clathrates the enthalpy value associated with the loss of the final pair of bases is approximately 20 kJ/mol less than for the removal of the first pair. Hence once the first two ligands have been removed from the host the two base compounds remaining are not as stable as their four base predecessors.

5.5 Thermal decomposition of compounds III to V

Fig 5.4 shows the TG and DTA curves for these clathrates. The shape of these curves is unusual compared to those obtained for other Werner clathrates e.g fig's 5.2 and 5.3. There is a peak with a negative $\triangle T$ value corresponding to an endothermic event which occurs between 160-180°C for the three compounds, and this is followed soon after by an exothermic event occurring at approximately 200°C.

Pure iodoform is reported to decompose on heating to liberate iodine[5,13], and so the DTA and TG curves of this decomposition were recorded in order to observe the temperature at which it occurs. These curves are shown below:

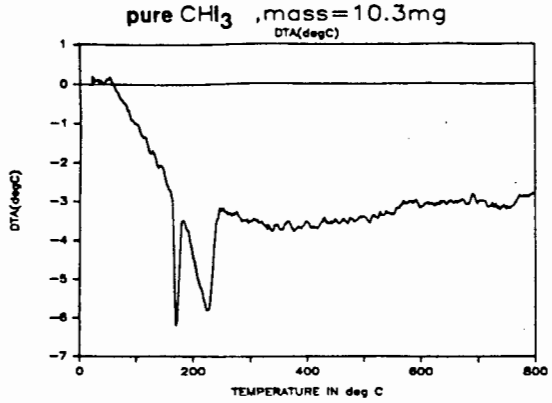

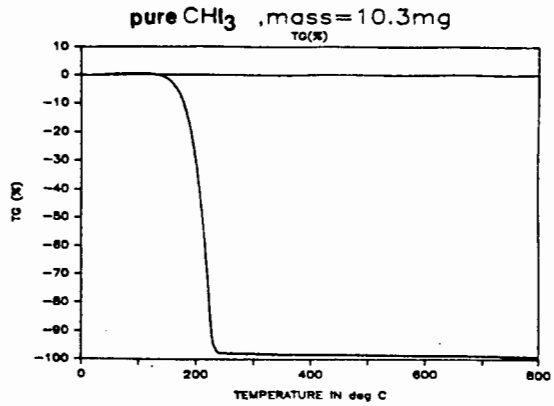

There are two endothermic peaks for this decomposition and the first peak occurs in the same region as the endothermic peak of the two CHI_3 clathrates. If this peak corresponds to CHI_3 liberating iodine, then a possible explanation for the exothermic reaction would be the iodine reacting with the host complex, possibly displacing two host bases, although the end product/products of this reaction are not clear. After this reaction there is gradual weight loss up until 800°C.

CH_2I_2 is a liquid (boiling $point_{760}$ = 181°C, d = 3.33g.cm²) and so on heating the $Ni(NCS)_2(4\text{-}ViPy)_4.1.8CH_2I_2$ clathrate, we might expect the guest molecules to be desorbed as they acquire enough energy to escape from the host lattice. CH_2I_2 is reported to partially decompose on boiling[5,14] to yield iodine. The study of the cavity system in the $Ni(NCS)_2(4\text{-}ViPy)_4.1.8CH_2I_2$ clathrate in Chapter 4 shows that the CH_2I_2 molecules must pass along the channels connecting the cavities in order to be liberated from their confines, and this study shows that they are far too bulky for this to happen. The only other way that they could have escaped is if a high enough temperature was attained to cause sufficient disruption of the host lattice to allow their release. However, before this temperature is reached the CH_2I_2 guest molecules decompose in their cavities to form iodine and again we see an endothermic event (guest decomposition) followed by an exothermic event, occurring at approximately the same temperature as for the CHI_3 clathrates, which again is probably due to I_2 reacting with the host complex.

Chapter 5 References

5.1 W.W Wendlandt, J.P Smith, 'The thermal properties of transition metal amine complexes', Elsevier, New York (1967)

5.2 G. Beech, C.T Mortimer and E.G Taylor, J. Chem. Soc., A, 925 (1967)

5.3 E. Koros, J. Chem. Soc., A, 1349 (1966)

5.4 W. Kemula and J. Czarnecki, Roczn. Chem., 41, 1463 (1967)

5.5 G. Beech and G.B Kauffmann, Thermochim. Acta, 1, 93 (1970)

5.6 E. Jona, T. Sramko and J. Gazo, Chem. Zvesti, 27, 145 (1973)

5.7 J. Zsako and C. Varhelyi, J. Therm. Anal., 7, 81 (1975)

5.8 F. Cassellato and B. Casu, Erdol Kohle Erdgas Petrochim, 22, 71 (1969)

5.9 V. Kemula, J. Lipkowski and D. Sybilska, Roczn.Chem., 48, 3 (1974)

5.10 M.H Moore, L.R Nassimbeni and M.L Niven, Inorganica Chimica Acta, 131, 45 (1987)

5.11 E. Dubler, A. Reller and H.R Oswald, Zeitschrift fur kristallog., 161, 265 (1982)

5.12 M.H Moore, unpublished results.

5.13 V. Vyskocil, Chem. Abstracts, 23, 4896 (1929)

5.14 A. Adams and H. Marvel, Organic Synthesis, Collective vol. I, 350

Chapter 6

General discussion and conclusions

As noted earlier the similarity of packing of these structures is of interest. STRUCTURE II may be compared with STRUCTURES I and its chloroform analogue, $Ni(NCS)_2(4\text{-}ViPy)_4.2CHCl_3$ which is isomorphous with STRUCTURE I.

Fig 6.1 shows these three structures projected along [010]. The dichloromethane and chloroform clathrates have symmetry $P2_1/n$ which is a subset of C2/c, and the host molecules are therefore not constrained to lie in special positions. Nevertheless, the packings bear certain similarities, with the host and guest molecules lying in bands parallel to a.

STRUCTURES IV and V display even greater similarity in their packing. STRUCTURE V crystallises in $P2_1/c$ which is not a subset of Pbca. The two sets of cell dimensions are similar, however, with the angle β only 6.58° distorted from 90°, and the two structures retaining the inversion centres and the two-fold screw axes parallel to b in common. The positions of the host and guest molecules are essentially the same, showing that the substitution of a tetrahydrofuran for a 4-vinylpyridine ligand has little effect on the crystal packing, as shown in fig 6.2.

It was observed that the sulphur to iodine distances in STRUCTURES III, IV and V were substantially shorter than the sum of their van der Waals radii. The type of interaction involved has been termed "Secondary bonding" and is discussed below.

6.1 Secondary bonding

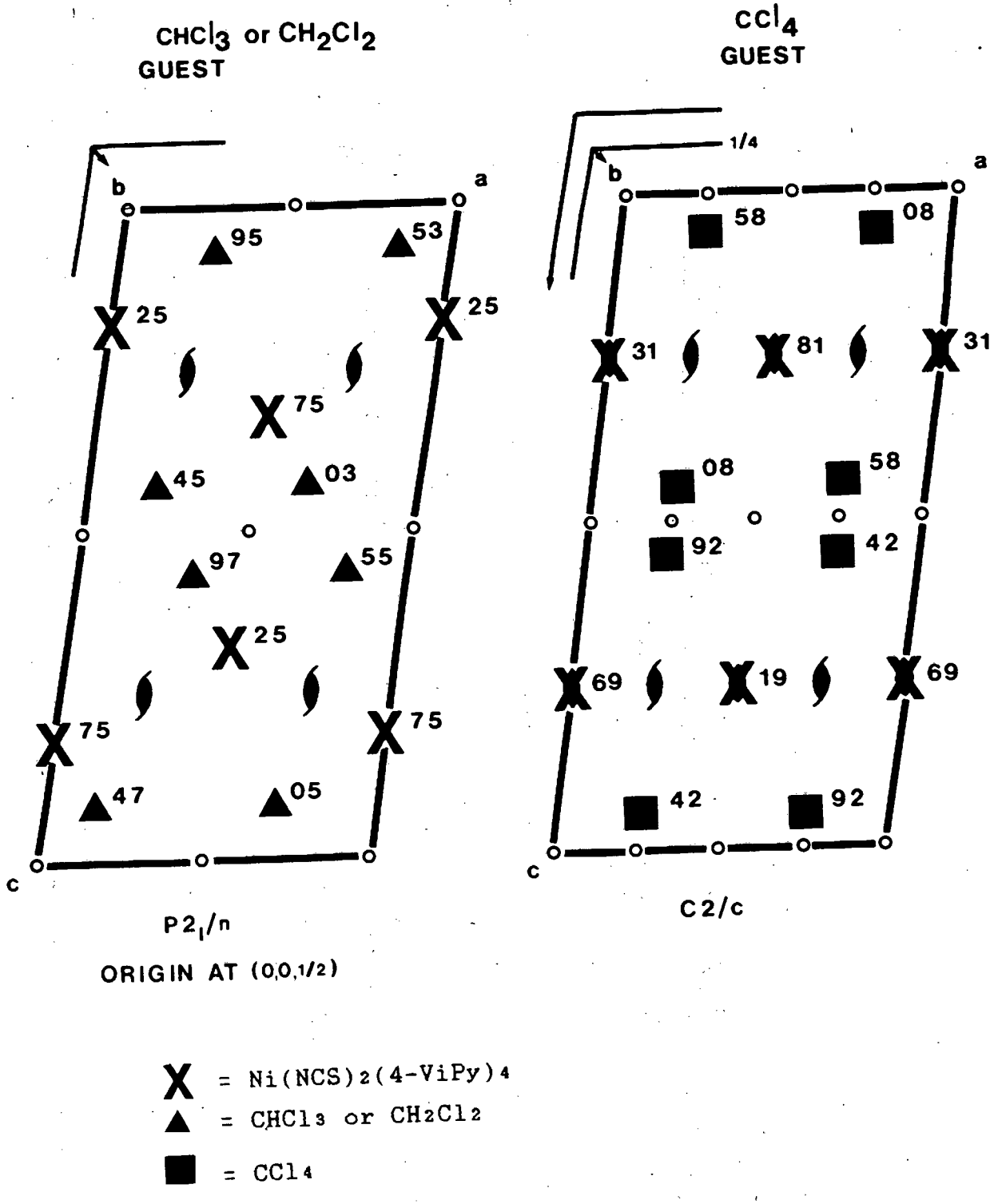

Fig 6.1 Structures containing CH_2Cl_2, $CHCl_3$ and CCl_4 guests viewed along [0 1 0] (heights along b alongside).

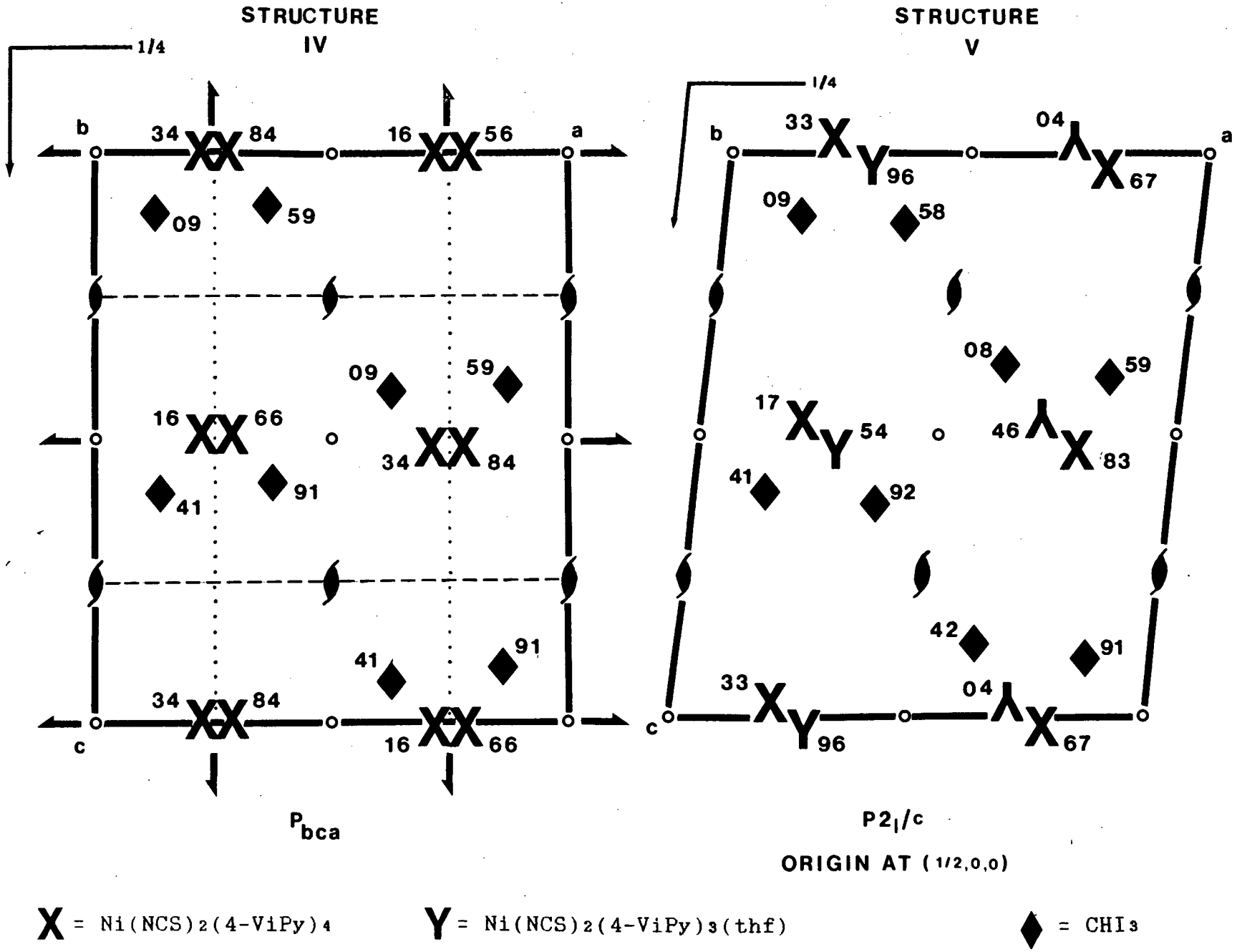

Fig 6.2 Structures IV and V viewed along [0 1 0].

Secondary bonding is an interaction of the type Y-A····· X, which is considered significant if the internuclear distance A·····X is shorter than the sum of the van der Waals radii of A and X. Such interactions may occur between the constituents of a crystal whether they are of the same type or different. Hydrogen bonding is a special case of these interactions. Alcock's review[6.1] has played an important role in classifying and understanding these interactions. The following rules appear to form a good basis for description and codification of structures exhibiting secondary bonds:

(a) The geometry of the primary bonds to the central atom is determined by the number of lone and bonding electron pairs(i.e Gillespie-Nyholm theory)

(b) Secondary bonds may form in any direction in line with primary bonds

(c) but not in the same direction as a lone pair on the central atom.

Rules (b) and (c) can be explained in terms of the orbitals involved in the interaction.

Although the potential for secondary bonding may exist in a crystal structure, packing considerations may limit the number of secondary bonds to any atom which may otherwise be formed. However, in the case of hydrogen bonding for instance, if the possibility for hydrogen bonding exists then the molecules invariably pack so as to maximise these interactions. Close - packing principles are still operative and the efficiency of the use of space is not lower than 60% i.e comparable with packing densities of non - polar molecules. In most cases molecular conformation can be arranged and a suitable space – group found such that a H -

bond can be formed. Nevertheless, the frequent departure from linearity and the variation in A to B distances in A-H·····B bonds for a given A and B pair indicate the need for the satisfaction of molecular packing requirements.

Although part of the shortening from the van der Waals distance is probably due to some electrostatic attraction, this cannot explain the magnitude of this shortening in many cases. A bonding scheme has been proposed by Alcock which explains the observed effects: the most likely form of interaction is a dative bond formed by donation of a lone pair by X into an empty σ^* orbital of the primary Y-A bond. This would account for the observed linearity of the Y-A·····X interaction. This model also accounts for the trends in the strength of the secondary bond as the electronegativity of A and X vary. As the electronegativity of A decreases, then so the strength of the interaction increases, a positive charge on A also being favourable. However, increasing the electronegativity of X does not increase the strength of the secondary bond as expected, and in some cases can even cause a weakening. As A becomes more electropositive, then so the σ and σ^* orbitals of the Y-A bond become more diffuse, which promotes better overlap with the lone pair on X. Similarly, as the electronegativity of X increases, then the lone pair of electrons become more tightly bound , which reduces the basicity of X.

Thus secondary bonding serves to bridge the gap between metallic and covalent bonding. This variation of bonding type with change in electronegativities of the participating atoms, for the system B - A - B is shown in fig 6.3.

Secondary bonding between iodine and sulphur is not uncommon. The 1,4 dithian - I_2 adduct exhibits significant secondary interaction[6·2], with a S····I distance of 2.87Å (the sum of the van der Waals radii of sulphur and iodine is

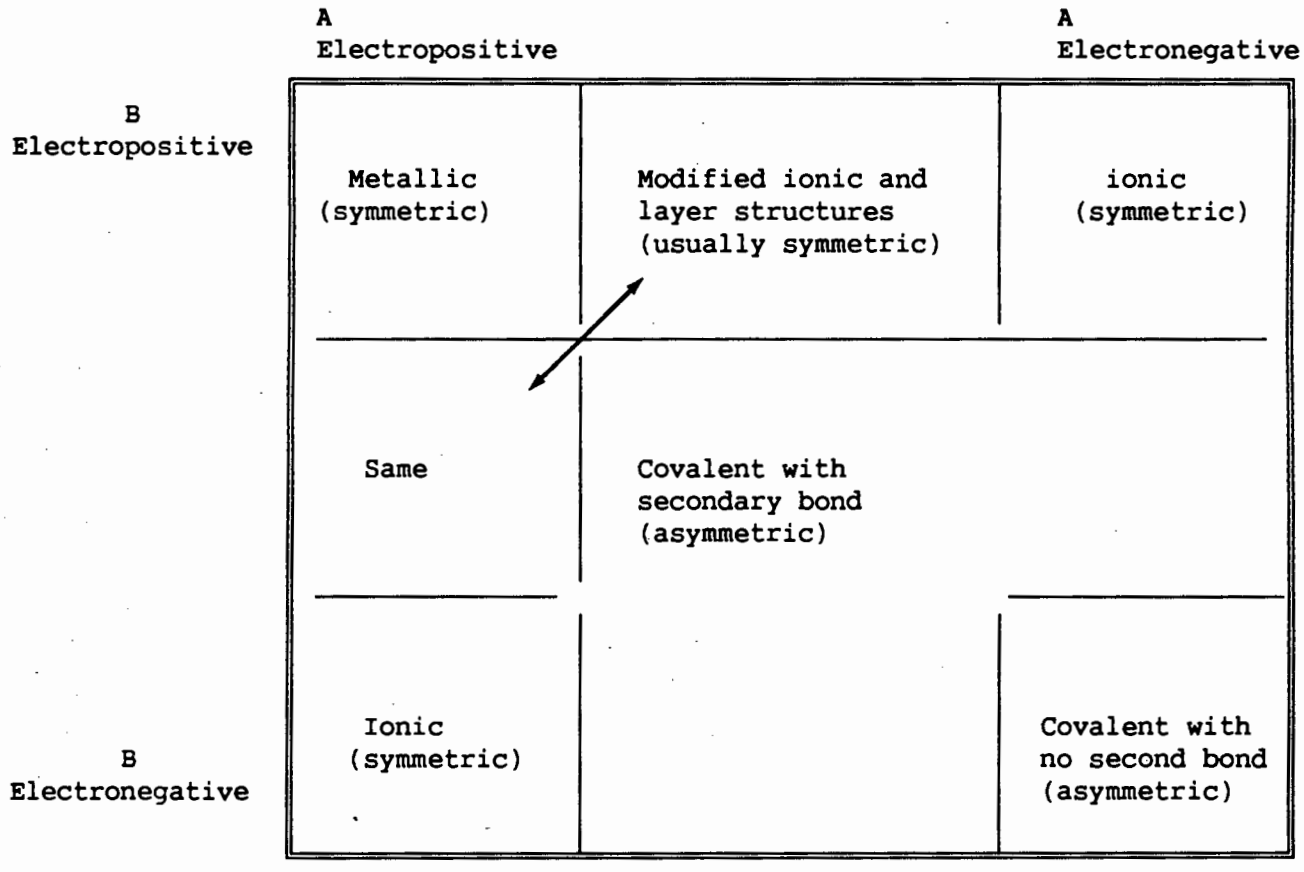

Fig 6.3. The variation of bond type with electronegativity in a system B - A - B. Taken from Alcock[6.1].

taken as 3.78Å[6.3]). The 1:1 addition compound of dibenzyl sulphide - I_2 has also been reported[6.4] with a S····I distance of 2.84Å. More relevant to this discussion is the 1:1 addition compound of dithian - iodoform[6.5] (S····I distance of 3.29Å) and the 1:3 addition compound of S_8 - CHI_3[6.5](S····I distance of 3.44Å). In the 1:1 addition compound only two of the iodoform iodine atoms are involved in secondary bonding, while in the 1:3 addition compound, all three iodines of a particular iodoform molecule are involved in secondary interaction. The C-I····S angles are almost linear which is expected for an interaction of this nature. The S····I distances of 3.29Å and 3.44Å in these two compounds are also of the same magnitude that is observed for the S····I interactions in STRUCTURES III,IV and V (TABLE 6.1).

6.2 Secondary bonding in STRUCTURES IV and V

There are two ways in which secondary bonding can occur between the isothiocyanate sulphur and the iodine of the guest molecule;

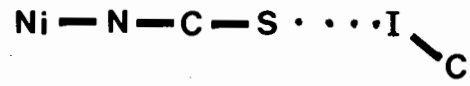

I donor

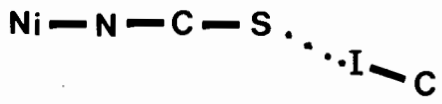

S donor

These are illustrated above, where the secondary bond is represented by the broken line. With iodine as donor we expect the Ni(NC) - S·····I angle to be in the vicinity of 180°, while with sulphur as donor we expect linearity in the S·····I - C_{guest} bond. The van der Waals radii for iodine and sulphur are taken to be $r_w(I)$ = 1.98Å and $r_w(S)$=1.80Å[6.3]. In all these structures S acts as the donor atom. In STRUCTURE IV we have three S·····I interactions

TABLE 6.1 Sulphur to iodine bond distances and angles for the S···I - C interaction in $NiX_2B_4.nG$ clathrates, where X = NCS, B = pyridine or 4-vinylpyridine and G = CH_2I_2 or CHI_3.

	d(S···I)	(d-3.78)/Å	S····I - C Angle	I moved through symmetry element
STRUCTURE III				
S1 ·· I2	3.66	-0.12	-	(i) x, y, z
S1 ·· I3	3.39	-0.39	-	(ii)y-.25,-x,-z+1.25
S1 ·· I4	3.91	+0.13	-	" "
S1 ·· I5	3.65	-0.13	-	" "
STRUCTURE IV				
S1 ·· I1	3.36	-0.42	172.83	(i) x,y + ½,z - ½
S1 ·· I2	3.63	-0.15	170.44	(ii) x + ½,y + ½,-z
S1 ·· I3	3.42	-0.36	168.04	(iii)x + ½,y + ½, z
STRUCTURE V				
S1A ·· I1A	3.57	-0.21	168.19	(i) x,y - 1, z - 1
S1A ·· I3A	3.84	+0.06	160.74	(ii)x + 1,y + 1,z+1
S1A ·· I2A	3.55	-0.23	170.04	(iii) x, y, z
S1B ·· I2A	3.30	-0.48	175.00	(iv)x + 1,y + 1,z+1
S1B ·· I1B	3.64	-0.14	168.64	(v) x + 1,y ,z + 1
S1B ·· I3B	3.50	-0.23	173.82	(vi) x + 1,y ,z
$Co(NCS)_2(Py)_4.2CHI_3$				
S ·· I1	3.36	-0.12	173.4	(i) x,y + ½, z + ½
S ·· I2	3.51	-0.27	176.5	(ii)x, y + ½,z + ½
S ·· I3	3.46	-0.32	170.3	(iii) x, y, z

with interatomic distances < 3.78Å occurring with only one of the S atoms of the host molecules. This pattern is repeated in STRUCTURE V where we find again the two different molecules of the host each involving one -NCS moiety in secondary bonding.

The details of these secondary bonds are listed in TABLE 6.1 which also gives the values for these interactions in the related compound, $Co(NCS)_2(py)_4.2CHI_3$[6·6].

The geometry of the S atom in STRUCTURE IV is shown in fig 6.4. The sulphur atom is surrounded by the three symmetry - related iodines and is almost coplanar with them. It lies 0.03 Å from the plane defined by the iodines.

Similar geometries are exhibited by the S atoms which are involved in secondary interaction in STRUCTURE V.

6.3 Secondary bonding in STRUCTURE III

Although the diiodomethane molecules are disordered, both iodines of the guest lie an appreciable distance within the van der Waals radii of the sulphur of the host. The distance from I2 to S is 3.66Å, but when this iodine moves onto the diad (I1) the S ··· I distance becomes 4.64Å.
As the other iodine varies from position I3 to I4 to I5 the S ···· I distances range from 3.39Å, 3.91Å to 3.65Å, respectively. Each sulphur has two secondary interactions and this arrangement around the $\bar{4}$ centre at 0, 3/4, 3/8 is shown in fig 6.5. Only peaks I2 and I3 are shown for clarity. The inset diagram shows peaks I3, I4 and I5 interacting with the sulphur.

In the other structures listed in TABLE 6.1 each sulphur interacts with three iodines, whereas in this case the sulphur interacts with only two. If the sulphur is thought

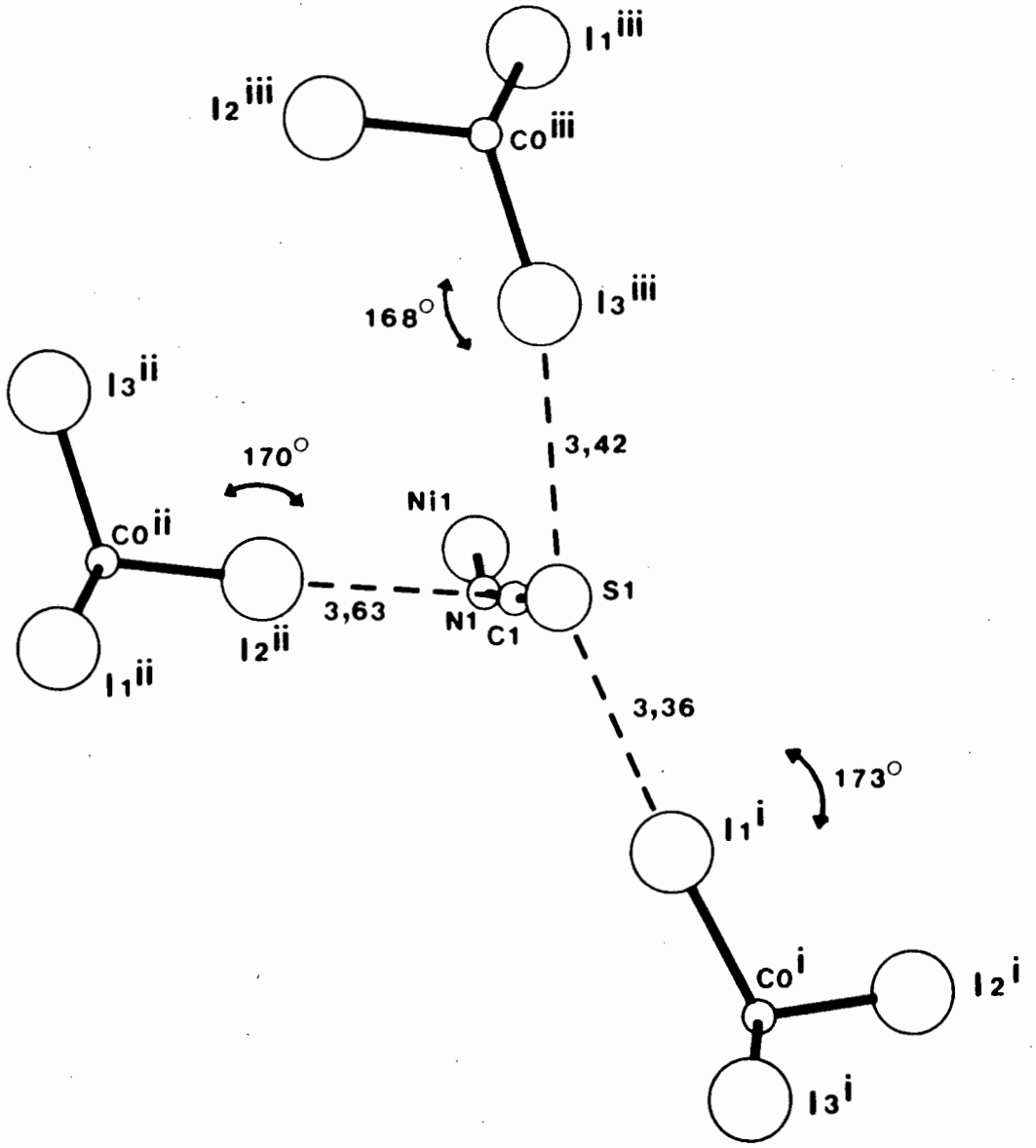

Fig 6.4 Perspective view of the secondary interaction about the sulphur in STRUCTURE IV. Postscripts refer to the symmetry elements that the iodines have been moved through. (Lengths in angstroms).

of as having a certain capacity for secondary bonding then in STRUCTURE III this ability to interact is only "spread" over two iodines, as opposed to three, and so we might expect stronger secondary bonds in STRUCTURE III. It would be interesting to solve this structure at even a lower temperature than -40 °C, firstly to see whether the strength of the interaction increases i.e shortening of the S ···· I distances as the iodines become less vibrant and secondly, to locate the carbon atom so that the C - I ····· S angles may be observed. From an orbital point of view the sulphur atom has two lone pairs of electrons in sp^2 hybrid orbitals, and these must be shared between the anti - bonding orbitals of the C - I bonds, which project into space at 180° to the covalent bond. The fewer σ^* orbitals these electrons must be shared between, the stronger the interaction.

STRUCTURES I and II, as well as other Werner clathrates of the form $Ni(NCS)_2(subst.\ pyridine)_4$ with chlorine containing guests, do not display significant secondary bonding in that all S ····· Cl distances are on the limit or greater than the sum of the van der Waals radii.

This study has served to show that secondary bonding may play a role in host - guest interactions, not only in Werner clathrates, but in Inclusion compounds as a whole, depending on whether the host and guest molecules contain atoms of suitable electronegativity for this interaction to occur.

Chapter 6 References

6.1 N.W Alcock, Adv. Inorg. Radiochem., 15, 2 (1972)
6.2 G.Y Chao and J.D McCullough, Acta Cryst.,13, 727 (1960)
6.3 A. Bondi, J. Phys. Chem., 68, 441 (1964)
6.4 O. Hassel, Proc. Chem. Soc., 250 (1957)
6.5 T. Bjorvatten, O. Hassel and C. Romming, Nature, 189, 137, (1961)
6.6 H. van Hartl and S. Steidel, Acta Cryst., B36, 65 (1980)

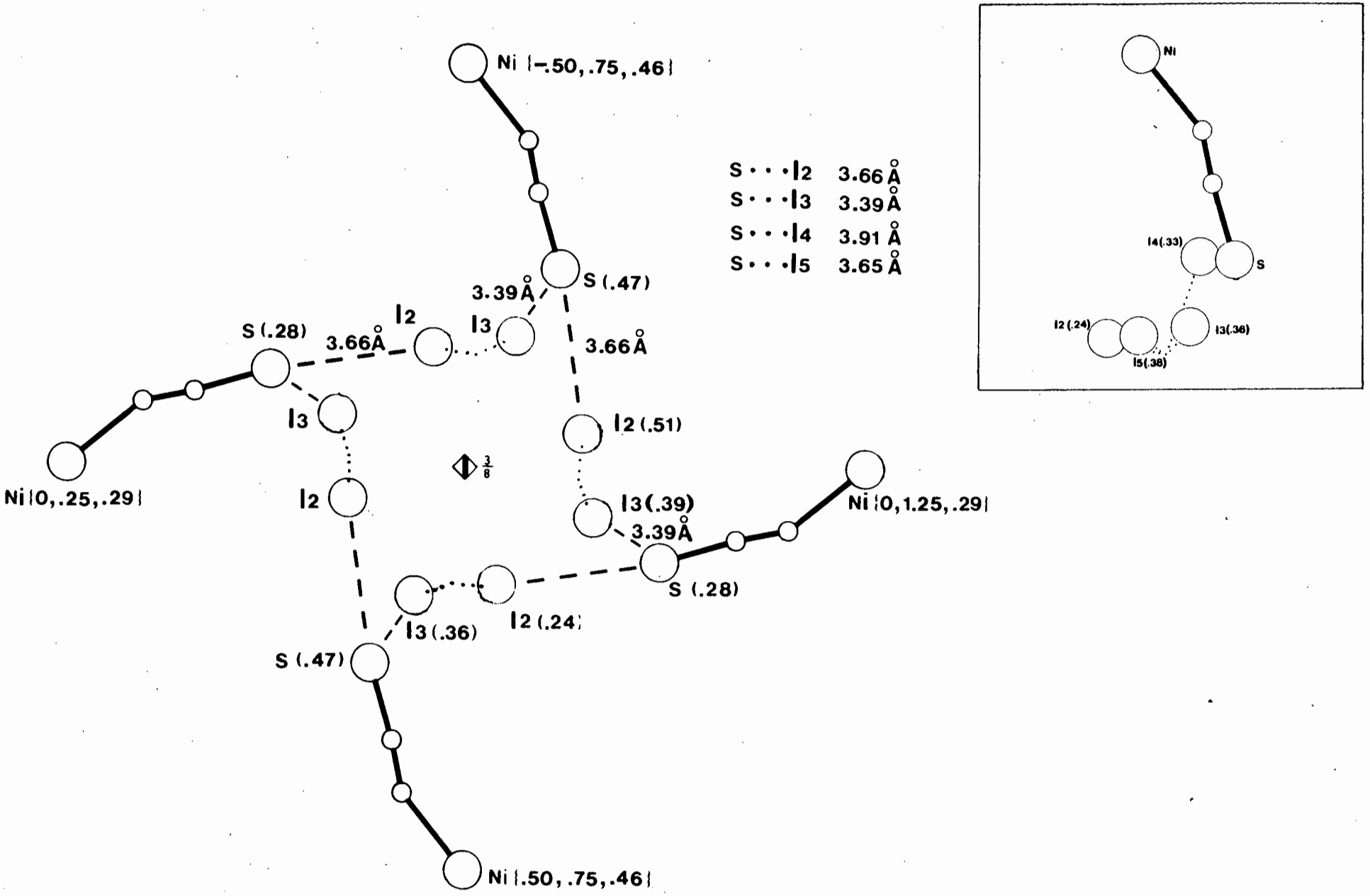

Fig 6.5 View down [0 0 1] of the secondary interaction in STRUCTURE V (heights along c in brackets). The inset diagram shows the relationship of peaks I3,I4 and I5 to the sulphur. Although the guest carbon atom was not located the C-I bonds are shown as dotted lines.

APPENDIX A

Comparison of STRUCTURE II solved in C2/c and Cc

* x,y,z is related to x*,y*,z* by the diad in C2/c i.e x = -x*, y = y* and z = ½ - z*.

Atomic * parameter	C2/c	Cc	$\triangle$(x10⁴)	$\bar{\sigma}$ (x10⁴)	$\frac{\triangle}{\bar{\sigma}}$
Ni					
y	0.3075(1)	0.3075(2)	0	1.5	0
N11					
x	0.0694(11)	0.0648(25)	46	18.0	2.6
y	0.3099(6)	0.3085(14)	14	10.0	1.4
z	0.1557(6)	0.1493(13)	64	9.5	6.7
x*	-0.0694(11)	-0.0791(31)	97	21.0	4.6
y*	0.3099(6)	0.3120(16)	21	11.0	1.9
z*	0.3443(6)	0.3337(15)	106	10.5	10.1
N21					
x	0.0000(0)	-0.0132(40)	132	20.0	6.6
y	0.4138(8)	0.4124(9)	14	8.5	1.6
z	0.2500(0)	0.2546(22)	46	11.0	4.2
N41					
x	0.0000(0)	-0.0053(39)	53	19.5	2.7
y	0.2037(8)	0.2020(11)	17	9.5	1.8
z	0.2500(0)	0.2612(16)	112	8.0	14
N1					
x	0.1951(12)	0.1924(45)	27	28.5	0.9
y	0.3090(6)	0.3044(22)	46	14.0	3.3
z	0.2947(6)	0.2990(21)	43	13.5	3.2
x*	-0.1951(12)	-0.1928(28)	23	20.0	1.2
y*	0.3090(6)	0.3105(14)	15	10.0	1.5
z*	0.2053(6)	0.2081(15)	28	10.5	2.7
S1					
x	0.4473(5)	0.4448(15)	25	10.0	2.5
y	0.3018(4)	0.3030(9)	12	6.5	1.8
z	0.3649(3)	0.3677(10)	28	6.5	4.3
x*	-0.4473(5)	-0.4458(25)	15	15.0	1.0
y*	0.3018(4)	0.2945(14)	73	9.0	8.1
z*	0.1351(3)	0.1364(15)	13	9.0	1.4
C12					
x	0.1794(15)	0.1823(52)	29	33.5	0.9
y	0.3445(7)	0.3447(24)	2	15.5	0.1
z	0.1458(8)	0.1503(28)	45	18.0	2.5

Atomic parameter	C2/c	Cc	$\triangle$(x10^4)	$\bar{\sigma}$(x10^4)	$\frac{\triangle}{\bar{\sigma}}$
C12					
x*	-0.1794(15)	-0.1758(51)	36	33.0	1.1
y*	0.3445(7)	0.3472(24)	27	15.5	1.7
z*	0.3542(8)	0.3565(27)	23	17.5	1.3
C13					
x	0.2149(16)	0.2162(39)	13	27.5	0.5
y	0.3528(7)	0.3556(18)	28	12.5	2.2
z	0.0871(8)	0.0932(20)	61	14.0	4.4
x*	-0.2149(16)	-0.2249(47)	100	31.5	3.2
y*	0.3528(7)	0.3439(22)	89	14.5	6.1
z*	0.4129(8)	0.4183(23)	54	15.5	3.5
C14					
x	0.1449(15)	0.1429(44)	20	29.5	0.7
y	0.3247(7)	0.3253(22)	6	14.5	0.4
z	0.0328(8)	0.0384(23)	56	15.5	3.6
x*	-0.1449(15)	-0.1382(42)	67	28.5	2.4
y*	0.3247(7)	0.3206(22)	41	14.5	2.8
z*	0.4672(8)	0.4730(21)	58	14.5	4.0
C15					
x	0.0315(17)	0.0265(46)	50	31.5	1.6
y	0.2864(8)	0.2863(23)	1	15.5	0.1
z	0.0433(9)	0.0460(25)	27	17.0	1.6
x*	-0.0315(17)	-0.0392(53)	77	35.0	2.2
y*	0.2864(8)	0.2887(27)	23	17.5	1.3
z*	0.4567(9)	0.4655(27)	88	18.0	4.9
C16					
x	0.0023(15)	-0.0171(50)	194	32.5	6.0
y	0.2795(7)	0.2836(24)	41	15.5	2.6
z	0.1056(8)	0.1050(26)	6	17.0	0.4
x*	-0.0023(15)	-0.0057(35)	34	25.0	1.4
y*	0.2795(7)	0.2771(17)	24	12.0	2.0
z*	0.3944(8)	0.3977(19)	33	13.5	2.4
C17					
x	0.1786(22)	0.1823(77)	37	49.5	0.7
y	0.3324(11)	0.3377(40)	53	25.5	2.1
z	-0.0342(11)	-0.0233(40)	109	25.5	4.3
x*	-0.1786(22)	-0.1810(41)	24	31.5	0.8
y*	0.3324(11)	0.3296(22)	28	16.5	1.7
z*	0.5342(11)	0.5367(22)	25	16.5	1.5

Atomic parameter	C2/c	Cc	$\triangle$(x10^4)	$\bar{\sigma}$(x10^4)	$\frac{\triangle}{\bar{\sigma}}$
C18					
x	0.2732(25)	0.2751(55)	19	40.0	0.5
y	0.3678(12)	0.3708(26)	30	19.0	1.6
z	-0.0509(13)	-0.0432(28)	77	20.5	3.8
x*	-0.2732(25)	-0.2715(85)	17	55.0	0.3
y*	0.3678(12)	0.3554(35)	124	23.5	5.3
z*	0.5509(13)	0.5633(46)	124	29.5	4.2
C22					
x	0.0490(16)	0.0484(38)	6	27.0	0.2
y	0.4472(8)	0.4449(20)	23	14.0	1.6
z	0.3002(9)	0.3012(20)	10	14.5	0.7
x*	-0.0490(16)	-0.0499(58)	9	37.0	0.2
y*	0.4472(8)	0.4524(31)	52	19.5	2.7
z*	0.1998(9)	0.1979(32)	19	20.5	0.9
C23					
x	0.0507(16)	0.0538(62)	31	39.0	0.8
y	0.5161(8)	0.5207(32)	46	20.0	2.3
z	0.3062(9)	0.3042(31)	20	20.0	1.0
x*	-0.0507(16)	-0.0467(46)	40	31.0	1.3
y*	0.5161(8)	0.5161(26)	0	17.0	0.0
z*	0.1938(9)	0.1960(25)	22	17.0	1.3
C24					
x	0.0000(0)	-0.0042(43)	42	21.5	2.0
y	0.5499(12)	0.5507(14)	8	13.0	0.6
z	0.2500(0)	0.2653(20)	153	10.0	15.3
C27					
x	0.0000(0)	0.0136(51)	136	25.5	5.3
y	0.6281(18)	0.6580(24)	299	21.0	14.2
z	0.2500(0)	0.2756(27)	256	13.5	19.0
C28					
x	0.0271(40)	0.0065(50)	206	45.0	4.6
y	0.6684(22)	0.6258(22)	426	22.0	19.4
z	0.2806(19)	0.2718(24)	88	21.5	4.1
x*	-0.0271(40)	-0.0070(56)	201	48.0	4.2
y*	0.6684(22)	0.6260(22)	424	22.0	19.3
z*	0.2194(19)	0.2282(26)	88	22.5	3.9
C42					
x	0.1042(16)	0.1066(37)	24	26.5	0.9
y	0.1671(9)	0.1713(20)	42	14.5	2.9
z	0.2375(8)	0.2304(19)	71	13.5	5.3

Atomic parameter	C2/c	Cc	$\triangle$ (x10^4)	$\bar{\sigma}$ (x10^4)	$\frac{\triangle}{\bar{\sigma}}$
C42					
x*	-0.1042(16)	-0.1115(42)	73	29.0	2.5
y*	0.1671(9)	0.1661(19)	10	14.0	0.7
z*	0.2625(8)	0.2539(22)	86	15.0	5.7
C43					
x	0.1101(16)	0.1062(43)	39	29.5	1.3
y	0.1018(8)	0.0993(20)	25	14.0	1.8
z	0.2368(8)	0.2326(20)	42	14.0	3.0
x*	-0.1101(16)	-0.1134(59)	33	37.5	0.9
y*	0.1018(8)	0.1033(27)	15	17.5	0.9
z*	0.2632(8)	0.2532(25)	100	16.5	6.1
C44					
x	0.0000(0)	-0.0152(48)	152	24.0	6.3
y	0.0614(15)	0.0660(14)	46	14.5	3.2
z	0.2500(0)	0.2593(24)	93	12.0	7.8
C47					
x	0.0000(0)	-0.0619(48)	619	24.0	26
y	-0.0108(18)	-0.0443(24)	335	21.0	16
z	0.2500(0)	0.2663(26)	163	13.0	12.5
C48					
x	0.0551(54)	0.0592(30)	41	42.0	1.0
y	-0.0514(26)	-0.0561(32)	47	29.0	1.6
z	0.2340(30)	0.2349(28)	9	29.0	0.3
x*	-0.0551(54)	-0.0573(20)	22	37.0	0.6
y*	-0.0514(26)	-0.0583(31)	69	28.5	2.4
z*	0.2660(30)	0.2679(13)	19	21.5	0.9